Manufacture and Characterization of 3D-Printed Sugar-Reduced Layered Chocolates and their Sensory Perception

by

Khemiga Khemacheevakul

A thesis submitted in partial fulfillment of the requirements for the degree of

Master of Science

in

Food Science and Technology

Department of Agricultural, Food and Nutritional Science

University of Alberta

Abstract

High global sugar consumption exceeding recommendations and an increased awareness of health concerns associated with excess sugar consumption have promoted the development of sugar-reduced foods by manufacturers, and consumption of sugar-reduced foods by consumers. As confectionary items are a major contributor to total sugars intake, sugar-reduction strategies should focus on this group of foods. 3D food printing (3DFP) is an emerging area of research, and previous studies have investigated single-extruder 3D printers, with a focus on optimizing material formulation and 3D printing parameters. However, few have addressed sensory perception of the printed foods, and none have utilized 3DFP for sugar-reduction. Furthermore, novel methods to optimize 3DFP can be developed as there are several ways to define a 'good' print. Therefore, this research comprises two studies that aimed to demonstrate the capability of a dual-extruder 3D food printer as an innovative tool to manufacture sugar-reduced 3D printed chocolates with desirable sensory qualities. A novel optimization procedure that compiles several previously proposed concepts for 3D printing parameters was also developed.

In the first study, six variations of a three-layered hollow cylinder (diameter 28.00 mm, height 10.80 mm, wall thickness 4.37 mm) was designed in CAD software. Each variation had different layering orders of H or L chocolate to create sugar-reduced and non-sugar-reduced chocolates with different total % sugar concentrations. A semi-quantitative procedure for optimizing 3D printing parameters was developed, and this four-step approach was used to optimize printing parameters for a dual-extruder 3D printer with L and H chocolate. 3D printer speed and flow rate settings were first quantified. Then, chocolate lines that were 3D printed at varying print speed and flow rate were assessed by qualitative criteria (non-linearity, localized bulging, localized thinning, and breakage) to determine optimal print settings. Then, printed

product accuracy and precision was validated by comparing measured mass and dimensions (height, wall thickness and diameter) of 3D chocolate prints to digital designs. Finally, 3D printed chocolate quality was evaluated by determining chocolate melting properties prior to and after 3D printing. The optimal print setting for both extruders was identified as print speed 35 (2.92-2.94 mm/s) and flow rate 100 (6.11-6.55 mm^3/s) as it manufactured 3D printed chocolates with no qualitative defects and with similar mass and dimensions compared to the digital designs. The six designs had mean total % sugar (g sugar/g chocolate) of 51.5%, 41.6%, 41.6%, 34.9%, 34.0%, and 26.7%. Melting properties suggested that a printing temperature between 28-30℃ was suitable for both chocolates, as the chocolates remained tempered after 3D printing at these temperatures.

In the second study, the temporal sensory profile, perceived sweetness intensity, and acceptance of the six manufactured sugar-reduced and non-sugar reduced 3D printed chocolates were investigated. The chocolate with 51.5% total sugar (printed with only H chocolate) was used as a high sugar control. A consumer panel (n=72) completed a temporal dominance of sensations (TDS) evaluation, rated overall sweetness intensity on a 5-point scale (1=not at all sweet, 5=extremely sweet), and rated liking on a 9-point hedonic scale (1=dislike extremely, 9=like extremely). 3D printed chocolates with 19% sugar reduction were perceived as similarly sweet compared to the high sugar control, while samples with 32% sugar reduction were perceived as less sweet. Layering order of H and L chocolates changed the temporal sensory attribute profile of the 3D printed chocolates, which influenced perceived overall sweetness. A sugar concentration gradient between layers improved the sweetness enhancement effect. All the manufactured 3D printed chocolates were similarly well-liked.

This research presented an alternative sugar-reduction method that utilized dual-extrusion 3DFP to create sugar-reduced 3D printed chocolates. The spatial distribution of sugar concentration in layers to reduce sugar in foods has not previously been demonstrated for chocolate, and not with 3DFP. A novel, semi-quantitative printing parameter optimization procedure was proposed and demonstrated for a dual-extruder 3D food printer with two types of chocolate. Manufactured sugar-reduced 3D printed chocolates were also evaluated for their temporal sensory perceptions. Although this research focused on chocolate, the printing parameter optimization procedure, and the sensory perception results can be used to guide the development of improved 3D food printing processes for further sugar-reduction and customization of a variety of 3D printed foods.

Preface

This thesis is an original work by Khemiga Khemacheevakul under the supervision of Dr. John Wolodko and Dr.Wendy Wismer, with funding from Alberta Innovates through the Strategic Chair Program, secured by Dr. John Wolodko.

A version of **Chapter 2** of this thesis will be submitted to *Journal of Food Engineering* for publication as K. Khemacheevakul, W. Wismer, A. Rana, and J. Wolodko. Optimization of a Dual-Extrusion 3D Food Printer for the Manufacturing of Sugar-Reduced Chocolates. The study was conceptualized by Dr. John Wolodko, Dr. Wendy Wismer, and I. Dr. John Wolodko, Dr. Anup Rana, and I designed the study. I collected, analysed, and interpreted the data and drafted the manuscript. Dr. Anup Rana contributed to data collection and provided technical support for 3D food printing. Dr. Anup Rana and Dr. John Wolodko provided editorial comments to the manuscript.

A version of **Chapter 3** of this thesis will be submitted to *Foods* as Khemiga Khemacheevakul, John Wolodko, Ha Nguyen and Wendy Wismer. Temporal Sensory Perceptions of Sugar-reduced 3D Printed Chocolates. The study was conceptualized and designed by Dr. Wendy Wismer, Dr. John Wolodko and I. Dr. Wendy Wismer and I designed the study. I completed participant recruitment and data collection (with the help of an undergraduate research student), data analysis and interpretation of the results and writing of the manuscript. Dr. Wendy Wismer provided editorial comments to the manuscript. Dr. Ha Nguyen assisted with statistical data analysis and conducted the principal components analysis (PCA). This study received ethics approval from the University of Alberta Human Research Ethics Board 2 (Pro00097545), under the project name “Sensory perception of layered chocolates.”

Dedication

I would like to dedicate this work to my beloved family. I am forever grateful for their unconditional love, continuous encouragement and support in everything that I do.

Acknowledgements

I would like to express my sincere gratitude and appreciation to my supervisors Dr. John Wolodko and Dr. Wendy Wismer for their kind support and providing me with the guidance and knowledge to complete this thesis. I am grateful for the opportunity to work under their supervision, and their encouragement in all research endeavors.

My sincere thanks to Anup Rana for your advice and invaluable input in these studies, and Ha Nguyen for your assistance and support with statistical analyses. I would also like to thank my former and current lab mates for their contributions towards different components of this thesis, especially Xiao Qin Feng, Susana De Leon Siller, Blanca Estela Enriquez Fernandez, and Ibironke Popoola. Thank you also to Michelle Feuereisen, Mariarosaria Savarese, Susan Gibson, and Samantha Biberdorf for their assistance in these studies. Thank you to Alberta Innovates for providing funding for this research through the Strategic Chair program.

I would also like to acknowledge several individuals for their technical assistance for lab equipment and analyses. Thank you to Ereddad Kharraz for your help with differential scanning calorimetry and gas pycnometry, Kelly Dunfield for your training on optical microscopy, Jingui Lan and Lisa Nikolai for their help with high performance liquid chromatography trials, Nathan Gerein for your help with the scanning electron microscope, as well as Dr. Michael Doschak for your help with X-ray microtomography.

A special thanks to my friends and family in Thailand and Canada, especially my mom, dad, brother and Raihan for their presence, advice, and continued support.

Table of Contents

List of Tables

List of Figures

List of Abbreviations

CAD	Computer-aided design
CATA	Check-all-that-apply sensory test
CCHS	Canadian Community Health Survey
CFIA	Canadian Food Inspection Agency
DSC	Differential scanning calorimetry
FR	Flow rate setting
H	High sugar concentration chocolate
HHH	3D printed chocolate with high sugar concentration chocolate in all three layers
HHL	3D printed chocolate (High sugar-High sugar-Low sugar chocolate)
HLH	3D printed chocolate (High sugar-Low sugar-High sugar chocolate)
HLL	3D printed chocolate (High sugar-Low sugar-Low sugar chocolate)
HSF	Heart and Stroke Foundation
LHL	3D printed chocolate (Low sugar-High sugar-Low sugar chocolate)
LLL	3D printed chocolate (Low sugar-Low sugar-Low sugar chocolate)
L	Low sugar concentration chocolate
PCA	Principal component analysis
PS	Print speed setting
RATA	Rate-all-that-apply sensory test
TDS	Temporal dominance of sensations
USDA	U.S. Department of Agriculture
WHO	World Health Organization

% (w/w)	% (g sugar/g chocolate)
3D	Three dimensional
3DFP	3D Food Printing
3DCP	3D Chocolate Printing

Chapter 1 - Introduction and Background

1.1 Introduction

Three-dimensional food printing (3DFP) is an emerging area in food science, and the continual development of sugar-reduced foods is needed to combat global excess consumption of sugar. As such, there are still potential applications of 3DFP and new methods of sugar-reduction to be explored. The topic of interest in this research is a sugar-reduction of chocolate based on a 'spatial distribution' of sugar concentration in layers, which can be accomplished by the layer-by-layer deposition of the chocolates through 3DFP. Optimization of 3DFP parameters by a semi-quantitative process and perceived temporal sensory perceptions, especially sweetness and liking, was considered in the manufacture of the sugar-reduced 3D printed chocolates.

1.2 Sugar-reduced foods

Government guidelines should be consulted when developing sugar-reduced foods. The Canadian Food Inspection Agency (CFIA) states that to include a "sugar-reduced" health claim, a food product must be "processed, formulated, reformulated, or otherwise modified so that it contains at least 25% less sugars, totaling at least 5 g less per reference amount of the food, than the reference amount of a similar reference food" (Canadian Food Inspection Agency, 2021). In this research, the sugar-reduced 3D printed chocolates were designed in CAD software to meet this requirement.

Increasing availability of sugar-reduced food options can be attributed to a greater understanding of the negative impacts of sugary foods, and a shift in consumer and food manufacturer attitudes towards health. The World Health Organization (WHO) indicates that excess sugars intake is associated with increased body weight, increased risk of dental caries and

poor oral health (World Health Organization, 2015). The increasing adoption of Ketogenic, Mediterranean and Paleo diets by consumers has promoted reduced consumption of carbohydrates and high sugar processed foods (Modi & Priefer, 2020). Globally, governments and organizations have identified sugar-reduction targets, and implemented strategies such as taxes on sugary beverages and advertising healthier food options, that have encouraged food manufacturers to reduce sugar in their products by reformulation (World Cancer Research Fund International, 2015). However, continued development of sugar-reduced foods is still needed to curb high global sugar consumption that exceeds recommendations.

From 2020 to 2029, global sugar consumption is projected to grow by 1.4% per year and reach 199 million tonnes by 2029 (OECD & FAO, 2020). The Heart and Stroke Foundation (HSF) of Canada and the U.S. Department of Agriculture (USDA) recommends less than 10% of calories from added sugars (Heart and Stroke Foundation of Canada, 2020; U.S. Department of Agriculture and U.S. Department of Health and Human Services, 2020), while the WHO and the Canadian Diabetes Association (Canadian Diabetes Association, 2021) recommends less than 10% of total energy intake from free sugars (World Health Organization, 2015). However, a Statistics Canada Health Report estimated that in 2015, only 49% of surveyed Canadians met the HSF and USDA recommendations for added sugars, and 33.8% met the WHO recommendation for free sugars (Liu et al., 2020). Further reduction in sugar consumption by consumers, and reduction of added sugars in processed foods by manufacturers is needed to meet recommendations.

Chocolate is a major contributor of total sugars in the Canadian diet for all age groups (Langlois et al., 2019). Considering this and the high global consumption of chocolate (outlined in section 1.3), it is important for industry sugar-reduction efforts to focus on this food product.

However, as sugar plays an important functional role by providing sweetness (taste), mouthfeel (texture) and color (appearance) in chocolate (Beckett et al., 2017), reduction or removal can affect the rheological and sensory properties of the chocolates. Thus, the taste, texture and acceptance of sugar-reduced chocolates should be evaluated.

1.3 Chocolate production, consumption and characterization

Chocolate is a widely known and commonly enjoyed food product all over the world. In 2012, the USA alone produced 1.9 million tonnes of chocolate confectionary and had sales in excess of 1.72 million tonnes (Beckett et al., 2017). In terms of per capita consumption (kg), European countries (Switzerland, Ireland, UK, Austria, Belgium, Germany, Norway, Denmark, France; 6.3-11.9kg) and Canada (6.4kg) were the world's leading chocolate consumers in 2012 (Beckett et al., 2017).

Chocolate is produced through a series of steps and is usually a combination of one or more of the following ingredients: cocoa liquor, cocoa butter, cocoa powder, and a sweetening ingredient (Beckett et al., 2017). First, the cocoa beans are fermented, dried, cleaned, and roasted, and then the shells are cracked to obtain the cocoa nib (Beckett et al., 2017). The cocoa nib is ground to produce the cocoa mass, which is mixed with sugar and then refined by grinding (Beckett et al., 2017). Cocoa butter produced by pressing the cocoa mass is added to the refined mixture, which is then conched (slowly mixed) to remove undesirable acidic and astringent flavors developed during the initial stages of cocoa bean processing, and to develop desirable flow properties and flavors (Beckett et al., 2017).

Differential scanning calorimetry (DSC) is a thermoanalytical technique that has been used to characterize fat crystal formation in non-3D-printed (Afoakwa et al., 2008; Fernandes et

al., 2013; Ostrowska-Ligęza et al., 2019; Svanberg et al., 2011; Svanberg et al., 2013) and 3D printed milk and dark chocolates (Hao et al., 2010; Lanaro et al., 2017). Fat in chocolate can exist in six polymorphic forms (I, II, III, IV, V, VI), where form I (ϑ) is the least stable, and form V (β2) is the most stable. Form V fat crystals give chocolate its characteristic glossy appearance, snap upon biting, desired rheological properties (non-Newtonian and shear thinning behavior) and prevents sugar and fat bloom (Beckett et al., 2017). The fat crystal polymorphs can be characterized by their melting ranges with DSC; form V (or β_2) fat crystals melt between 29-34℃ (van Malssen et al., 1999).

Tempering is the most important process in chocolate making to create form V fat crystals and involves heating the chocolate to a temperature that melts all fat crystal forms (~50℃), cooling down the chocolate to promote the formation of form IV and V fat crystals (~27℃) and again increasing the temperature (~30-32℃) to melt out the form IV crystals (Lanaro et al., 2019).

1.4 Sugar-reduction methods for chocolates

To reduce sugar but maintain sweetness, food manufacturers often reformulate their products with high-intensity sweeteners (e.g., aspartame, sucralose, saccharin) and sugar alcohols (e.g., isomalt, maltitol, xylitol, lactitol, sorbitol, mannitol) (Beckett et. al., 2017). Less popularly, sucrose can be substituted with natural sweeteners (e.g., lucuma, yacon, dried carrot, acacia flowers, liquorice powder, and stevia leaves and stevioside), dietary fibers (e.g., inulin, oligofructose), and syrups (rice syrup, agave syrup) (Belščak-Cvitanović et al., 2015). These alternatives are all known to enhance sweetness, but can impart undesirable flavor, aftertaste, and

texture to foods (de melo et al., 2009). Therefore, sugar reduction methods other than substitution should be examined.

The spatial distribution method is a tastant-reduction strategy where foods with different concentrations of the tastant are layered to create a heterogeneous distribution of tastants in the food matrix. Spatial distribution of sugar or salt concentration in layers enhanced sweetness perception for agar and gelatin gels, saltiness perception for bread, and liking for sausages. A 10% sugar agar/gelatin gel with a spatial distribution of sucrose in layers tasted sweeter than a homogeneous sample with 12% sucrose (Mosca et al., 2010). For two gelatin gels with 9% sugar, the gel with an inhomogeneous distribution of sugar tasted sweeter than the homogenous sample (Holm et al., 2009). A spatial distribution of salt enhanced liking in sausages (Mosca et al., 2013) and achieved a 28% salt reduction in bread without affecting saltiness intensity (Noort et al., 2010). Tastant-reduction was achieved without compromising acceptance and desired sensory perceptions, and without substitution of sucrose with alternative sweeteners.

As 3DFP technology fabricates 3D objects by adding food materials in successive layers, it can be applied to create sugar-reduced foods by the spatial distribution method. It is also more efficient than conventional chocolate molding methods and does not require expertise in chocolate making.

1.5 3D food printing (3DFP)

3DFP is the process of creating 3D structures from food materials that are deposited in a layer-by-layer fashion. Extrusion 3D printing is currently the most common type of food printing, and the process starts by designing a digital 3D model in dedicated computer-aided design (CAD) software (Sun et al., 2018). A slicing software is used to convert this model into

individual layers and to generate a G-code that is understood by the 3D printer. After a desired food material is loaded into an extruder of the 3D printer, an appropriate G-code is selected and run in the printing software. The printing process starts, and a 3D object is created by dispensing the desired food material from the extruder nozzle onto a print bed in layers, following the predetermined path of the loaded design. Each layer binds to the next as the material is deposited until the 3D structure is complete.

3DFP has promising applications from creating personalized foods for individuals with special dietary needs, including children (Derossi et al., 2018) and individuals with dysphagia (RTDS Group., 2020), to developing geometrically complex and novel food structures (Hertafeld et al., 2019; Lanaro et al., 2017; Liu, Zhang, & Yang, 2018; Yang et al., 2018) using alternative food ingredients such as insects and mushroom powder (Caporizzi et al., 2019; Keerthana et al., 2020; Severini, Azzollini et al., 2018), and modification of textural and mouth-feel properties of foods (Cohen et al., 2009). However, printing efficiency and quality of final prints can be improved to increase adoption of 3DFP in food manufacturing and other culinary settings.

In extrusion 3DFP, printing parameters (e.g., print speed, flow rate, nozzle size, nozzle height and layer height), food material properties (e.g., physicochemical and rheological), and post-processing methods determine material printability, and the accuracy and precision of printed products compared to 3D model designs (Liu et al., 2017). These parameters and properties must be optimized for 3D printing and have been investigated by several researchers. In general, food materials must have a low enough viscosity for extrusion through the nozzle, but a sufficiently high viscosity to maintain the 3D structure after printing (Godoi et al., 2016). Rheological tests have been completed to determine printability of Vegemite and Marmite, and it was revealed that among the two, Vegemite had better printability due to a lower yield point

which required less pressure to start the extrusion process (Hamilton et al., 2018). The effect of NaCl addition on fish surimi printability has also been evaluated, and it was determined that 1.5g NaCl/100g fish surimi improved printability by decreasing the viscosity and improved the stability of surimi gels post-deposition by enhancing gel strength and water holding capacity (Wang et al., 2018). The importance of optimizing print speed and flow rate together to prevent under- or over- deposition has been established through 3D printing of a mixture of pureed fruits and vegetables (carrots, pears, kiwi fruit, broccoli, avocado) (Derossi et al., 2018). Under deposition resulted in broken internal infill lines, while over-deposition resulted in cross-over of printed lines (Derossi et al., 2018). Post-processing conditions have been optimized for fiber-enriched 3D printed snacks that were printed with a mixture containing mushroom powder and wheat flour (Keerthana et al., 2020). Microwave cooking at 800W for 10 min was identified to be the optimal power level for the 3D printed snacks as it caused the least shrinkage, and the snacks retained their crispy texture and geometry (Keerthana et al., 2020).

After optimization of 3DFP materials and printing parameters, the sensory and consumer perceptions of the novel 3D printed foods should be identified. Untrained panelists liked the overall appearance of 3D printed triangular pyramids with pureed fruits and vegetables more than non-3D-printed smoothies containing the same fruits and vegetables, and liking for other sensory characteristics (color, odor, taste) was similar for both products (Derossi et al., 2018). Among two fiber-enriched snacks 3D printed with mushroom powder and wheat flour, the sensory attributes (flavor, color, taste, after-taste, aroma, appearance, texture) of the spiced snacks were liked more compared to the sweet-flavored snacks (Keerthana et al., 2020).

Future research could investigate consumer “willingness to purchase” newly developed 3D printed food formulations, and sensory perceptions in addition to acceptance (liking of

sensory characteristics). Check-all-that-apply (CATA) and rate-all-that-apply (RATA) sensory tests can identify differences between the developed 3D printed foods and their conventional counterparts, and guide 3DFP material re-formulation to maximize consumer liking. Temporal sensory perceptions (e.g., time-intensity and temporal dominance of sensations) can be generated for 3D printed foods with complex taste and texture profiles such as 3D printed cheese and chocolate to capture important perceptions such as creaminess and melting characteristics that occur and change over time.

1.6 3D chocolate printing (3DCP)

Previous research has investigated the complex 3DCP process, from design and implementation of chocolate printers (Xie et al., 2016; Zeleny & Ruzicka, 2017; Zhuoqun & Jiazhe, 2018) to optimization of 3DCP parameters (Hao et al., 2010; Lanaro et al., 2017; Mantihal et al., 2017) and development of chocolate formulations with good printability (Karyappa & Hashimoto, 2019; Mantihal, Prakash, Godoi et al., 2019). These aspects were investigated as the 3DCP process is influenced by both chocolate formulation and the print settings used (Lanaro et al., 2019). Print settings (e.g., print speed, flow rate, nozzle size and height, layer height, temperature of the chocolate and the print bed, and active cooling) affect chocolate deposition and printing efficiency, and the formulation influences chocolate printability (i.e., chocolate thermal and rheological properties). However, both can be optimized to improve chocolate printability and stability after 3D printing.

Researchers have approached 3DCP parameter optimization from different perspectives as a ‘good’ print can be defined in several ways (Lanaro et al., 2019). An example of a method to optimize print speed and flow rate is the determination of print settings that printed chocolate

lines with a diameter equal to the nozzle diameter (Hao et al., 2010). Another method is to observe the ability of deposited chocolate lines to span distances without collapsing at various print speed, flow rate, and cooling rate to optimize those parameters (Lanaro et al., 2017). For other parameters, such as layer height, optimization has been completed by visually discerning geometrical accuracy of 3D printed chocolate squares with varying layer heights compared to the design (Hao et al., 2010). Optimization of printing parameters can improve printing efficiency, as well as the accuracy, visual appeal, structural height and stability of final prints compared to digitally designed 3D models.

A group of Australian researchers optimized 3DCP through a series of experiments. A texture analyzer was used to evaluate the structural stability and snap (an important texture property for high quality chocolate) of dark chocolates 3D printed with different support structures (cross-support, parallel support and no support) (Mantihal et al., 2017). The melting properties (onset, peak and end temperatures) before and after (immediately, 30 min, 1 h and 24 h) 3D printing and the viscosity of dark chocolates with and without magnesium stearate (a flow enhancer) were determined to establish optimal 3D print settings (print speed, extrusion rate, extrusion temperature and print bed temperature) (Mantihal et al., 2017). The quality of the 3D printed chocolates with and without support structures (printed with optimal settings) compared to pre-designed 3D models was also evaluated by comparing weight and dimensions (wall thickness, height and diameter) (Mantihal et al., 2017). Finally, the effect of two additives (magnesium stearate and plant sterol powder) on chocolate 3D printability (peak melting temperature, enthalpy of melting, apparent viscosity and yield stress) (Mantihal et al., 2019) and the effect of varying internal infill percentage on texture of 3D printed chocolate was investigated (Mantihal et al., 2019).

After 3DCP optimization, the same group of Australian researchers evaluated consumer and sensory perceptions of 3DFP, and texture-modified 3D printed dark chocolates. Preference ranking of appearance and hardness was used to evaluate chocolates with different honeycomb pattern infill percentages (25, 50 and 100%), and overall preference between 3D printed chocolate (100% infill) and non-3D-printed chocolate was determined (Mantihal, Prakash, & Bhandari, 2019). Finally, a consumer survey revealed an awareness of 3D printing processes and a positive attitude towards 3DFP (Mantihal et al., 2019).

Several 3D printers currently available in the market are limited to a one extruder system and require the use of specific cartridges provided by the manufacturer. Manufacturer specific information about printing parameters and the ingredients in the cartridges are not consistently publicly available. A multi-printhead 3D system can fabricate geometrically complex 3D structures with more than one food material, and more efficiently compared to conventional casting methods such as molding. Therefore, the 3Drag Choco printer (Futura group srl, Gallarate, Italy) was used in this research. It is an open-source, dual-extruder, syringe-based 3D chocolate printer that can be used with any chocolate material chosen by the user. At the time of writing, commercially available 3D printers with chocolate printing capabilities include the Choc Creator (Choc Edge Ltd, Exeter, Devon, England, United Kingdom), Focus 3D Food Printer (byFlow, Eindhoven, The Netherlands), Procusini® (Procusini, Freising, Germany), and the Foodini (Natural Machines, Barcelona, Spain).

Although several 3D chocolate printers are commercially available, published 3DCP research is limited. Novel applications of 3DCP using different types of chocolates should be explored, and novel optimization procedures for printing parameters should be developed. Further optimization of 3DCP and multi-extruder 3DFP systems is required to increase

efficiency and customization capabilities. In the process, chocolate material properties (e.g., rheological, thermal and mechanical properties), printed object properties (e.g., morphology, microstructure and dimensions), sensory properties (e.g., appearance, taste, texture, aroma and flavor) and shelf-life of printed chocolates should be evaluated to improve the final quality of prints.

In the present thesis, a novel semi-quantitative optimization method for print settings is presented for a multi-extruder printer for two chocolate materials. A novel application of 3DFP was also demonstrated through the manufacture of sugar-reduced 3D printed chocolates. The manufactured 3D printed chocolates were characterized by their melting properties to assess quality changes (chocolate temper) due to 3D printing. Finally, the consumer temporal sensory perceptions and acceptance of the prototype sugar-reduced 3D printed chocolates were evaluated.

1.7 Research hypotheses and objectives

This research comprises two studies (Chapter 2 & Chapter 3) that aimed to demonstrate the capability of a dual-extruder 3D food printer as an innovative tool to create sugar-reduced 3D printed chocolates with desirable sensory qualities. A novel optimization process for 3D printing parameters was also presented. The specific hypotheses and objectives for each study are outlined below.

1.7.1 Hypotheses

- Sugar-reduced chocolates can be created by layering chocolates with different sugar concentrations using a dual-extruder 3D food printer (Chapter 2).

- 3D printing parameters (extruder print speed and flow rate) can be optimized to create 3D printed chocolates with mass and dimensions (height, wall thickness and diameter) as designed in computer-aided design (CAD) software (Chapter 2).
- The 3D printing process will not affect 3D printed chocolate quality (i.e., chocolate tempering) (Chapter 2).
- The temporal sensory profile of the sugar-reduced chocolates will be influenced by the layering order, and this is expected to influence overall sweetness intensity and overall liking (Chapter 3).
- 3D printed sugar-reduced chocolates with high sugar chocolate as the bottom layer will taste similarly sweet to non-sugar-reduced 3D printed chocolates due to the high density of taste buds on the tongue (Chapter 3).

1.7.2 Objectives

- Select designs for the manufacture of sugar-reduced 3D printed chocolates by the spatial distribution method. This design should be suited to study both optimization of 3D printing parameters and consumer sensory assessment of 3D printed chocolate attributes, especially sweetness (Chapter 2).
- Optimize 3D printing parameters (extruder print speed and flow rate) for a dual-extruder 3D printer by a proposed four-step, semi-quantitative approach:
    1. Quantify actual print speeds and flow rates
    2. Conduct qualitative screening trials to assess 3D printing parameters
    3. Determine accuracy and precision of 3D printed products compared to digital designs

4. Assess quality changes due to 3D printing

- Validate the amount of total % sugar in the sugar-reduced 3D printed chocolates with different layering order and determine variability in sugar concentration between multiple prints of the same design (Chapter 2).
- Investigate and compare the temporal sensory profiles, overall sweetness, and overall liking between the manufactured sugar-reduced and non-sugar-reduced 3D printed chocolates (Chapter 3).

1.8 References

Afoakwa, E. O., Paterson, A., Fowler, M., & Vieira, J. (2008). Characterization of melting properties in dark chocolates from varying particle size distribution and composition using differential scanning calorimetry. *Food Research International, 41*(7), 751-757. https://doi.org/10.1016/j.foodres.2008.05.009

Beckett, S. T., Fowler, M. S., & Ziegler, G. R. (2017). *Beckett's industrial chocolate manufacture and use* (Fifth ed.). John Wiley & Sons Ltd. https://doi.org/10.1002/9781118923597

Belščak-Cvitanović, A., Komes, D., Dujmović, M., Karlović, S., Biškić, M., Brnčić, M., & Ježek, D. (2015). Physical, bioactive and sensory quality parameters of reduced sugar chocolates formulated with natural sweeteners as sucrose alternatives. *Food Chemistry, 167*, 61-70. https://doi.org/10.1016/j.foodchem.2014.06.064

Canadian Diabetes Association. (2021). *Sugar & diabetes.* https://www.diabetes.ca/advocacy---policies/our-policy-positions/sugar---diabetes#b

Canadian Food Inspection Agency. (2021). *Specific nutrient content claim requirements: Carbohydrate and sugars claims.* https://inspection.canada.ca/food-label-requirements/labelling/industry/nutrient-content/specific-claim-requirements/eng/1389907770176/1389907817577?chap=11

Caporizzi, R., Derossi, A., & Severini, C. (2019). *Cereal-based and insect-enriched printable food*. Elsevier. https://doi.org/10.1016/b978-0-12-814564-7.00004-3

Cohen, D., Lipton, J., Cutler, M., Coulter, D., Vesco, A., & Lipson, A. (2009). Hydrocolloid printing: A novel platform for customized food production. Paper presented at the *20th Annual International Solid Freeform Fabrication Symposium, SFF 209,* 807-818. https://search.datacite.org/works/10.1080/10408398.2015.1094732

de melo, Bolini, & Efraim. (2009). Sensory profile, acceptability, and their relationship for diabetic/reduced calorie chocolates. *Food Quality and Preference, 20*(2), 138-143. https://doi.org/10.1016/j.foodqual.2008.09.001

Derossi, A., Caporizzi, R., Azzollini, D., & Severini, C. (2018). Application of 3D printing for customized food. A case on the development of a fruit-based snack for children. *Journal of Food Engineering, 220*, 65-75. https://doi.org/10.1016/j.jfoodeng.2017.05.015

Fernandes, V. A., Müller, A. J., & Sandoval, A. J. (2013). Thermal, structural and rheological characteristics of dark chocolate with different compositions. *Journal of Food Engineering, 116*(1), 97-108. https://doi.org/10.1016/j.jfoodeng.2012.12.002

Godoi, F. C., Prakash, S., & Bhandari, B. R. (2016). 3d printing technologies applied for food design: Status and prospects. *Journal of Food Engineering, 179*, 44-54. https://doi.org/10.1016/j.jfoodeng.2016.01.025

Hao, L., Mellor, S., Seaman, O., Henderson, J., Sewell, N., & Sloan, M. (2010). Material characterisation and process development for chocolate additive layer manufacturing. *Virtual and Physical Prototyping, 5*(2), 57-64. https://doi.org/10.1080/17452751003753212

Hamilton, C. A., Alici, G., & in het Panhuis, M. (2018). 3D printing vegemite and marmite: Redefining "breadboards". *Journal of Food Engineering, 220*, 83-88. https://doi.org/10.1016/j.jfoodeng.2017.01.008

Heart and Stroke Foundation of Canada. (2020). *Reduce sugar.* https://www.heartandstroke.ca/healthy-living/healthy-eating/reduce-sugar

Hertafeld, E., Zhang, C., Jin, Z., Jakub, A., Russell, K., Lakehal, Y., Andreyeva, K., Bangalore, S. N., Mezquita, J., Blutinger, J., & Lipson, H. (2019). Multi-material three-dimensional food printing with simultaneous infrared cooking. *3D Printing and Additive Manufacturing, 6*(1), 13-19. https://doi.org/10.1089/3dp.2018.0042

Holm, K., Wendin, K., & Hermansson, A. (2009). Sweetness and texture perceptions in structured gelatin gels with embedded sugar rich domains. *Food Hydrocolloids, 23*, 2388-2393.

Karyappa, R., & Hashimoto, M. (2019). *Chocolate-based ink three-dimensional printing (Ci3DP)*. Springer Science and Business Media LLC. https://doi.org/10.1038/s41598-019-50583-5

Keerthana, K., Anukiruthika, T., Moses, J. A., & Anandharamakrishnan, C. (2020). Development of fiber-enriched 3D printed snacks from alternative foods: A study on button mushroom. *Journal of Food Engineering, 287*, 110116. https://doi.org/10.1016/j.jfoodeng.2020.110116

Lanaro, M., Forrestal, D. P., Scheurer, S., Slinger, D. J., Liao, S., Powell, S. K., & Woodruff, M. A. (2017). 3D printing complex chocolate objects: Platform design, optimization and evaluation. *Journal of Food Engineering, 215*, 13-22. https://doi.org/10.1016/j.jfoodeng.2017.06.029

Lanaro, M., Desselle, M. R., & Woodruff, M. A. (2019). In Godoi F. C., Bhandari B. R., Prakash S. and Zhang M.(Eds.), *3D printing chocolate: Properties of formulations for extrusion, sintering, binding and ink jetting*. Academic Press Ltd-Elsevier Science Ltd. https://doi.org/10.1016/B978-0-12-814564-7.00006-7

Langlois, K., Garriguet, D., Gonzalez, A., Sinclair, S., & Colapinto, C. K. (2019). Change in total sugars consumption among canadian children and adults. *Health Reports, 30*(1), 10-19. https://www.ncbi.nlm.nih.gov/pubmed/30649778

Liu, S., Munasinghe, L. L., Ohinmaa, A., & Veugelers, P. J. (2020). Added, free and total sugar content and consumption of foods and beverages in canada. *Health Reports, 31*(10), 14-24. https://doi.org/10.25318/82-003-x202001000002-eng

Liu, Z., Bhandari, B., Prakash, S., & Zhang, M. (2018). Creation of internal structure of mashed potato construct by 3D printing and its textural properties. *Food Research International, 111*, 534-543. https://doi.org/10.1016/j.foodres.2018.05.075

Liu, Z., Zhang, M., Bhandari, B., & Wang, Y. (2017). 3D printing: Printing precision and application in food sector. *Trends in Food Science & Technology, 69*, 83-94. https://doi.org/10.1016/j.tifs.2017.08.018

Liu, Z., Zhang, M., & Yang, C. (2018). Dual extrusion 3D printing of mashed potatoes/strawberry juice gel. *Food Science & Technology, 96*, 589-596. https://doi.org/10.1016/j.lwt.2018.06.014

Mantihal, S., Prakash, S., & Bhandari, B. (2019). Textural modification of 3D printed dark chocolate by varying internal infill structure. *Food Research International, 121*, 648-657. https://doi.org/10.1016/j.foodres.2018.12.034

Mantihal, S., Prakash, S., & Bhandari, B. (2019). Texture-modified 3D printed dark chocolate: Sensory evaluation and consumer perception study. *Journal of Texture Studies, 50*(5), 386-399. https://doi.org/10.1111/jtxs.12472

Mantihal, S., Prakash, S., Godoi, F. C., & Bhandari, B. (2017). Optimization of chocolate 3D printing by correlating thermal and flow properties with 3D structure modeling. *Innovative Food Science & Emerging Technologies, 44*, 21-29. https://doi.org/10.1016/j.ifset.2017.09.012

Mantihal, S., Prakash, S., Godoi, F. C., & Bhandari, B. (2019). Effect of additives on thermal, rheological and tribological properties of 3D printed dark chocolate. *Food Research International, 119*, 161-169. https://doi.org/10.1016/j.foodres.2019.01.056

Modi, N., & Priefer, R. (2020). Effectiveness of mainstream diets. *Obesity Medicine, 18*, 100239. https://doi.org/10.1016/j.obmed.2020.100239

Mosca, A. C., Bult, J. H. F., & Stieger, M. (2013). Effect of spatial distribution of tastants on taste intensity, fluctuation of taste intensity and consumer preference of (semi-)solid food products. *Food Quality and Preference, 28*(1), 182-187. https://doi.org/10.1016/j.foodqual.2012.07.003

Mosca, A. C., Velde, F. v. d., Bult, J. H. F., van Boekel, Martinus A. J. S, & Stieger, M. (2010). Enhancement of sweetness intensity in gels by inhomogeneous distribution of sucrose. *Food Quality and Preference, 21*(7), 837-842. https://doi.org/10.1016/j.foodqual.2010.04.010

Noort, M. W. J., Bult, J. H. F., Stieger, M., & Hamer, R. J. (2010). Saltiness enhancement in bread by inhomogeneous spatial distribution of sodium chloride. *Journal of Cereal Science, 52*(3), 378-386. https://doi.org/10.1016/j.jcs.2010.06.018

OECD, & FAO. (2020). *OECD-FAO agricultural outlook 2020-2029*. OECD Publishing. https://doi.org/10.1787/1112c23b-en

Ostrowska-Ligęza, E., Marzec, A., Górska, A., Wirkowska-Wojdyła, M., Bryś, J., Rejch, A., & Czarkowska, K. (2019). A comparative study of thermal and textural properties of milk, white and dark chocolates. *Thermochimica Acta, 671*, 60-69. https://doi.org/10.1016/j.tca.2018.11.005

RTDS Group. (2020). *PERFORMANCE (development of personalised food using rapid manufacturing for the nutrition of elderly consumers)*. https://www.rtds-group.com/services/projects-performance/?portfolioID=100

Severini, C., Azzollini, D., Albenzio, M., & Derossi, A. (2018). On printability, quality and nutritional properties of 3D printed cereal based snacks enriched with edible insects. *Food Research International, 106*, 666-676. https://doi.org/10.1016/j.foodres.2018.01.034

Severini, C., Derossi, A., Ricci, I., Caporizzi, R., & Fiore, A. (2018). Printing a blend of fruit and vegetables. new advances on critical variables and shelf life of 3D edible objects. *Journal of Food Engineering, 220*, 89-100. https://doi.org/10.1016/j.jfoodeng.2017.08.025

Svanberg, L., Ahrné, L., Lorén, N., & Windhab, E. (2011). Effect of pre-crystallization process and solid particle addition on microstructure in chocolate model systems. *Food Research International, 44*(5), 1339-1350. https://doi.org/10.1016/j.foodres.2011.01.018

Svanberg, L., Ahrné, L., Lorén, N., & Windhab, E. (2013). Impact of pre-crystallization process on structure and product properties in dark chocolate. *Journal of Food Engineering, 114*(1), 90-98. https://doi.org/10.1016/j.jfoodeng.2012.06.016

Sun, J., Zhou, W., Yan, L., Huang, D., & Lin, L. (2018). Extrusion-based food printing for digitalized food design and nutrition control. *Journal of Food Engineering, 220*, 1-11. https://doi.org/10.1016/j.jfoodeng.2017.02.028

U.S. Department of Agriculture and U.S. Department of Health and Human Services. (2020). *Dietary guidelines for americans, 2020-2025* (9th ed.)

van Malssen, K., van Langevelde, A., Peschar, R., & Schenk, H. (1999). Phase behavior and extended phase scheme of static cocoa butter investigated with real-time X-ray powder diffraction. *Journal of the American Oil Chemists' Society, 76*(6), 669-676. https://doi.org/10.1007/s11746-999-0158-4

Wang, L., Zhang, M., Bhandari, B., & Yang, C. (2018). Investigation on fish surimi gel as promising food material for 3D printing. *Journal of Food Engineering, 220*, 101-108. https://doi.org/10.1016/j.jfoodeng.2017.02.029

World Cancer Research Fund International. (2015). *Curbing global sugar consumption: Effective food policy actions to help promote healthy diets & tackle obesity.*

World Health Organization. (2015). *Guideline: Sugars intake for adults and children.*

Xie, Y., Tan, Y., Ma, G., Zhang, J., & Zhang, F. (2016). *Design and implementation of chocolate 3D printer*. Destech Publications, Inc.

Yang, F., Zhang, M., Bhandari, B., & Liu, Y. (2018). Investigation on lemon juice gel as food material for 3D printing and optimization of printing parameters. *Food Science & Technology, 87*, 67-76. https://doi.org/10.1016/j.lwt.2017.08.054

Zeleny, P., & Ruzicka, V. (2017). The design of the 3d printer for use in gastronomy. *MM Science Journal, 2017*(1), 1744-1747. https://doi.org/10.17973/MMSJ.2017_02_2016187

Zhuoqun, L., & Jiazhe, Y. (2018). PID control of chocolate 3D printer heating system. Paper presented at the 298-301.

Chapter 2 - Optimization of a Dual-Extrusion 3D Food Printer for the Manufacturing of Sugar-Reduced Chocolates

2.1 Introduction

3D printing technology (also known as "additive manufacturing") was developed in the 1980s, and has since been widely researched and applied in the engineering and manufacturing sectors using plastics, ceramics, and metals as printing materials (Noorani, 2017). 3D printing is a multi-step process which involves both a hardware component (i.e., a printer capable of three-dimensional translation of a printing head or surface) and associated software which allows the user to create and print intricate virtual designs. The first step involves the generation of a 3D solid model using computer-aided-design (CAD) software. This digital model is then virtually sectioned using "slicer" software to create patterns for successive layering of materials. Finally, this digital rendering is converted to a machine ready code (G-code) which is used directly by the 3D printer control system to generate the final physical product.

3D food printing (3DFP) is an emerging technology that fabricates digitally designed 3D objects by depositing or adding food materials in successive layers (Sun et al., 2015). Edible food materials have only recently been used for 3D printing, with 93% of the current published research being from 2015 onwards (Baiano, 2020). Of the various 3D printing technologies, extrusion-based 3DFP using liquid or paste materials has been the most studied method in the food science and engineering literature. A wide variety of food types have been assessed including cheese (Kern et al., 2018; Le Tohic et al., 2018), fruit and vegetable puree (Derossi et al., 2018; Severini, Derossi et al., 2018) mashed potatoes (Liu et al., 2018; Yang et al., 2018) cookie dough, almond paste, pastry dough, sesame paste, chicken paste and shrimp paste

(Hertafeld et al., 2019). 3DFP has been used to deliver personalized nutrition (Derossi et al., 2018; RTDS Group., 2020; Severini et al., 2018) and to modify texture and mouthfeel of food products (Cohen et al., 2009). Researchers have also utilized novel materials in 3DFP, such as insects that may not otherwise be accepted by consumers have also been 3D printed (Caporizzi et al., 2019; Severini et al., 2018).

Another topic of interest in 3DFP research is the development of methodologies to determine optimal printing parameters. These guidelines are important to systematically and efficiently determine the best print settings for a given combination of food type and 3D food printer. 3D printing parameters have often been optimized by assessing quality changes due to 3D printing. The geometrical accuracy (shape and dimension), morphology and microstructure of 3D printed fruit-based snacks (Derossi et al., 2018; Severini et al., 2018), surimi gels (Wang et al., 2018), and lemon juice gels (Yang et al., 2018) was evaluated to optimize extruder print speed, extruder flow rate, nozzle diameter and nozzle height. 3D printing processing temperature has also been optimized by evaluating textural properties, thermo-rheological properties and shear behavior of processed cheese (Kern et al., 2018; Le Tohic et al., 2018). The textural, structural and dimensional properties of 3D printed foods have also been evaluated to optimize infill level, infill pattern and number of shell perimeters (Liu et al., 2018) For a dual-extruder 3D printer, extruder offset can be optimized to prevent overlapping of printed materials or gaps between printed lines, and retraction values can be optimized to prevent oozing of materials when one extruder is inactive (Liu et al., 2018).

The selected food material and its properties are also important factors that need to be considered for the implementation of 3DFP (Godoi et al., 2019). Chocolate was one of the first materials used in 3DFP because it is natively printable and suitable for melt extrusion 3DFP. Its

viscoelastic properties allow it to be easily deposited in a molten state and solidify quickly during post-deposition (Voon et al., 2019). Chocolate, however, can be sensitive to thermal processes (such as those found in 3DFP) which may alter its desirable sensory and quality characteristics. Tempering is an important process in traditional chocolate manufacturing, and involves heating and cooling the chocolate to specified temperatures and time frames. Properly tempered chocolates are shelf-stable (resistant to sugar and fat bloom), have a glossy appearance, smooth texture, and characteristic "snap" when consumed (Beckett et al., 2017). Well-tempered chocolates contain homogeneously dispersed fat crystals in the stable form V (or β2), corresponding to a melting temperature between 29-34℃ (Mantell et al., 2015; van Malssen et al., 1999).

There have been numerous studies in recent years focused specifically on chocolate 3DFP. The creation of intricate chocolate structures (Hertafeld et al., 2019; Karyappa & Hashimoto, 2019), chocolate texture modification by 3DFP (Mantihal et al., 2019) and administration of pain relief and fever reduction drugs using 3D printed chocolate as an excipient (Karavasili et al., 2020) has been explored. Optimization of 3D chocolate printing has also been investigated through thermal and rheological characterization (Mantihal et al., 2017; Mantihal et al., 2019; Rando & Ramaioli, 2021), the addition of additives to improve chocolate printability (Mantihal et al., 2019) and deposition experiments focused on specific printing parameters (Hao et al., 2010; Hertafeld et al., 2019; Lanaro et al., 2017).

In addition to 3DFP, another area of research which is receiving considerable attention over the past decade is the development of sugar-reduced foods. This topic has become increasingly important due to the global rise in health risks such as diabetes and obesity that are associated with overconsumption, particularly due to high sugar content in typical diets. Global

consumption of sugars exceeds the recommendation of 10% of total energy intake from sugars by the World Health Organization (World Health Organization, 2015). In Canada, food products in the category "sugars, syrups and confectionary" were found to be one of the top sources of total sugars intake for all age groups (Langlois et al., 2019). Since chocolate belongs to this group, it is not surprising that there has been some effort to reduce sugar content in these food products. Aside from gradual reduction or replacement with alternative sweeteners, a successful sugar reduction approach has included the arrangement of different concentrations of sucrose within layers of foods. The potential advantage of this approach is that layered products with an overall lower sugar concentration may be perceived to be as sweet as a conventional, non-layered product with a higher overall sugar concentration. For example, sweetness enhancement was achieved in gels that contained different sugar concentrations in each layer (Holm et al., 2009; Mosca et al., 2010; Mosca et al., 2012). Similar results were also described for other tastants, including salt in bread (Noort et al., 2010; Noort et al., 2012) and cream-based snacks (Emorine et al., 2015), and fat in gels and sausages (Mosca et al., 2012; Mosca et al., 2013).

To reduce sugar levels in chocolate, 3DFP technology with multiple extruders could be used to arrange layers of chocolate with different sugar concentrations. To the authors' knowledge, there has been no studies which demonstrate the use of 3DFP techniques in strategically reducing sugar levels in chocolate confectionaries. This method would be particularly useful for product development and testing, and more efficient in creating chocolate layers compared to conventional casting methods using molds. Further investigation into multiple extruder 3DFP systems would also provide the freedom to create more novel and complex 3D structures (Hertafeld et al., 2019; Liu et al., 2018). Current 3DFP research often

used single extruder systems that are incapable of producing multi-material prints without requiring a changeover of material in the extrusion barrel.

This study aims to demonstrate the use of a two-extruder 3D printing system as an innovative tool to manufacture sugar-reduced chocolates. The design of a dual-extruder system using open-sourced components is presented, followed by the selection and creation process for sugar-reduced designs. A novel, four-step optimization procedure was demonstrated to determine optimal print settings (print speed and extruder flow rate), and to validate product accuracy, precision and quality (i.e., to ensure that chocolate tempering is not affected by 3D printing). In addition to demonstrating both the dual-extruder manufacturing process and the novel optimization procedure, the cross-sectional dimensions and shape of extruded chocolate lines were also examined to better understand chocolate layering effects. The goal is to create a platform for manufacturing accurate and repeatable sugar reduced chocolate products for further development and sensory testing (presented in chapter 3).

2.2 Materials and Methods

2.2.1 Chocolate material and preparation for 3D printing

Two types of chocolates, Swiss dark chocolate bars with 47% cocoa (51.5% high sugar concentration; denoted as "H") and 72% cocoa (26.7% low sugar concentration; denoted as "L"), were locally purchased for use in this study (Western Family™, Overwaitea Food Group, Vancouver, BC). The nutrition facts information (which provides the overall sugar content for each chocolate type) can be found in the appendix **(Table A1).** To ensure that the thermal history remained uniform across all tests, L and H chocolates were tempered prior to placement in the 3D food printer using the seeding method. "Seed chocolate" is added in this method to promote the formation of form V fat crystals that provide chocolate with desirable rheological and sensory qualities (e.g., a glossy appearance, smooth texture, and characteristic "snap" upon biting). Chocolate (45 g) was slowly heated to 45-55℃ using a double boiler with constant gentle stirring. Chocolates were taken off the heat when a temperature of 47℃ was reached. Seed chocolate (5 g) was added to the melted chocolate whilst stirring, and the mixture was cooled to a working temperature of 28-32℃. At this point, the chocolate was transferred to a 60 mL syringe that was placed in the 3D food printer extruder barrel for product manufacturing.

2.2.2 Dual-extruder 3D Printer and cooling system

The 3Drag 3D Printer with chocolate extruder (Open Electronics, Futura Group srl) is an open source, fused deposition modeling 3D printer that was modified by replacing the plastic filament extruder with a screw-based extruder capable of printing soft foods (Landoni, 2014). Using this flexible model and platform, the final dual-extruder system used for experiments was manually assembled based on available components **(Figure 2.1)**. Unlike many commercially

available 3D food printers, this system can create prints made from two materials. Each extruder barrel and nozzle jacket is made from heat conductive aluminum, and wrapped with a Kapton heater pad to heat the material inside the syringe. Each extruder barrel supported a 60 mL Luer Lock syringe attached with a 1.2 mm diameter (0.9 mm internal diameter) nozzle. In order to create an accurate and self-standing 3D structure, each layer that is printed must be cooled before the next layer is deposited. A Peltier cooling system with fans and a water pump was installed for this purpose. A PC laptop was connected to the printer's control board to enable conversion and transfer of 3D printing files to the printer.

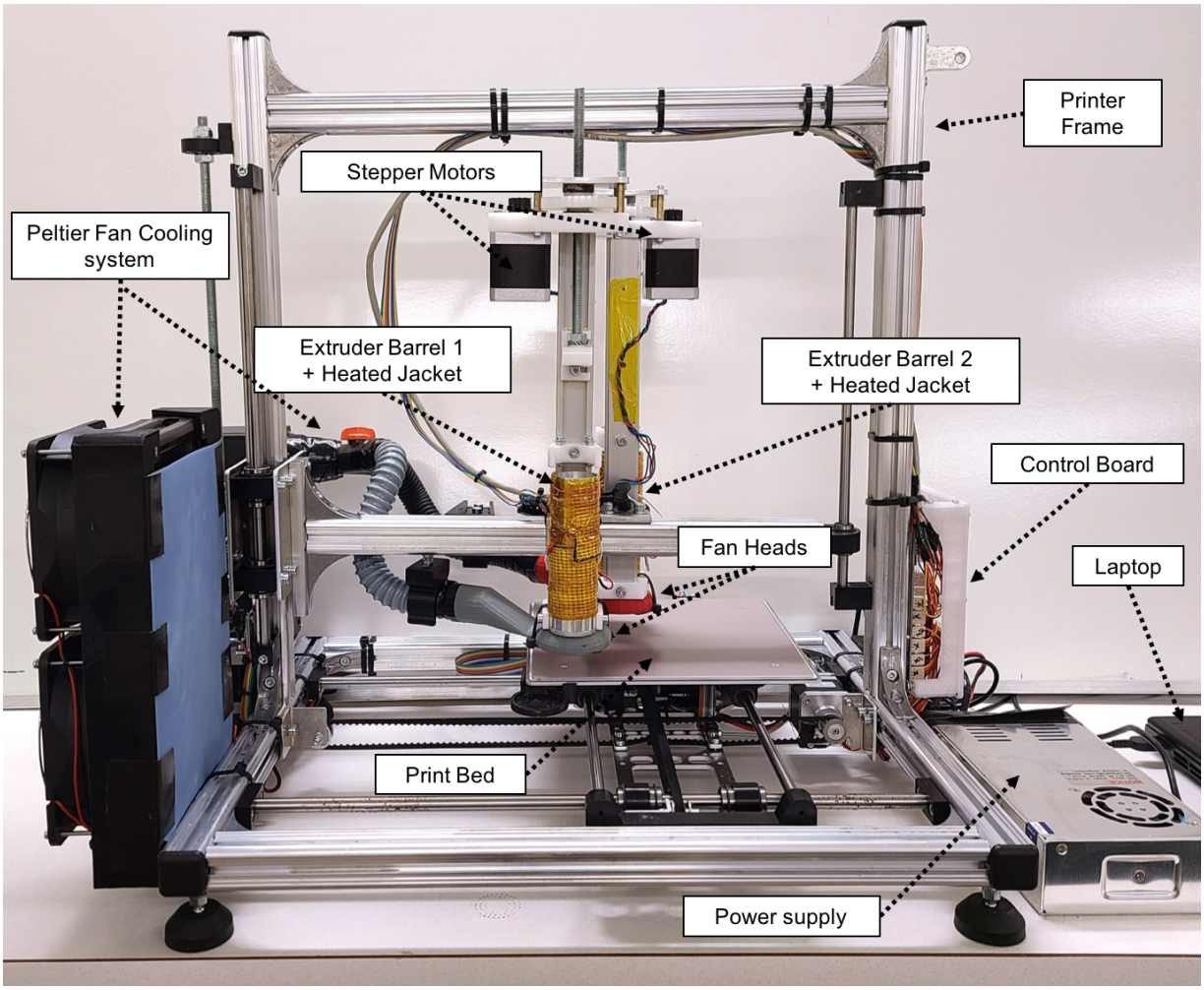

Figure 2.1 Dual-extruder 3Drag 3D Chocolate printer with labelled parts.

2.2.3 Selection and creation of chocolate designs

A three-layered hollow cylinder with a diameter of 28.00 mm, height of 10.80 mm and wall thickness of 4.37 mm was chosen as the final design for this study **(Figure 2.2a).** It was selected from preliminary printing trials of various basic, complex and novel chocolate shapes. From eight possible layering combinations of high (H) and low (L) sugar chocolate, the following six were used for experiments: HHH, HLH, HHL, LHL, HLL, and LLL **(Figure 2.3)**. The chocolates were named by the order in which the three layers were printed from the bottom to the top; for example, HLL had H chocolate at the bottom layer, L chocolate in the middle layer, and L chocolate at the top layer. Sample HHH was considered the non-sugar-reduced control, while LLL was considered the low sugar control. Since the objective was to manufacture sugar-reduced chocolates, the other four designs were selected to create two levels of sugar reduction. Samples with 2 H chocolate layers (HLH and HHL) would have a similar % sugar to each other, but less compared to HHH. Similarly, samples with 2 L chocolate layers (LHL and HLL) would have a similar % sugar to each other, but less compared to HLH and HHL, as well as HHH. The final 3D designs were created and downloaded in ".stl" format using Tinkercad online CAD software (AutoDesk Inc.) **(Figure 2.2a)**. The designs were then "sliced" (converted into layers) and translated into G-code (code that is understood by the 3D printer) by Slic3r software (RepRap) **(Figure 2.2b)**. The G-code was then imported into RepetierHost software (Hot-World GmbH & Co. KG, Germany) to 3D print chocolates **(Figure 2.2c)**.

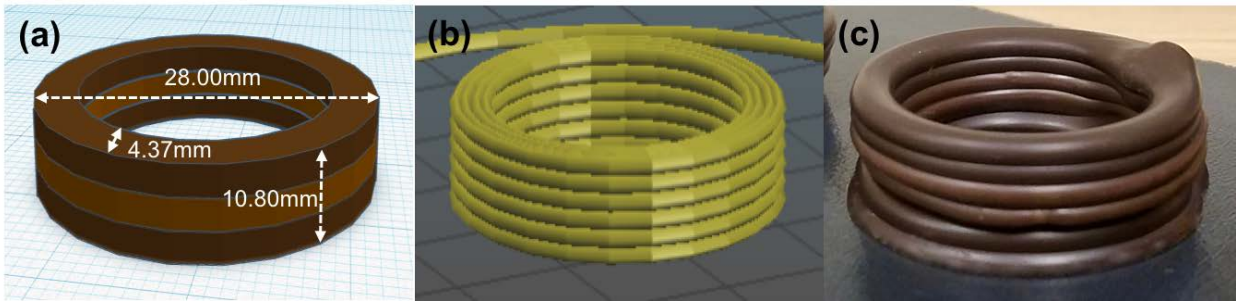

Figure 2.2 The three-layered hollow cylinder (LHL) (a) 3D model designed in CAD software (b) "sliced" 3D model (converted into layers to be 3D printed) (c) 3D printed chocolate.

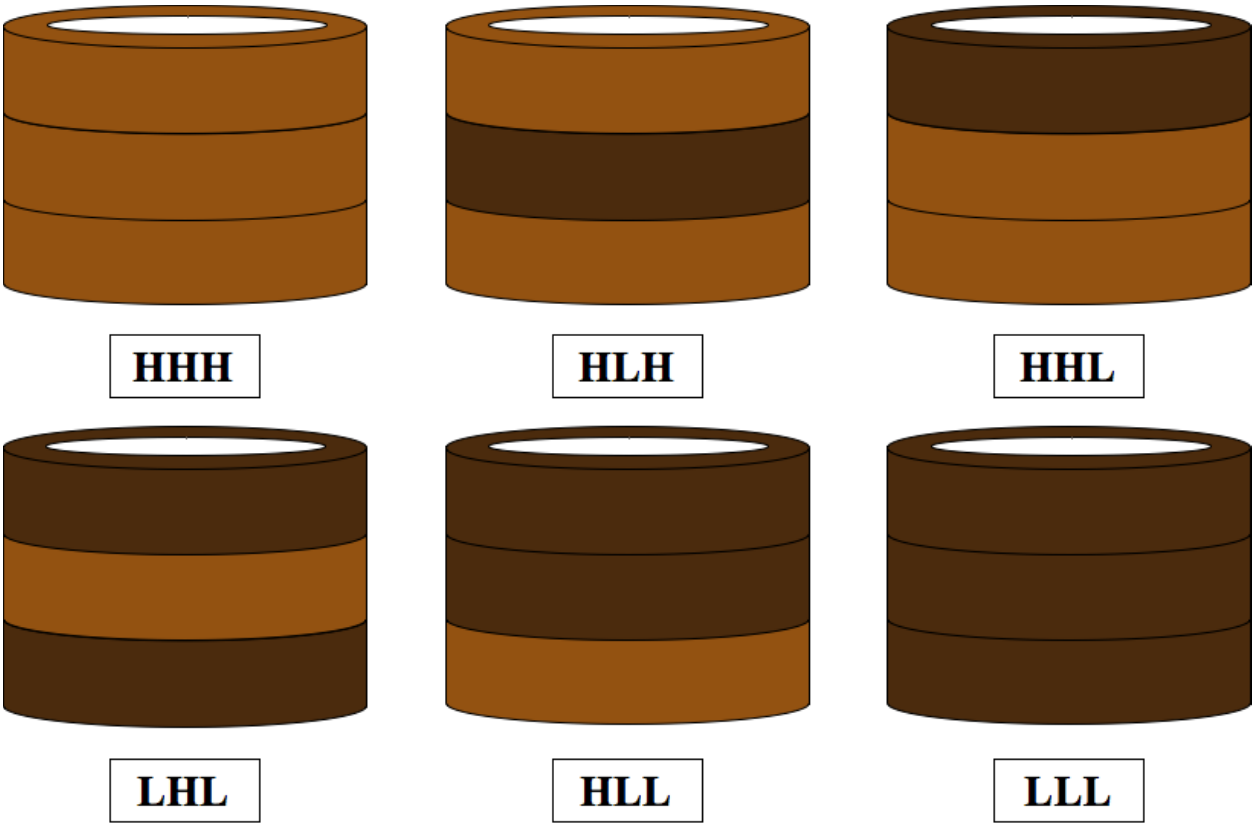

Figure 2.3 The six layering combinations for H and L chocolates used for experiments.

2.2.4 Optimization procedure

A novel, four-step methodology was developed to optimize and validate printer settings for the layered chocolate design used in this study. These steps include both quantitative and qualitative assessments, as shown in the flowchart in **Figure 2.4**. This methodology brings together several previous 3DFP optimization concepts that have been proposed (Azam et al., 2018; Hao et al., 2010; Lanaro et al., 2017; Mantihal et al., 2017; Rando & Ramaioli, 2021; Wang et al., 2018; Yang et al., 2018), and provides an efficient way to optimize print settings for a variety of 3D printed foods. As part of this procedure, the screening trials provide a rapid method to eliminate combinations of printing parameters such as print speed and extruder flow rate that do not produce acceptable prints. This step can be expanded to include other parameters such as nozzle diameter and height, printing temperatures and rheological properties. In this study, both nozzle diameter and height, as well as printing temperature was fixed.

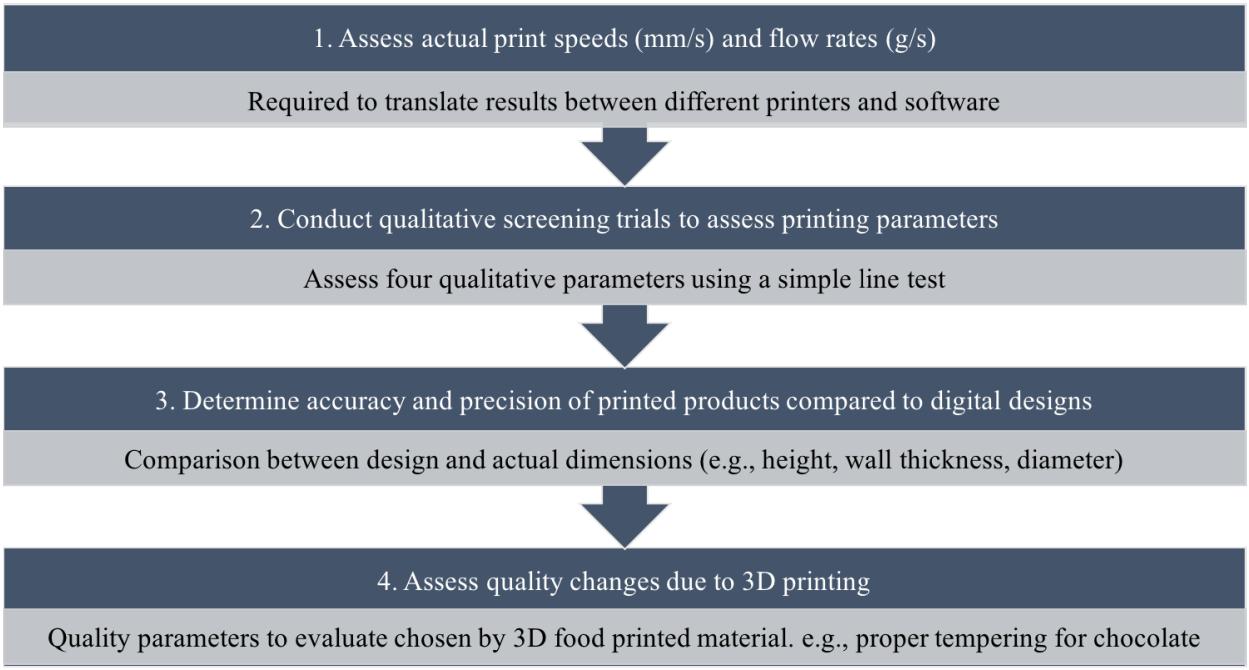

Figure 2.4 The proposed four-step, semi-quantitative approach for optimizing print settings for a dual-extruder 3D food printer.

2.2.4.1 Step 1: Assessment of actual print speeds and flow rates

For the first step in **Figure 2.4**, the actual print speeds and extruder flow rates were measured for a range of possible print settings. The purpose of this exercise was to convert print speed (PS) and flow rate (FR) settings in the control software (commonly presented in 3D printers as non-dimensional values) to actual speeds in mm/s and volumetric flow rates in mm^3/s. This conversion allows users to transfer print settings between different 3D food printers.

Preliminary printing trials were conducted using the full range of PS settings (25-300) and FR settings (50-150) as selected in the control software (RepetierHost) to narrow down a possible range for further screening. Based on these results, PS settings of 35, 65 and 95, and FR settings of 70, 100 and 130 were selected for further evaluation. Videos of four lines (100 mm x 1 mm x 1mm) printed in the shape of a square **(Figure 2.5)** at the selected nine print settings **(Table 2.1)** were recorded using a Logitech C920 Pro HD WebCam as they were being 3D printed. For each print setting combination, the time (in seconds) that was required to print each of the four lines was determined from the video, and was used to calculate the average actual print speed (mm/s). The mass of each line (printed on a transferable sheet) was measured with an electronic weighing scale. The mass of each line and the density of each chocolate **(Table A2)** was used to calculate the average actual flow rate (in mm^3/s). This experiment was completed for both H and L chocolates and the two extruders.

Table 2.1 The print speed and flow rate combinations used to assess print quality and accuracy.

Software Print Speed Setting (no units)	Software Flow Rate setting (no units)
35	70
35	100
35	130
65	70
65	100
65	130
95	70
95	100
95	130

2.2.4.2 Step 2: Qualitative screening trials to assess 3D printed chocolate printing parameters

For the second step in **Figure 2.4**, a simple line test was used as a screening tool to narrow down the nine print settings to the ones that were most optimal for L and H chocolate. Four lines (100mm x 1mm x 1mm) in the shape of a square were printed using each setting for both types of chocolate **(Figure 2.5).** This was repeated twice for each print setting (8 lines total). Images were taken for each replicate using a Logitech C920 Pro HD WebCam, and each line was weighed. The images were used to assess each print setting on four qualitative criteria: non-linearity, localized bulging, localized thinning and breakage **(Table 2.2)** to identify acceptable and unacceptable prints. Acceptable prints were ones that did not violate any of the four criteria.

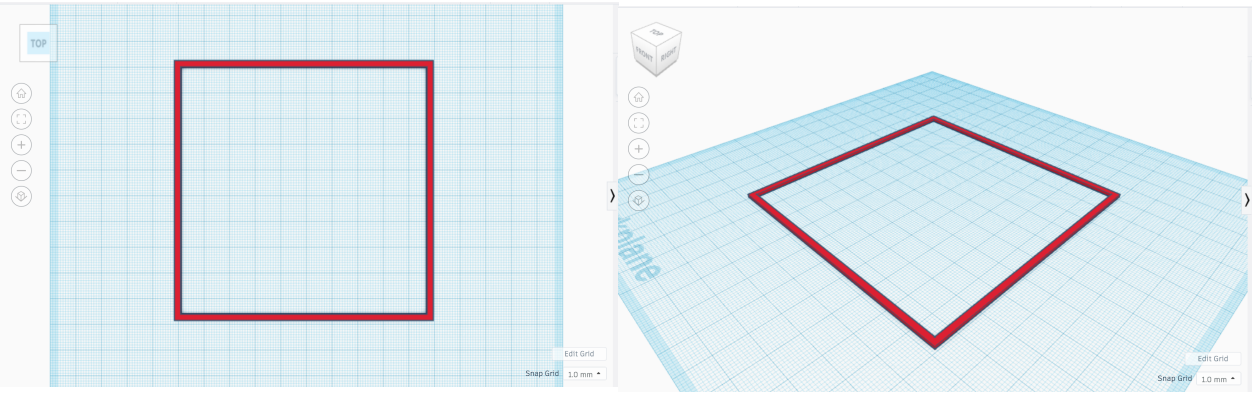

Figure 2.5 The TinkerCad square 3D design of four lines (100mm x 1mm x 1mm) that was used to determine the optimal print speed and flow rate settings.

Table 2.2 The criteria used for qualitative screening of lines printed at various print speed and flow rate settings.

Criteria number	Criteria	Description
1	Non-linearity	Sections in the line that are not straight
2	Localized bulging	Sections in the line with larger widths
3	Localized thinning	Sections in the line with reduced widths
4	Breakage	Discontinuities in the line

2.2.4.3 Step 3: Accuracy and precision of 3D printed chocolates compared to digital designs

2.2.4.3.1 Evaluation of 3D printed chocolate mass and dimensions

Once the best PS and FR settings were identified using the qualitative screening criteria, these printer settings were then used to evaluate print accuracy and repeatability for the six layered chocolate combinations outlined in Section 2.2.3. The mass (g), height (mm), wall thickness (mm), and diameter (mm) were measured for three replicates using a digital caliper at three equidistant points for each chocolate, and the % error in the mean of each parameter from the design was calculated. Gloves were worn to prevent the chocolate from melting during handling. Design mass was determined by the 3D model theoretical volume multiplied by the density of the chocolate **(Table A2)**. Images of each printed replicate were taken using the Logitech C920 Pro HD WebCam to visually compare the two final print settings. The print setting that produced visually appealing designs with a small % error in measured parameter values from the design was chosen as the final optimal print setting for both L and H chocolates.

To evaluate the repeatability of prints, eight replicates of each of the six chocolate designs **(Figure 2.3)** were printed using the final optimal print settings. Each of the three layers in the design were printed separately to evaluate the precision of each layer. For each replicate, the mass (g) was recorded, and height (mm), wall thickness (mm), and diameter (mm) were measured at three equidistant points for each layer using a digital caliper. Gloves were worn to prevent the chocolate from melting during handling. Averages were calculated for each parameter and the % error of each parameter from the design was calculated. A two-way ANOVA with layer number and chocolate type (H or L) as independent variables was performed using RStudio (Version 1.1.463, R Studio Inc., 2009-2018) for each parameter.

2.2.4.3.2 Evaluation of total sugar concentration

To validate that sugar-reduced chocolates could be created using a dual-extruder 3D printer, the total % sugar (g sugar/g chocolate) was calculated for each sample. This was also important because the 3D printed chocolates were planned for use in a subsequent sensory study. **Equations (1)** and **(2)** were used to determine the theoretical total % sugar based on proportional weights and sugar amounts as indicated on the nutritional facts table **(Table A1)**. The actual total % sugar was calculated using the same equations, but using measured mass (g) of chocolate layers.

$$Mass\ of\ sugar\ in\ layer\ (g) = mass\ of\ layer\ (g\ chocolate) \times concentration\ of\ sugar\ in\ layer\ \left(\frac{g\ sugar}{g\ chocolate}\right) \quad \textbf{(1)}$$

$$Total\ \%\ sugar = \frac{Total\ mass\ of\ sugar\ in\ each\ layer\ (g\ sugar)}{Total\ weight\ of\ chocolate\ (g\ chocolate)} \times 100 \quad \textbf{(2)}$$

2.2.4.4 Step 4: Assessment of chocolate quality changes due to 3D printing

Differential scanning calorimetry (DSC) is a thermoanalytical technique that has been used to characterize melting properties and identify the resulting fat crystal formation in chocolates (Afoakwa et al., 2008; Fernandes et al., 2013; Ostrowska-Ligęza et al., 2019; Svanberg et al., 2011; Svanberg et al., 2013). DSC was used to evaluate the crystalline phase of fat in the high and low sugar chocolates prior to printing (L1, H1) and after 3D printing (L2, H2). Approximately 5mg of chocolate was placed into the sample holder of a DSC Q100 V9.8 Build 296 (TA Instruments), and melting curves were obtained from 25-40℃ at 5℃ intervals. Three samples for each chocolate (L1, H1, L2, H2) were analysed by DSC to obtain the melting curves. Onset temperature (T_o), peak temperature (T_{peak}), end temperature (T_e) and enthalpy of melting

(ΔH_{melt}) were computed by integrating the DSC curves using TA Universal Analysis software (TA Instruments), and the melting index (T_{index}) was calculated as (T_e-T_o) (Afoakwa et al., 2008). The average of the three replicates was calculated for each melting property. The chocolate polymorphic form was categorized by comparing the peak temperature to previously reported melting ranges for the different fat crystal polymorphic forms (Marangoni & McGauley, 2003).

2.2.5 Determination of chocolate density

Density was determined for both L and H chocolates (values are shown in **Table A2**) using a gas pycnometer (Micromeritics AccuPyc II 1340 - FoamPyc V1.05, Folio Instruments Inc, Kitchener, Ontario, Canada). Approximately 2.8g of each sample was placed into the cylindrical sample holder of the pycnometer for analysis.

2.2.6 Characterization of 3D printed chocolate cross-sectional shape and dimensions

A scalpel was used to section lines (100mm x 1 mm x 1mm) that were printed using the two best printer settings (as determined by the qualitative screening methodology in Section 2.2.4.2). Cross-section images of the printed lines were taken by an optical microscope (SteREO Discovery.V8, ZEISS Microscopy) with color microscope camera (Axiocam ERc 5s, ZEISS Microscopy) at 2.5x magnification to evaluate the shape of the printed chocolate bead. Cross-sectional dimensions were measured using ZEISS ZEN 2.3 Lite software. Several cross-sections were sampled from various chocolate line tests. These images were used to better understand characteristics of how the printed lines were deposited on the printer surface.

2.3 Results and Discussion

2.3.1 Optimal 3D print settings for a dual-extruder 3D food printer

Qualitative and quantitative assessment revealed that the optimal print setting that could be used for both H and L chocolates was a print speed setting of 35 (2.92-2.94 mm/s) and flow rate setting of 100 (6.11-6.55 m^3/s), denoted as PS 35, FR 100. This combination of printing parameters produced visually appealing and accurate 3D chocolate prints with similar mass and dimensions to digital designs.

A dual-extruder system with one control board can be challenging to use if the optimal print settings are different for each material in the two extruders. This would require the user to change the settings in the RepetierHost software (Hot-World GmbH & Co. KG, Germany) during printing each time that a new layer of a different material is being printed. As there is a delay of up to 30 seconds between inputting new settings into the software and the printer following the command, the printing would not be seamless. Therefore, the determined optimal print setting eliminated the need for a switchover of settings for each extruder during 3D printing.

2.3.1.1 Actual print speeds and flow rates

Actual print speeds (mm/s) and volumetric flow rates (mm^3/s) were quantified for each print setting combination and extruder. In general, this step is important if one wants to transfer settings from one 3D printer to another, and the results can be used to check for interaction effects between print speed and flow rate. The actual volumetric flow rates were calculated based on a mean density of 1.3244 g/cm^3 for the high sugar concentration chocolate (H), and a mean density of 1.2478 g/cm^3 for the low sugar concentration (L) chocolate **(see Table A2)**.

Actual print speeds for extruder 1 (L chocolate) and 2 (H chocolate) are shown in **Tables 2.3 and 2.5** respectively, while volumetric flow rates are shown in **Tables 2.4 and 2.6**. Both extruders had similar average print speeds and volumetric flow rates. As the PS settings are increased, the actual print speeds (mm/s) demonstrate a fairly linear increase and are unaffected by flow rate setting. However, as FR settings are increased, the volumetric flow rates (mm^3/s) generally increase, but are more inconsistent (non-linear). The volumetric flow rates are also seen to be affected by print speed setting, which indicates interaction effects. This step highlights the necessity to quantify actual rates for all print setting combinations investigated.

Table 2.3 Average print speed (mm/s) ± standard deviation for extruder 1 (L chocolate) at various print setting combinations.

Print Setting	FR 70*	FR 100*	FR 130*	Average print speed for all flow rate settings**
PS 35	2.94 ± 0.07	2.92 ± 0.04	2.92 ± 0.04	2.93 ± 0.05
PS 65	5.56 ± 0.00	5.63 ± 0.30	5.56 ± 0.00	5.59 ± 0.16
PS 95	8.33 ± 0.00	8.00 ± 0.37	8.33 ± 0.00	8.23 ± 0.25

*Values in the column represent four replicates.

**Values in the column represent twelve replicates.

Table 2.4 Average extruder volumetric flow rate (mm^3/s) ± standard deviation for extruder 1 (L chocolate) at various print setting combinations.

Print Setting	PS 35*	PS 65*	PS 95*	Average volumetric flow rate for all print speed settings**
FR 70	4.78 ± 0.33	9.68 ± 0.43	14.19 ± 1.00	9.55 ± 4.06
FR 100	6.55 ± 0.52	13.35 ± 2.18	19.91 ± 0.92	13.27 ± 5.83
FR 130	9.02 ± 1.26	12.47 ± 0.36	24.71 ± 1.64	15.40 ± 7.12

*Values in the column represent four replicates.

**Values in the column represent twelve replicates.

Table 2.5 Average print speed (mm/s) ± standard deviation for extruder 2 (H chocolate) at various print setting combinations.

Print Setting	FR 70*	FR 100*	FR 130*	Average print speed for all flow rate settings**
PS 35	2.94 ± 0.00	2.94 ± 0.00	2.92 ± 0.08	2.93 ± 0.05
PS 65	5.56 ± 0.25	5.56 ± 0.25	5.48 ± 0.15	5.59 ± 0.16
PS 95	8.33 ± 1.09	8.16 ± 0.99	7.69 ± 0.49	8.23 ± 0.25

*Values in the column represent four replicates.

**Values in the column represent twelve replicates.

Table 2.6 Average extruder volumetric flow rate (mm^3/s) ± standard deviation for extruder 2 (H chocolate) at various print setting combinations.

Print Setting	PS 35*	PS 65*	PS 95*	Average volumetric flow rate for all print speed settings**
FR 70	3.55 ± 0.65	8.19 ± 1.30	12.16 ± 1.83	7.97 ± 3.87
FR 100	6.11 ± 0.59	12.31 ± 1.59	15.74 ± 2.05	11.39 ± 4.39
FR 130	8.49 ± 0.77	14.19 ± 1.58	16.54 ± 3.5	13.07 ± 4.08

*Values in the column represent four replicates.

**Values in the column represent twelve replicates.

2.3.1.2 Qualitative screening of printing parameters

A qualitative assessment of the various print setting combinations was performed to determine acceptable and unacceptable printing parameters based on the evaluated criteria in Table 2.2. Out of the nine combinations of print settings tested for each chocolate type (H and L), both acceptable and unacceptable printed lines were observed **(Table 2.7)**. For L chocolate, 6 out of 9 settings produced acceptable prints based on the exclusion criteria, while for H chocolate, only 4 out of 9 were deemed acceptable. Only two of the print setting combinations produced acceptable prints for both chocolate types (PS 35, FR 100 and PS 65, FR 70). The differences in the resulting acceptable versus unacceptable print settings between the H and L

chocolate groupings could be explained by possible differences in rheological properties between the two chocolate types. From **Table 2.7**, it can also be seen that various combinations of print settings produced unacceptable prints due to line non-linearities (denoted as 1 in **table 2.7**) and/or breakages (denoted as 4 in **table 2.7**). For both chocolates used in this study, localized bulging or thinning effects were not observed for the print settings considered.

Table 2.7 Matrix showing acceptable (green) and unacceptable (red) prints for each chocolate and print setting combination based on visual observation of qualitative criteria.

	L chocolate			H chocolate		
	PS 35	**PS 65**	**PS 95**	**PS 35**	**PS 65**	**PS 95**
FR 70	**1**	✓			✓	**1,4**
FR 100	✓	**1**		✓	**1**	**1**
FR 130	**1**				**1**	**1**

*** Numbers indicate violated criteria (1: Non-linearity, 2: Localized bulging, 3: Localized thinning, 4: Breakage)**

"✓" denotes settings that produced acceptable prints common to both chocolate types.

Figure 2.6 shows representative images of acceptable and unacceptable line prints for both H and L chocolates. Acceptable prints had linear, continuous lines with no localized bulging or thinning as shown in **Figure 2.6a-c**. When comparing Figure 2.6b to Figure 2.6c (same PS but different FR settings), the latter setting produced thicker lines (due to a higher flow rate setting), but the lines themselves are still continuous and linear in nature. As such, the print in Figure 2.6c is still considered to be an acceptable print. This is not the case when one compares the prints in Figures 2.6a to Figure 2.6d (again, same PS but different FR settings), or the prints in Figures

2.6a to Figure 2.6e (same FR but different PS settings). In the former case, the change in flow rate results in non-linear features (waviness) to occur in the printed lines as shown in Figure 2.6d. For the latter case, the increased print speed setting causes both non-linear features and line breakage as shown in Figure 2.6e. As a result, the printing parameter combinations used in both Figures 2.6d and 2.6e were considered unacceptable. These examples highlight the importance of balancing print speed and flow rate settings to produce an acceptable and continuous print.

From this screening exercise, the two common print settings that were found acceptable for both types of chocolates (PS 35, FR 100 and PS 65, FR 70) were subsequently used in the next step of the optimization process (i.e., step 3 in **Figure 2.4)**. Of course, a greater resolution could have been achieved in this screening assessment by testing combinations of settings at smaller increments (e.g., 35, 40, 45 … 95 versus 35, 65, 95). This would have more precisely determined the relationship between print speed and flow rate for each chocolate type. However, with increased resolution comes an increase in the number of screening tests required. Even with the relatively coarse test matrix used in this study (i.e., 3 PS settings and 3 FR settings), this qualitative screening method has demonstrated its utility in greatly reducing the number of full 3D samples needed for subsequent steps in the optimization process.

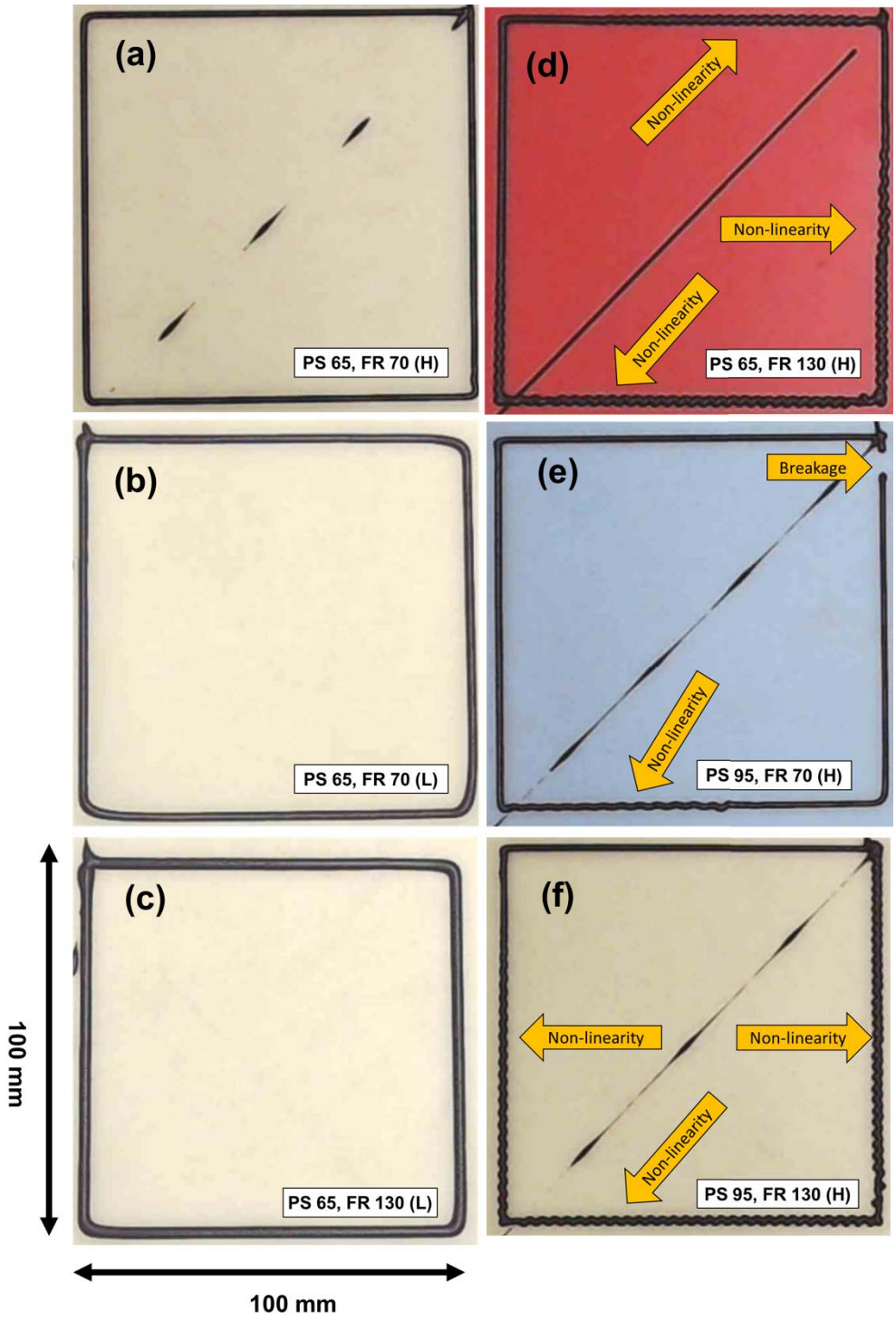

Figure 2.6 Representative lines showing acceptable prints (a,b,c) or qualitative criteria violations (d,e,f) for L and H chocolate. Diagonal lines in the center of the square are travel lines and are ignored for this analysis. The chocolate lines were 3D printed on different colored print beds.

2.3.1.3 Accuracy of 3D printed chocolates compared to digital designs

The accuracy of two chocolate designs (HHH and LLL) printed using the two print setting combinations outlined in the previous section is shown in **Figure 2.7**. The % error between the design and actual measurements was calculated for four parameters: mass, height, wall thickness, and outer diameter. Overall, print setting PS 35, FR 100 produce a more dimensionally accurate representation (least error) of the 3D printed design compared to print setting PS 65, FR 70.

The % error in mean measured parameters suggested that mass and height were most affected by adjusting print speed and flow rate **(Figure 2.7,** see **Table A3** for exact values**)**. The prints at PS35, FR100 were considered to be accurate as the % error in mean for all four measured parameters were ≤10% of the design value, except for a 14.80% error in wall thickness for the low sugar sample. The observed variation in mass also did not greatly influence the actual total % sugar (g sugar/g chocolate) in the sample **(Table 2.8)**, which will be important for subsequent sensory testing (Chapter 3).

The setting PS 65, FR 70 produced high (HHH) and low (LLL) sugar samples that were much lower in mass and height compared to the design (-29.01% to -36.98% error). The lower height can clearly be seen in the side view pictures **(Figure 2.8)**. A faster print speed setting (65 vs 35) and slower flow rate setting (70 vs 100) extrudes less material at a faster rate, which could explain the observed decreased mass and height at PS 65, FR 70. There was a greater % error in wall thickness for low sugar chocolate at PS 35, 100 compared to PS 65, FR70, while the % error was similar for high sugar chocolate at both print settings, but in opposite directions. Percent error in average diameter was greater at PS 65, FR 70 compared to PS 35, FR 100 for both high and low sugar chocolate.

Based on these results from the dimensional analysis, printer setting PS35, FR100 was selected as the optimal parameters for the 3D printed chocolates in subsequent tests. The remaining optimization steps were used to evaluate precision of individually printed layers, and also to confirm that the quality characteristics (i.e., tempering) were not affected by the printing process.

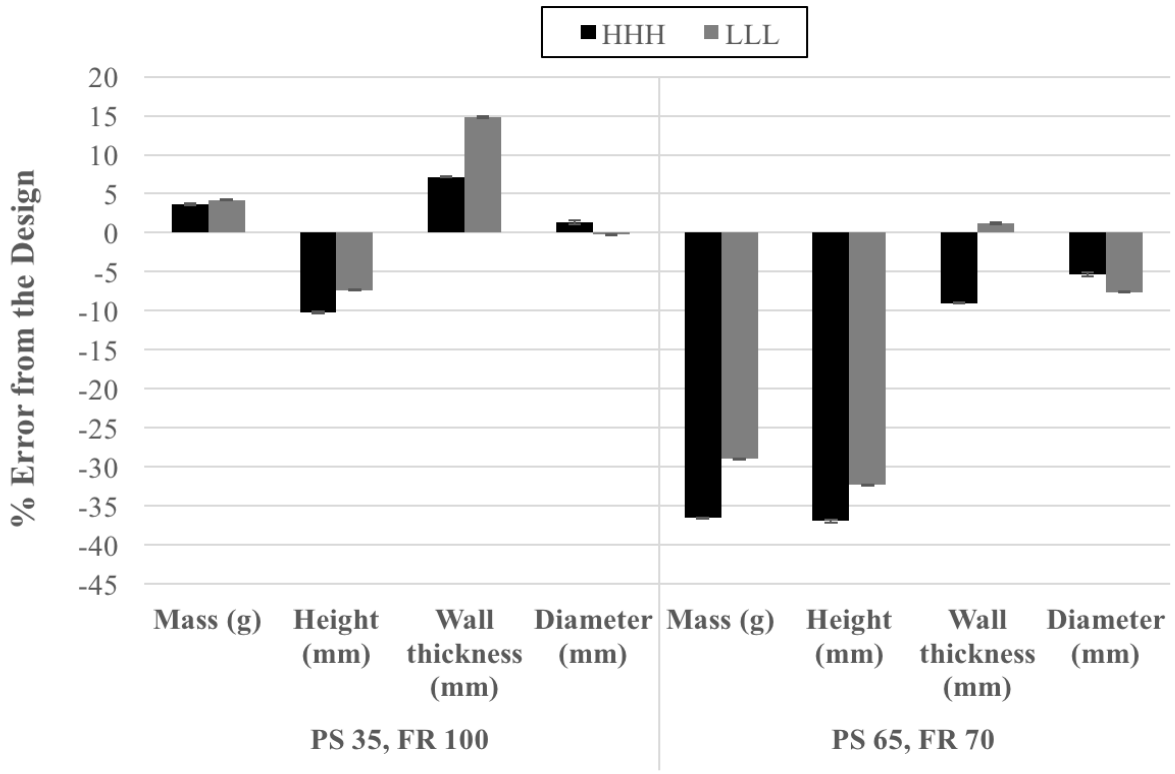

Figure 2.7 The % error in mean measured parameters from the design for high (HHH) and low (LLL) sugar 3D printed chocolates using two print settings (PS 35, 100 and PS 65, FR 70).

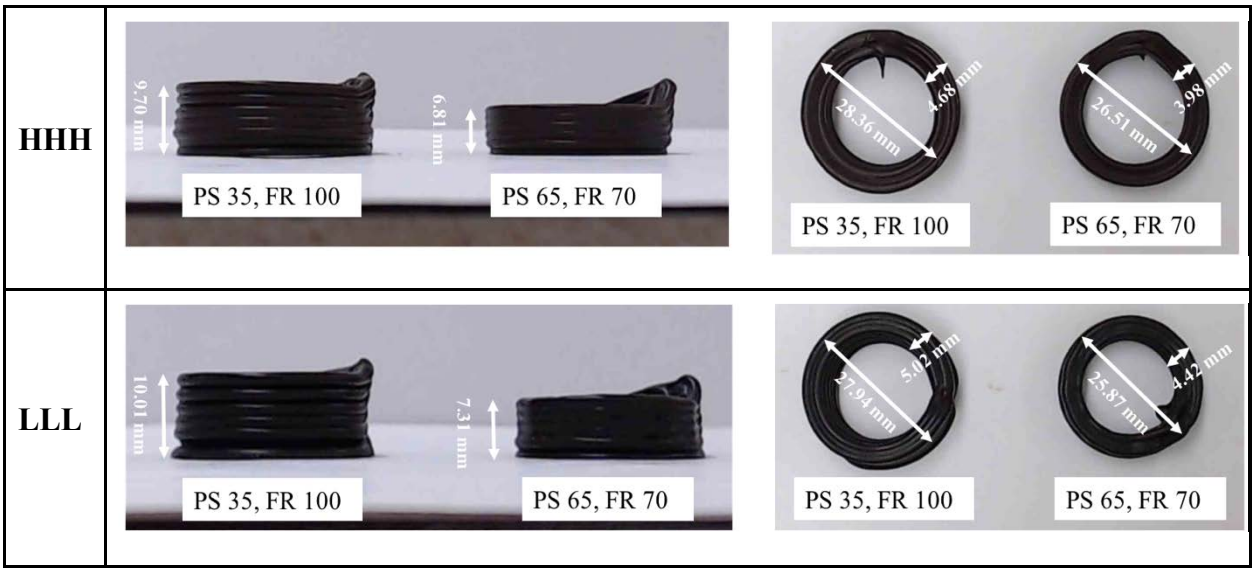

Figure 2.8 Top view (right) and side view (left) of high sugar (HHH) and low sugar (LLL) chocolates printed using acceptable printing parameters determined from qualitative assessment (PS 35, FR 100 or PS 65, FR 70). Indicated measurements are average height, wall thickness and diameter values for the corresponding print settings.

2.3.1.4 Precision of 3D printed chocolates compared to digital designs

The precision of each deposited layer was evaluated for the three-layered 3D printed chocolates to validate that a proper layer geometry was achieved. This analysis examines the deposition of each layer independently and is critical in determining the accuracy and repeatability of the final sugar reduced 3D printed chocolates. Based on the results from the previous assessment steps, the optimal print setting of PS35, FR 100 was used in this analysis.

Changes in mass, diameter and wall thickness were comparable to the design for all three layers and both H and L chocolate **(Figure 2.9)**. All mean measured parameters varied within ± 12% from the design except for the height. Mean mass for all high sugar chocolate layers (-3.01% to -10.78%) was lower than the design value, but was greater for all low sugar chocolate layers (3.60% to 9.21%). The error in mean diameter was small; 0.50% to 1.04% for all high sugar chocolate layers and -0.46% to -1.35% for all low sugar chocolate layers. Mean height was

lower than the design value for both H and L chocolate and all three chocolate layers, with layer 3 having the greatest error (-22.44% high sugar, -15.01% low sugar). For high sugar chocolate, mean wall thickness was lower than the design for layers 1 (-2.20%) and 2 (-0.02%), but greater than the design for layer 3 (3.42%). For low sugar chocolate, wall thickness was greater than the design for all layers (4.90% to 11.93%). As both L and H chocolates were molten when printed and did not solidify instantly once deposited, spreading likely occurred while the chocolate cooled, resulting in a lower height compared to the design for all layers and a corresponding greater wall thickness compared to the design at the top layer (layer 3). To prevent spreading, a faster cooling rate or larger design where there is more time for the chocolate to cool between layers could be used.

Two-way ANOVA revealed that there were no significant differences in average mass and height by layer nor chocolate type, and there was no interaction between layer and chocolate type ($p \leq 0.05$). Between layers 1, 2, and 3, there were no significant differences in any of the parameters ($p \leq 0.05$). Between chocolate type, H chocolate had significantly thinner mean wall thickness ($p=0.02054$) and larger mean diameter ($p= 0.01616$) (4.36 ± 0.20mm, 28.17 ± 0.26mm) compared to L chocolate (4.76 ± 0.30mm, 27.78 ± 0.29mm) **(Table A3).** The presence of emulsifiers in chocolate reduces rheological values (yield stress, apparent viscosity, thixotropy) while a higher fraction of non-fat cocoa solids increases them (Beckett et al., 2017; Glicerina et al., 2016). As H chocolate contains the emulsifier soy lecithin that promotes a reduced viscosity, more spreading may have occurred, which resulted in a larger diameter compared to L chocolate. Furthermore, H chocolate may have solidified faster due to decreased thixotropic behavior influenced by soy lecithin, which contributed to thinner walls. Conversely, L chocolate that contains more non-fat particles (e.g., chocolate liquor and cocoa powder) may have had

increased viscosity and thixotropic behavior, resulting in less spreading and slower solidification, which could explain the smaller diameter, but thicker walls compared to H chocolate.

This assessment determined that precise chocolate layers were 3D printed with a dual-extruder 3D food printer for the six chosen designs. The % error in the evaluated parameters (mass, height, wall thickness, and outer diameter) compared to the design was small among several prints of the same layer and/or chocolate type. A slight difference in mean diameter and wall thickness was observed between H and L chocolate.

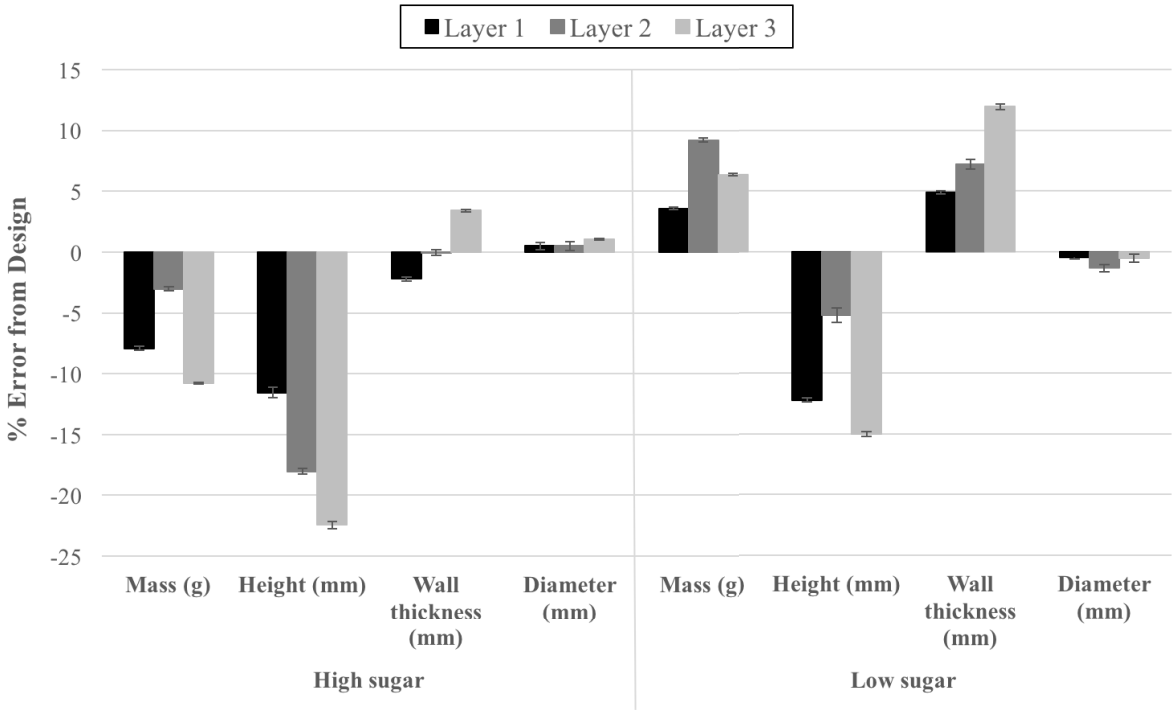

Figure 2.9 The % error in mean measured parameters from the design for each layer (1, 2, or 3) and chocolate type (high or low sugar).

2.3.1.5 Total % sugar concentration for the manufactured sugar-reduced 3D printed chocolates

For all samples, the mean actual total % sugar was similar to the theoretical total % sugar with small standard deviation **(Table 2.8).** This validates that sugar reduced 3D printed chocolates were successfully created by printing alternating layers of L and H chocolate in the three-layered hollow cylinder design. Two levels of percent sugar reduction from control (HHH) were created by this method. There were two chocolates with a 19.3% sugar reduction (HLH, HHL) and two with a 32.3-34.0% sugar reduction (LHL, HLL). Additionally, a 48.2% reduction in sugar was seen with sample LLL that had three layers of L chocolate. The difference between the two samples within the 19.3% and 32.3-34.0% sugar reduction groups was the layering order of H and L chocolates.

The sugar-reduced 3D printed chocolates that were created in this research were suitable for subsequent sensory analysis. The amount of sugar reduction achieved in this study (19% and 34.0-34.9%) was comparable to other tastant reduction studies, and different concentration gradients were produced by positioning the H layer at either the bottom layer (HLL), middle layer (LHL), bottom and middle layer (HHL), or bottom and top layer (HLH). In agar/gelatin gels, approximately a 20% sugar reduction was achieved without affecting sweetness when there was a large sugar concentration gradient between layers (Mosca et al., 2010). Similarly, a 28% salt reduction was achieved in bread without compromising saltiness intensity (Noort et al., 2010). A review of studies that successfully used a layering method to reduce sugar/salt in foods without affecting acceptability and sweetness/saltiness suggested that the amount of sugar reduction and position of high concentration layers are important factors that should be evaluated in sensory testing. Too much sugar reduction may be perceived by consumers, and the position of the high concentration layers affects the sensory contrast between the layers.

Table 2.8. Mean theoretical and actual total % sugar (g sugar/g chocolate) for the 3D printed chocolates and the percent sugar reduction from the high sugar sample (HHH).

Sample	Mean Theoretical Total % sugar	Mean Actual Total % sugar ± SD*	Difference between Mean Theoretical and Actual Total % content	Actual Percent Sugar Reduction based on HHH***
HHH	51.5	51.5 ± 0.0	-	-
HLH	43.6	41.6 ± 0.7**	2.0	19.3
HHL	43.6	41.6 ± 0.8	2.0	19.3
LHL	35.3	34.9 ± 0.6	0.4	32.3
HLL	35.3	34.0 ± 0.9	1.3	34.0
LLL	26.7	26.7 ± 0.0	-	48.2

*Values represent the mean and standard deviation of eight replicates.

**Value represents the mean and standard deviation of twelve replicates.

***Calculated using mean actual total % sugar values

2.3.1.6 Validation of chocolate quality

For the final step in the optimization process, the quality (temper) of the 3D printed chocolate was confirmed using DSC thermal analysis. Both chocolate types (H and L) were analyzed before and after 3D printing to assess any changes in temper based on the measured peak melting temperature. Based on these values, the crystallization form (I-VI) was determined. As shown in **Figure 2.10 & Table 2.9,** both chocolate types before 3D printing (H1, L1) and after 3D printing (H2, L2) had peak melting temperature in the range of 29-34℃which corresponded to the favorable form V (or β_2) fat crystals (van Malssen et al., 1999). These form V fat crystals are desired in chocolate products as they are stable, which prolongs shelf-life and gives desirable attributes such as a smooth and glossy finish and a characteristic "snap" when chewed (Beckett et al., 2017). As shown in Figure 2.10, the melting curves for both chocolate types (before and after 3D printing) were similar in shape. However, a double melting peak was observed for L2 chocolate. This could either be due to melting of the milk fat in the low sugar chocolate rather than cocoa butter, or to the presence of amorphous forms of sugar (Afoakwa et al., 2008). These results confirmed that the initial seed tempering process used was successful in forming the desired fat crystals, and that the 3D printing process did not alter the tempering in the chocolate.

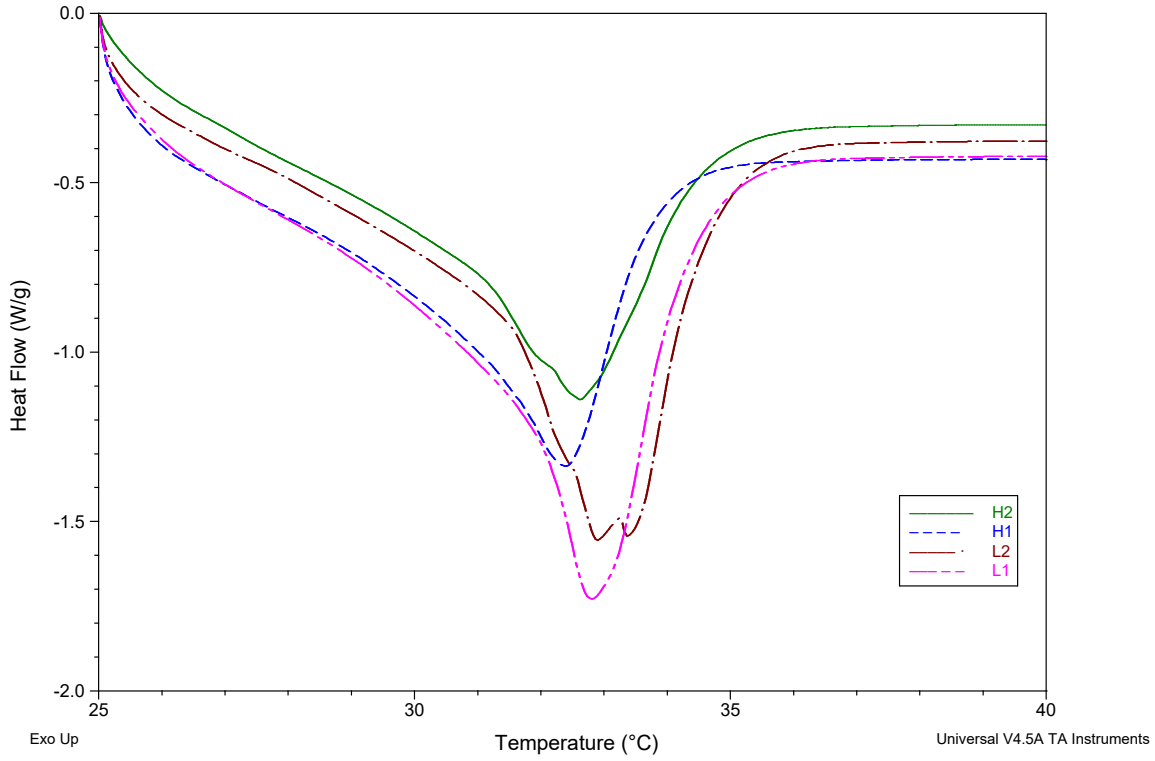

Figure 2.10 Typical DSC melting curves of high and low sugar chocolates pre-printing (H1, L1) and after 3D printing (H2, L2).

Table 2.9 Mean ± standard deviation for the melting properties of high and low sugar chocolates pre-printing (H1, L1) and after 3D printing (H2, L2), and the corresponding fat crystal polymorphic form.

Sample	Melting properties					Fat crystal polymorphic form
	T_{onset} (℃)	T_{end} (℃)	T_{index}	T_{peak}	△ H melt (J/g)	
H1	31.69 ± 1.85	35.75 ± 1.86	4.06 ± 0.07	33.66 ± 1.24	35.01 ± 2.08	β_2 (form V)
H2	29.64 ± 2.03	36.22 ± 1.21	6.58 ± 2.12	34.33 ± 1.59	33.00 ± 1.70	β_2 (form V)
L1	32.49 ± 1.15	36.15 ± 1.32	3.66 ± 0.32	34.01 ± 1.05	42.61 ± 4.90	β_2 (form V)
L2	32.47 ± 1.15	36.36 ± 1.77	3.89 ± 0.94	34.39 ± 1.32	47.53 ± 4.35	β_2 (form V)

*Values represent the mean and standard deviation of three replicates.

2.3.2 Observed cross-sectional shape and dimensions of various 3D print settings

The shape and dimensions of the 3D printed lines for the optimal chocolate print settings were examined using optical microscopy to better understand how these materials are being deposited. The final cross-sectional shape and dimensions of a 3D printed line or layer will depend on several factors including food properties (e.g., rheology, heat capacity), printing parameters (e.g., print speed, extrusion flow rate, and nozzle diameter), process temperature (e.g., heated extruder), ambient or post-print temperature (e.g., room conditions versus forced cooling), and printing substrate (e.g., hard/flat surface versus previously printed food layers). The shape of a printed line or layer can also influence the ability to deposit even and stable successive layers.

Cross-sectional images of printed lines (L chocolate) using the two best printer settings (as determined by the qualitative screening methodology in Section 2.2.4.2) is shown in **Figure 2.11**. The shapes of the chocolate lines are semi-circular in nature with a flat bottom which is due to the hard, flat printing surface. This flatter shape is suggested to increase stability by enabling proper alignment of successive layers (Derossi, Antonio et al., 2019).

In previous 3DFP studies, "optimal" printing settings were often selected, in part, when the deposited line diameter was equal to the inside diameter of the printer nozzle (Hao et al., 2010; Lanaro et al., 2017). This is a reasonable apriori assumption since the 3D printer software which converts solid models to printing code needs to assume a cross-sectional shape to calculate the printing pathways, number of lines required in a layer, and estimated height of successive layers. For example, some studies have assumed that the cross-sectional shape of 3D printed materials are cylindrical (Wang & Shaw, 2005; Yang et al., 2018), while the Slic3r program (RepRap) assumes that the printed cross-sectional shape is a rectangle with semicircular ends

(Hodgson et al., 2021). When these shapes are compared to the semi-circular cross-section in the current study, neither are representative. Furthermore, the cross-sectional dimensions of the line (i.e., width and height shown in **Figure 2.11**) are significantly greater that the inside diameter of the printer nozzle used in this study (0.9 mm). This suggests that optimization procedures based on the nozzle diameter may not be valid.

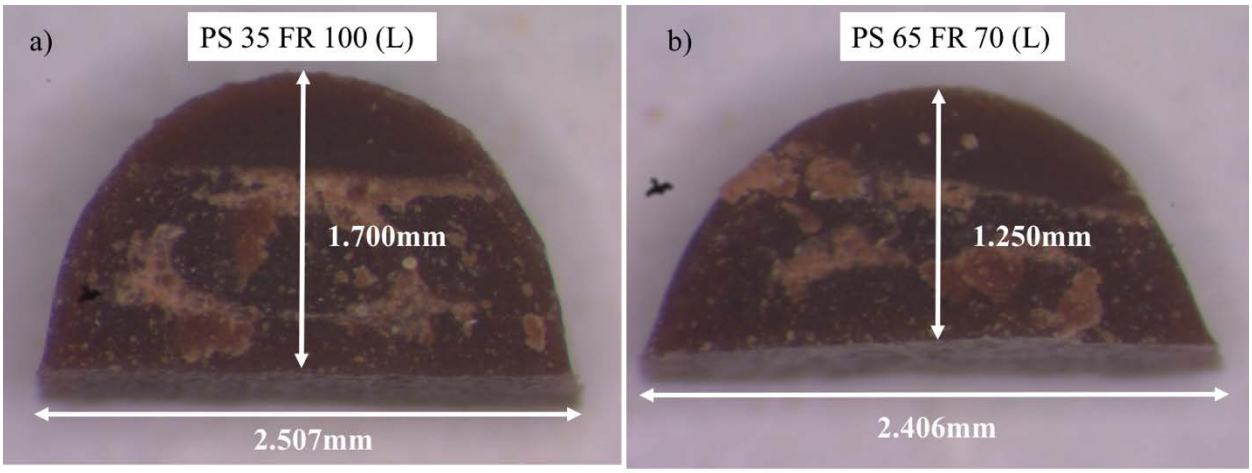

Figure 2.11 Representative cross-section optical microscope images (2.5x magnification) of printed lines (100mm x 1mm x 1mm) at a) PS35, FR 100 and b) PS 65, FR 70.

In order to better compare different cross-sectional print shapes from various line tests, the calculation of an "effective cross-sectional diameter" is proposed. This derivation assumes that each printed line is a cylinder with a volume equivalent to the experimental line deposited (irrespective of cross-sectional shape). By measuring the mass of the printed line, m (in g), the line length, l (in mm), and material density, ρ (in g/mm^3), the effective diameter, d_e (in mm) can be calculated using Equation 3, as follows:

$$d_e = 2\sqrt{\frac{m}{\pi\rho l}} \qquad (3)$$

Using Equation 3, the average effective diameters were plotted against print speed setting (35, 65 or 95) for each flow rate setting (70, 100 or 130) as shown in **Figure 2.12**. For each combination of parameters, data was combined from extruder 1 and 2, with a total of eight replicates for each line test performed (four replicates each of the two extruders). It can be observed that the average effective diameter of the lines generally increases with increasing extruder flow rate setting (FR) but is relatively constant with respect to printer speed setting (PS). This is expected since the deposition of mass is solely dependent on the print extruder. It can also be seen that the effective diameters calculated are significantly larger compared to the internal diameter of the nozzle (0.9 mm), which further suggests that optimization procedures based on the nozzle diameter may not be as relevant as other criteria.

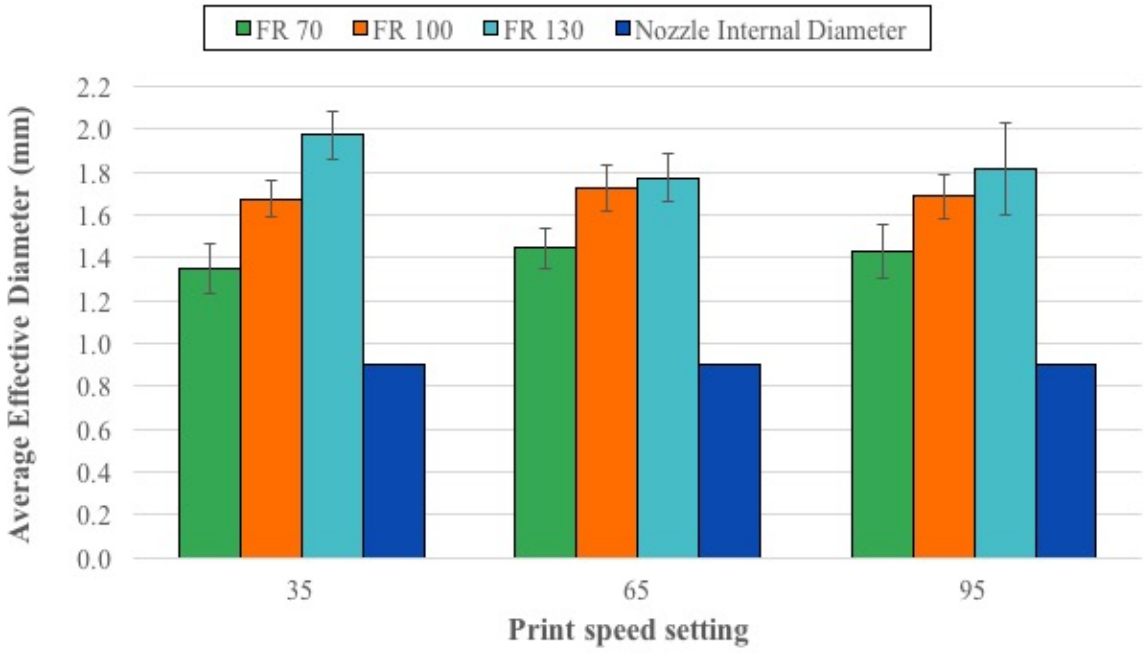

Figure 2.12 Calculated average effective diameter (mm) for print speed setting (PS 35, 65, 95) and flow rate setting combinations (FR 70, 100 and 130) compared to the nozzle internal diameter.

In the current study, the optimal print setting of PS35, FR100 produced a printed chocolate with a reasonably good dimensional accuracy compared to the 3D design, even though the printed cross-sectional shape was not circular, and the dimensions (including effective diameter) were much greater than the internal nozzle diameter. In the end, the main goal of a valid optimization method for 3DFP should be to determine the best printer settings in an easy, systematic manner to create an accurate, repeatable and stable representation of a 3D model without an impact on quality parameters. This has been demonstrated in this study.

2.4 Conclusion

This study demonstrated that a dual-extruder 3D food printer can be used to create three-layered, sugar-reduced 3D printed chocolates by printing high and low sugar chocolate in alternating layers. Two levels of sugar reduction were achieved by this method; 19% and 32-34% less total sugar compared to the high sugar control. A novel, semi-quantitative approach was proposed to optimize 3D chocolate printing parameters, and was used to assess the accuracy, precision and quality of the 3D printed chocolates. An optimal print speed setting and flow rate setting combination was determined for the tested chocolates that created 3D printed chocolates with small % error in average measured mass, height, wall thickness, and diameter of the 3D printed chocolates compared to 3D digital designs. Analysis of chocolate melting properties revealed that form V fat crystals that impart important chocolate properties such as a glossy finish and snap upon biting were present in the 3D printed chocolates, and the 3D printing process did not alter the thermal profile of the seed tempered chocolate. Overall, the optimization procedure proposed in this study provides an efficient way to optimize print settings for a variety

of 3D printed foods to create an accurate, repeatable and stable representation of a 3D model while ensuring that quality parameters are met.

2.4 References

Afoakwa, E. O., Paterson, A., Fowler, M., & Vieira, J. (2008). Characterization of melting properties in dark chocolates from varying particle size distribution and composition using differential scanning calorimetry. *Food Research International, 41*(7), 751-757. https://doi.org/10.1016/j.foodres.2008.05.009

Azam, S. M. R., Zhang, M., Mujumdar, A. S., & Yang, C. (2018, Apr 6,). Study on 3D printing of orange concentrate and material characteristics. *Journal of Food Process Engineering, 0*, e12689. https://doi.org/10.1111/jfpe.12689

Beckett, S. T., Fowler, M. S., & Ziegler, G. R. (2017). *Beckett's industrial chocolate manufacture and use* (Fifth ed.). John Wiley & Sons Ltd. https://doi.org/10.1002/9781118923597

Baiano, A. (2020). 3D printed foods: A comprehensive review on technologies, nutritional value, safety, consumer attitude, regulatory framework, and economic and sustainability issues. *Food Reviews International, ahead-of-print*(ahead-of-print), 1-31. https://doi.org/10.1080/87559129.2020.1762091

Caporizzi, R., Derossi, A., & Severini, C. (2019). *Cereal-based and insect-enriched printable food*. Elsevier. https://doi.org/10.1016/b978-0-12-814564-7.00004-3

Derossi, A., Caporizzi, R., Azzollini, D., & Severini, C. (2018). Application of 3D printing for customized food. A case on the development of a fruit-based snack for children. *Journal of Food Engineering, 220*, 65-75. https://doi.org/10.1016/j.jfoodeng.2017.05.015

Derossi, A., Caporizzi, R., Ricci, I., & Severini, C. (2019). *Critical variables in 3D food printing*. Elsevier. https://doi.org/10.1016/b978-0-12-814564-7.00003-1

Emorine, M., Septier, C., Andriot, I., Martin, C., Salles, C., & Thomas-Danguin, T. (2015). Combined heterogeneous distribution of salt and aroma in food enhances salt perception. *Food & Function, 6*(5), 1449-1459. https://doi.org/10.1039/c4fo01067a

Fernandes, V. A., Müller, A. J., & Sandoval, A. J. (2013). Thermal, structural and rheological characteristics of dark chocolate with different compositions. *Journal of Food Engineering, 116*(1), 97-108. https://doi.org/10.1016/j.jfoodeng.2012.12.002

Glicerina, V., Balestra, F., Dalla Rosa, M., & Romani, S. (2016). Microstructural and rheological characteristics of dark, milk and white chocolate: A comparative study. Journal of Food Engineering, 169, 165-171. https://doi.org/10.1016/j.jfoodeng.2015.08.011

Godoi, F. C., Bhandari, B. R., Prakash, S., & Zhang, M. (2019). *An introduction to the principles of 3D food printing*. Elsevier. https://doi.org/10.1016/b978-0-12-814564-7.00001-8

Hao, L., Mellor, S., Seaman, O., Henderson, J., Sewell, N., & Sloan, M. (2010). Material characterisation and process development for chocolate additive layer manufacturing. *Virtual and Physical Prototyping, 5*(2), 57-64. https://doi.org/10.1080/17452751003753212

Hertafeld, E., Zhang, C., Jin, Z., Jakub, A., Russell, K., Lakehal, Y., Andreyeva, K., Bangalore, S. N., Mezquita, J., Blutinger, J., & Lipson, H. (2019). Multi-material three-dimensional food printing with simultaneous infrared cooking. *3D Printing and Additive Manufacturing, 6*(1), 13-19. https://doi.org/10.1089/3dp.2018.0042

Holm, K., Wendin, K., & Hermansson, A. (2009). Sweetness and texture perceptions in structured gelatin gels with embedded sugar rich domains. *Food Hydrocolloids, 23*, 2388-2393.

Lanaro, M., Forrestal, D. P., Scheurer, S., Slinger, D. J., Liao, S., Powell, S. K., & Woodruff, M. A. (2017). 3D printing complex chocolate objects: Platform design, optimization and evaluation. *Journal of Food Engineering, 215*, 13-22. https://doi.org/10.1016/j.jfoodeng.2017.06.029

Landoni, B. (2014). *3Drag is now printing with chocolate!* Open Electronics. https://www.open-electronics.org/3drag-is-now-printing-with-chocolate/

Langlois, K., Garriguet, D., Gonzalez, A., Sinclair, S., & Colapinto, C. K. (2019). Change in total sugars consumption among canadian children and adults. *Health Reports, 30*(1), 10-19. https://www.ncbi.nlm.nih.gov/pubmed/30649778

Le Tohic, C., O'Sullivan, J. J., Drapala, K. P., Chartrin, V., Chan, T., Morrison, A. P., Kerry, J. P., & Kelly, A. L. (2018). Effect of 3D printing on the structure and textural properties of processed cheese. *Journal of Food Engineering, 220*, 56-64. https://doi.org/10.1016/j.jfoodeng.2017.02.003

Liu, Z., Bhandari, B., Prakash, S., & Zhang, M. (2018). Creation of internal structure of mashed potato construct by 3D printing and its textural properties. *Food Research International, 111*, 534-543. https://doi.org/10.1016/j.foodres.2018.05.075

Liu, Z., Zhang, M., Bhandari, B., & Yang, C. (2018). Impact of rheological properties of mashed potatoes on 3D printing. *Journal of Food Engineering, 220*, 76-82. https://doi.org/10.1016/j.jfoodeng.2017.04.017

Liu, Z., Zhang, M., & Yang, C. (2018). Dual extrusion 3D printing of mashed potatoes/strawberry juice gel. *Food Science & Technology, 96*, 589-596. https://doi.org/10.1016/j.lwt.2018.06.014

Karavasili, C., Gkaragkounis, A., Moschakis, T., Ritzoulis, C., & Fatouros, D. G. (2020). Pediatric-friendly chocolate-based dosage forms for the oral administration of both hydrophilic and lipophilic drugs fabricated with extrusion-based 3D printing. *European Journal of Pharmaceutical Sciences, 147*, 105291. https://doi.org/10.1016/j.ejps.2020.105291

Karyappa, R., & Hashimoto, M. (2019). *Chocolate-based ink three-dimensional printing (Ci3DP)*. Springer Science and Business Media LLC. https://doi.org/10.1038/s41598-019-50583-5

Kern, C., Weiss, J., & Hinrichs, J. (2018). Additive layer manufacturing of semi-hard model cheese: Effect of calcium levels on thermo-rheological properties and shear behavior. *Journal of Food Engineering, 235*, 89-97. https://doi.org/10.1016/j.jfoodeng.2018.04.029

Mantell, D. A., Hays, A. W., & Langford, Z. C. (2015). In XEROX CORPORATION, Norwalk, CT (US) (Ed.), *Printing 3D tempered chocolate*

Mantihal, S., Prakash, S., Godoi, F. C., & Bhandari, B. (2017). Optimization of chocolate 3D printing by correlating thermal and flow properties with 3D structure modeling. *Innovative Food Science & Emerging Technologies, 44*, 21-29. https://doi.org/10.1016/j.ifset.2017.09.012

Mantihal, S., Prakash, S., & Bhandari, B. (2019). Textural modification of 3D printed dark chocolate by varying internal infill structure. *Food Research International, 121*, 648-657. https://doi.org/10.1016/j.foodres.2018.12.034

Mantihal, S., Prakash, S., Godoi, F. C., & Bhandari, B. (2019). Effect of additives on thermal, rheological and tribological properties of 3D printed dark chocolate. *Food Research International, 119*, 161-169. https://doi.org/10.1016/j.foodres.2019.01.056

Marangoni, A. G., & McGauley, S. E. (2003). Relationship between crystallization behavior and structure in cocoa butter. *Crystal Growth & Design, 3*(1), 95-108. https://doi.org/10.1021/cg025580l

Mosca, A. C., Bult, J. H. F., & Stieger, M. (2013). Effect of spatial distribution of tastants on taste intensity, fluctuation of taste intensity and consumer preference of (semi-)solid food products. *Food Quality and Preference, 28*(1), 182-187. https://doi.org/10.1016/j.foodqual.2012.07.003

Mosca, A. C., Rocha, J. A., Sala, G., van de Velde, F., & Stieger, M. (2012). Inhomogeneous distribution of fat enhances the perception of fat-related sensory attributes in gelled foods. *Food Hydrocolloids, 27*(2), 448-455. https://doi.org/10.1016/j.foodhyd.2011.11.002

Mosca, A. C., van de Velde, F., Bult, J. H. F., van Boekel, Martinus A. J. S, & Stieger, M. (2012). Effect of gel texture and sucrose spatial distribution on sweetness perception. *LWT - Food Science and Technology, 46*, 183-188.

Mosca, A. C., Velde, F. v. d., Bult, J. H. F., van Boekel, Martinus A. J. S, & Stieger, M. (2010). Enhancement of sweetness intensity in gels by inhomogeneous distribution of sucrose. *Food Quality and Preference, 21*(7), 837-842. https://doi.org/10.1016/j.foodqual.2010.04.010

Noorani, R. (2017). *3D printing technology, applications, and selection* (1st ed.). CRC Press.

Noort, M. W. J., Bult, J. H. F., & Stieger, M. (2012). Saltiness enhancement by taste contrast in bread prepared with encapsulated salt. *Journal of Cereal Science, 55*(2), 218-225. https://doi.org/10.1016/j.jcs.2011.11.012

Noort, M. W. J., Bult, J. H. F., Stieger, M., & Hamer, R. J. (2010). Saltiness enhancement in bread by inhomogeneous spatial distribution of sodium chloride. *Journal of Cereal Science, 52*(3), 378-386. https://doi.org/10.1016/j.jcs.2010.06.018

Ostrowska-Ligęza, E., Marzec, A., Górska, A., Wirkowska-Wojdyła, M., Bryś, J., Rejch, A., & Czarkowska, K. (2019). A comparative study of thermal and textural properties of milk, white and dark chocolates. *Thermochimica Acta, 671*, 60-69. https://doi.org/10.1016/j.tca.2018.11.005

Rando, P., & Ramaioli, M. (2021). Food 3D printing: Effect of heat transfer on print stability of chocolate. *Journal of Food Engineering, 294.* https://doi.org/10.1016/j.jfoodeng.2020.110415

Severini, C., Azzollini, D., Albenzio, M., & Derossi, A. (2018). On printability, quality and nutritional properties of 3D printed cereal based snacks enriched with edible insects. *Food Research International, 106*, 666-676. https://doi.org/10.1016/j.foodres.2018.01.034

Severini, C., Derossi, A., Ricci, I., Caporizzi, R., & Fiore, A. (2018). Printing a blend of fruit and vegetables. new advances on critical variables and shelf life of 3D edible objects. *Journal of Food Engineering, 220*, 89-100. https://doi.org/10.1016/j.jfoodeng.2017.08.025

Svanberg, L., Ahrné, L., Lorén, N., & Windhab, E. (2011). Effect of pre-crystallization process and solid particle addition on microstructure in chocolate model systems. *Food Research International, 44*(5), 1339-1350. https://doi.org/10.1016/j.foodres.2011.01.018

Svanberg, L., Ahrné, L., Lorén, N., & Windhab, E. (2013). Impact of pre-crystallization process on structure and product properties in dark chocolate. *Journal of Food Engineering, 114*(1), 90-98. https://doi.org/10.1016/j.jfoodeng.2012.06.016

Sun, J., Peng, Z., Zhou, W., Fuh, J. Y. H., Hong, G. S., & Chiu, A. (2015). A review on 3D printing for customized food fabrication. *Procedia Manufacturing, 1*, 308-319. https://doi.org/10.1016/j.promfg.2015.09.057

van Malssen, K., van Langevelde, A., Peschar, R., & Schenk, H. (1999). Phase behavior and extended phase scheme of static cocoa butter investigated with real-time X-ray powder diffraction. *Journal of the American Oil Chemists' Society, 76*(6), 669-676. https://doi.org/10.1007/s11746-999-0158-4

Voon, S. L., An, J., Wong, G., Zhang, Y., & Chua, C. K. (2019). 3D food printing: A categorised review of inks and their development. *Virtual and Physical Prototyping, 14*(3), 203-218. https://doi.org/10.1080/17452759.2019.1603508

Yang, F., Zhang, M., Bhandari, B., & Liu, Y. (2018). Investigation on lemon juice gel as food material for 3D printing and optimization of printing parameters. *Food Science & Technology, 87*, 67-76. https://doi.org/10.1016/j.lwt.2017.08.054

Wang, J., & Shaw, L. L. (2005). Rheological and extrusion behavior of dental porcelain slurries for rapid prototyping applications. *Materials Science & Engineering. A, Structural Materials: Properties, Microstructure and Processing, 397*(1), 314-321. https://doi.org/10.1016/j.msea.2005.02.045

Wang, L., Zhang, M., Bhandari, B., & Yang, C. (2018). Investigation on fish surimi gel as promising food material for 3D printing. *Journal of Food Engineering, 220*, 101-108. https://doi.org/10.1016/j.jfoodeng.2017.02.029

World Health Organization. (2015). *Guideline: Sugars intake for adults and children*

Chapter 3 - Temporal Sensory Perceptions of Sugar-reduced 3D Printed Chocolates

3.1 Introduction

Globally, there is an increasing need for sugar-reduced foods due to the negative impacts of high sugar consumption on human health and a higher dietary consumption of total sugars than recommended. Health impacts of a high sugar diet include increased body weight, dental caries and poor oral health, and the World Health Organization (WHO) recommends less than 10% of total energy intake from free sugars (World Health Organization, 2015). However, 2015 data revealed that free sugars, added sugars and total sugars intake contributed to 13.3%, 11.1% and 21.6% of total daily energy intake of Canadians, respectively (Liu et al., 2020). Although total sugar intake declined from 2004 to 2015 for the "sugars, syrups and confectionary" category of food products, they remained among the top sources of total sugars intake for all age groups (Langlois et al., 2019). Moreover, the "desserts and sweets" group was the greatest contributor of free (57.5%), added (67.3%) and total sugar (41.4%) in the Canadian diet (Liu et al., 2020). Considering the importance of reducing sugar in this food category and its popularity, prototype sugar-reduced chocolates were evaluated in this research.

Arranging different concentrations of tastants in layers within a food structure can alter the sensory profile, thereby allowing a reduction in the tastant without affecting desirable sensory perceptions. This spatial distribution by layering has been demonstrated with sugar in gels (Holm et al., 2009; Mosca et al., 2010; Mosca et al., 2012), salt in bread (Noort et al., 2010) and cream-based snacks (Emorine et al., 2015), and fat in gels (Mosca et al., 2012) and sausages (Mosca et al., 2013). Bread samples with a heterogeneous distribution of salt permitted a reduction of up to 28% overall salt content without compromising saltiness intensity (Noort et

al., 2010). For sausages with 2% (w/w) total salt, the sample with an inhomogeneous distribution of salt was liked significantly more than the sausage with a homogeneous distribution, suggesting the method can be used to reduce salt in food without lessening consumer tastant acceptance (Mosca et al., 2013). Sweetness intensity was enhanced by an inhomogeneous distribution of sugar particles in gels. Of two gelatin gels with 9% sugar (w/w), a seven layered sample with an inhomogeneous distribution of sugar particles was perceived to be sweeter than a five-layered homogeneous sample (Holm et al., 2009). Of two four-layered agar/gelatin gels, a 10% sugar (w/w) sample with an inhomogeneous distribution of sucrose and a large concentration gradient of sucrose between the layers, tasted sweeter than a homogeneous sample with 12% (w/w) sucrose (Mosca et al., 2010).

Spatial distribution of sugar can be achieved by 3D food printing (3DFP) using a dual-extruder 3D food printer to create alternating chocolate layers of different sugar concentrations (Sun et al., 2015). 3DFP is a more accurate and efficient method to create chocolate layers compared to conventional methods using molds and provides the user with flexibility to create layered designs of different shapes as desired. The research described here studied the effect of a spatial distribution of sugar in three-layered 3D printed chocolates on their sensory attribute profile, perceived sweetness and overall liking.

Temporal dominance of sensations (TDS) is a sensory methodology that provides a dynamic view of the evolution of dominant sensory attributes for a food product during the tasting period (Pineau & Schilch, 2015). Chocolate has a complex sensory profile influenced by its chemical composition and post-harvest processing. Appearance, aroma, flavor, and texture attributes, coupled with a phase change during consumption, contribute to a rich temporal chocolate experience that could influence overall perceived sweetness. A developed chocolate

sensory wheel and lexicon indicated that milk chocolate was most associated with the attributes "creaminess", "milk/cream" flavor and "sweet" while dark chocolate was more associated with "hardness," "snap," and "bitter" (De Pelsmaeker et al., 2019). Therefore, a temporal evaluation of key sensory attributes associated with milk and dark chocolate is valuable to determine chocolate sensory attribute interactions with sweetness perception.

This research aimed to investigate how layering order of chocolates with different concentrations of sugar would influence the temporal sensory attribute profile, and if changes in the sensory profile influenced perceived sweetness intensity and overall acceptance of sugar-reduced and non-sugar-reduced 3D printed chocolates. It was hypothesized that the sensory profile of chocolates with similar total % sugar would change as a result of the layering, and this was expected to affect overall liking. It was also hypothesized that layering combinations with the high sugar chocolate as the bottom layer would allow chocolate samples with a lower total % sugar to taste just as sweet, if not sweeter, than samples with a higher total % sugar because the tongue has the highest density of taste buds in the oral cavity.

3.2 Materials and Methods

The plan for this study (Study ID: Pro00097545) was reviewed for its adherence to ethical guidelines and approved by the Research Ethics Board at the University of Alberta. All participants completed written informed consent.

3.2.1 Chocolate samples

Bars of 47% Cocoa Swiss Dark Chocolate (high sugar: H) and 72% Cocoa Swiss Dark Chocolate (low sugar: L) (Western Family TM, Overwaitea Food Group, Vancouver, BC) were

purchased from a local supermarket. Three-layered 3D printed chocolates were created in the shape of a hollow cylinder (diameter: 28.00mm, height: 10.80mm, thickness: 4.37mm). The six samples used for sensory testing had different sugar concentrations and layering combinations from the bottom to the top layer **(Figure 3.1)** to generate four % sugar (w/w) concentrations: 51.5%, 41.6%, 34.0-34.9% or 26.7%. Two samples were homogeneous (HHH, LLL) and four were inhomogeneous (HLH, HHL, LHL, HLL). The % sugar (w/w) in HHH (51.5%) is comparable to conventional chocolates sold at grocery stores in North America, therefore the HHH sample was used in this experiment as the non-sugar-reduced control.

The samples were manufactured in a food grade laboratory following the process described in Chapter 2. Briefly, digital 3D designs were converted into G-code and loaded into the RepetierHost printing software. Then, the chocolates were tempered by heating to 45-55℃, followed by cooling to 27℃ using the seeding method. Cooled chocolates were fed into the dual extruders of the 3D printer, and printed at a set temperature of 28℃ (L chocolate) or 32℃ (H chocolate) using an average print speed of 3 mm/s and an average flow rate of 6 mm^3/s. Samples were prepared in batches for each week of sensory paneling and stored at room temperature (20℃) for no more than one week prior to sensory evaluation to ensure similar freshness. For maximum freshness, the chocolates were placed into plastic cups with lids, the cups were put into air-tight freezer bags and the bags were placed inside plastic containers which were stored in a dark and dry cupboard.

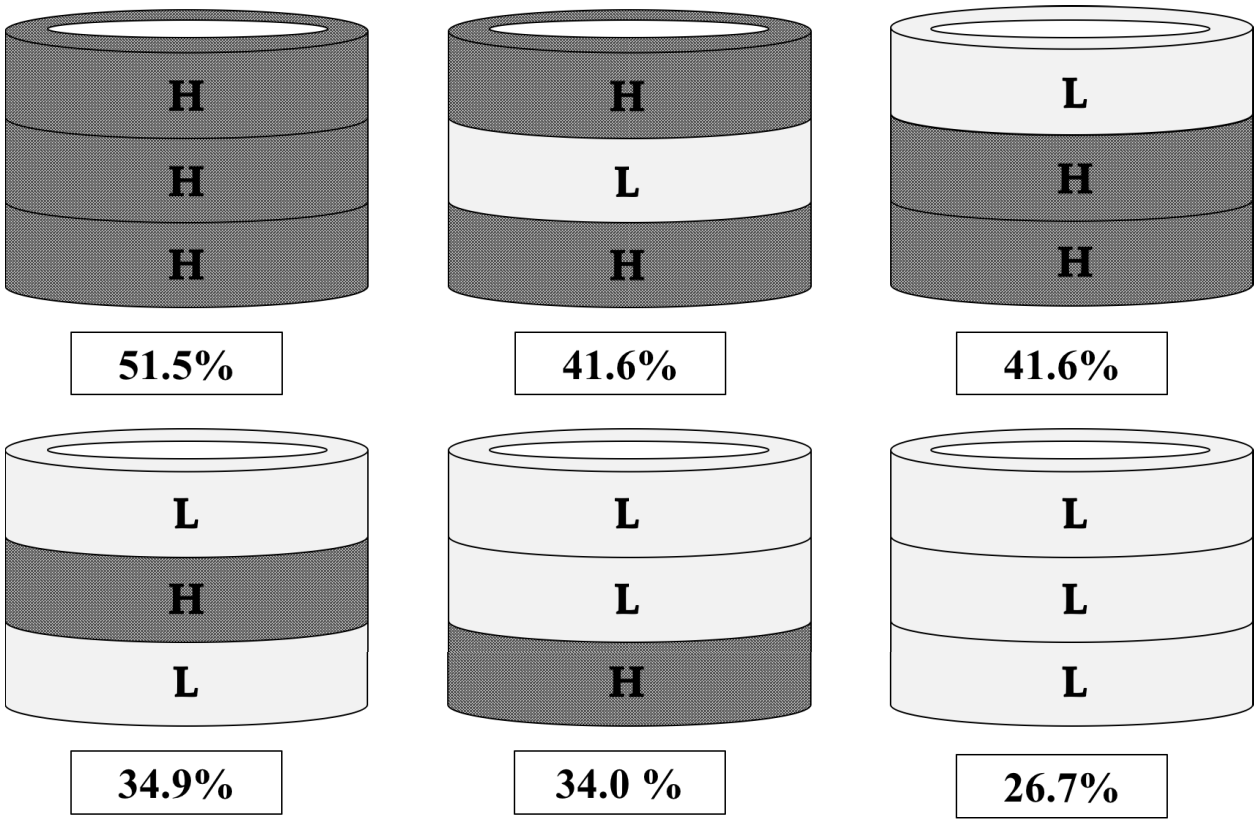

Figure 3.1 The six three-layered hollow cylinder samples and their total % (w/w) sugar concentration where H represents a high sugar layer (51.5%) and L a low sugar layer (26.7%).

3.2.2 Sensory panel

Students and staff (n=72) at the University of Alberta, age 18 and older who liked and were regular consumers of both milk and dark chocolate **(Table 3.2)** were recruited as participants for the study through flyers and university email lists. Immediately prior to evaluations participants were trained by the following procedure:

1. Familiarization with the chocolate TDS attributes based on the attribute definition list **(Table 3.1).**
2. Introduction to the TDS methodology, sweetness intensity scale, and overall liking scale.

3. Familiarization with the interface in the Compusense® Cloud sensory software (Compusense Inc., Guelph, Ontario, Canada) by performing the sensory evaluation procedure using a square of H chocolate as a warm-up sample.

Table 3.1 Sensory attribute definition list for TDS evaluations.

Attribute[1]	**Type of attribute**	**Definition**	**Examples**
Sweet	Taste	The taste of table sugar	Table sugar
Bitter	Taste	A sharp, pungent taste	Dark chocolate, strong black coffee, tonic water, or aspirin
Milky flavor	Taste	Reminiscent of the taste of fresh milk or the characteristic dairy note of milk chocolate	Fresh milk, milk chocolate
Chocolate flavor	Taste	The characteristic flavor of chocolate products	Cocoa powder, hot chocolate, chocolate milk, Hershey's kisses, Cadbury Dairy Milk Chocolate bars
Creamy	Texture	The fatty mouthfeel or thick coating on the tongue	Milkshake, heavy cream
Melting	Texture	A change in the chocolate from a solid to liquid	Ice cream melting in the mouth
Hard/ Brittle	Texture	High resistance to pressure from front teeth when biting through the sample, and breaks or shatters into crumbs or pieces	Shortbread, vanilla wafer, peanut brittle, gingersnap cookies

[1] Soft was included in the list of attributes for the TDS evaluation; a definition was not presented in the sensory attribute definition list.

3.2.3 Sensory evaluation

For each sample, participants completed an online questionnaire on Compusense® Cloud sensory software. They were asked to:

1. Complete a TDS evaluation by selecting from a list of 8 attributes, the most dominant attribute perceived over 120 seconds.
2. Indicate their opinion of the sweetness of the sample on a 5-point intensity category scale (1=not at all sweet, 5=extremely sweet).
3. Rate the sample for overall liking on a 9-point hedonic scale (1=dislike extremely, 9=like extremely).
4. Fill out a demographics and product use questionnaire.

TDS attributes to be evaluated by the panel were selected by first reviewing attributes and their definitions used in published chocolate sensory (De Pelsmaeker et al., 2019; International Organization for Standardization, 2008; Thamke et al., 2009) and TDS research (Ares et al., 2017; Oberrauter et al., 2018; Olegario et al., 2020; Ramón-Canul et al., 2020; Rodrigues et al., 2016; Rodrigues et al., 2016; van Bommel et al., 2019). Preliminary testing within the research group determined that eight sensory attributes were appropriate for the samples: sweet, bitter, chocolate flavor, milky flavor, creamy, melting, hard/brittle and soft. An appropriate training procedure, the maximum amount of time needed to complete the evaluation (2 minutes) and the correct orientation for placing samples into the mouth for evaluations were also trialed by the group.

The TDS evaluation procedure followed recommended guidelines in ISO 13299:2016(E) (International Organization for Standardization, 2016). Participants were instructed to start the evaluation by pressing the "play" button as soon as they put the sample into their mouth, and to chew each sample 3 times and let it melt on their tongue for the remainder of the time. They were asked to pick up and eat the sample in the orientation presented in the cup to ensure the bottom layer of each sample was on the tongue. While eating, they were asked to select the attribute that stood out to them the most from the list provided and re-select as the strongest attribute changed. Subjects were told that an attribute was considered dominant until another attribute was chosen. Moreover, they were informed that they could only select one attribute at a time but could select an attribute more than once and didn't have to use all the attributes. They pressed the "stop" button when the chocolate sample was gone from their mouth.

3.2.4 Testing conditions

Sensory evaluations were conducted at the sensory panel rooms in individual sensory booths under controlled light and air conditions. A balanced incomplete block design for 6 treatments was used to determine the sample presentation order. Participants were asked to taste and evaluate 3 of the 6 samples in one 30-minute session. Each sample (approximately 3.3g) was presented in 60mL plastic cups (P200N, Solo® translucent portion containers, Dart Container Corporation, Michigan, USA) with plastic lid (PL200N) at room temperature (20℃). A 30 second break was provided between each evaluation in order to cleanse the palate with deionized water.

3.2.5 Statistical analysis

All analyses were performed using R studio (Version 1.1.463, R Studio Inc., 2009-2018). TDS data were analyzed following the procedure described for TDS curves and TDS difference curves computation in (Pineau et al., 2009) using the tempR package (Castura, 2020). The data from each panelist was standardized from X=0.00 (first selection of dominant attribute) to X=1.00 (no more attributes selected) to account for differences in duration in the mouth. The dominance rates (proportion of participants that cited an attribute as dominant at each moment in time) were calculated, smoothed, and plotted against standardized time. TDS curves of all attributes were plotted on the same graph for each sample. The chance and significance level were calculated and indicated by dotted lines on the graph (Pineau et al., 2009). TDS difference curves were plotted to compare among all products and among products with similar overall perceived sweetness based on the mean perceived sweetness intensity. TDS difference curves were computed by subtracting the dominance rates of two samples for each attribute at each point of time. To highlight the differences between products over the evaluation period, only the significantly different dominance rates were plotted.

Overall sweetness and liking data were analysed by one-way ANOVA with Tukey's HSD Test ($p \leq 0.05$) using the nlme (Pinheiro et al., 2020) and lsmeans (Lenth, 2016) packages to investigate differences in perceived sweetness intensity and overall acceptance among samples. Samples were set as a fixed factor and panelists as a random factor using the nlme package.

Principal component analysis (PCA) was conducted with the tempR package and was used to visualize product differences during the temporal evaluation. Product trajectories were plotted for each 3D printed chocolate using a data frame with attributes tested in the columns and

dominance rates over standardized time in rows (Lenfant et al., 2009). Descriptive statistics were used for demographics and consumption habits data.

3.3 Results

3.3.1 Participants

Most participants were females (67%) aged 18-25 (58%) who consumed chocolate once per week or more often (86%) **(Table 3.2).** About half of the participants (54%) preferred milk chocolate to dark chocolate.

3.3.2 Overall sweetness and liking

All samples were rated as "not very sweet" to "moderately sweet" (2.3-3.3) on the 5-point scale, and three sweetness groups were identified **(Table 3.3)**. Samples with 41.6% sugar (HLH, HHL) were similar in sweetness to the control sample (HHH) with 51.5% sugar. This suggested that 3D printed sugar-reduced chocolates created by spatial distribution of sugar in layers, with up to 19% reduction in sugar (HLH, HHL) can taste as sweet as a non-sugar-reduced 3D printed chocolate (HHH). On the other hand, samples with 34.0% (HLL) and 34.9% (LHL) were similar in sweetness to the lowest sugar sample (LLL) with 26.7% sugar, but not to the control sample (HHH). This indicated that a sugar reduction of 32% from control was detected by participants. Although LHL was similar to LLL, it was also similar to HLH and HHL which had 19% more sugar. This further supports that a sugar reduction of 19% by spatial distribution in layers in chocolate can be achieved without changes in sweetness perception.

There were no significant differences in overall liking between the six samples **(Table 3.3)**. They were all liked slightly to moderately (6.4-6.9).

Table 3.2 Demographic and product use results of the consumer panelists (n=72).

	Category	Number (% frequency)
Sex	Male	24 (33)
	Female	48 (67)
Age	18-25 years	42 (58)
	26-35 years	19 (26)
	Greater than 36 years	11 (16)
Preference for sweet or savory food	Savory food	15 (21)
	Sweet food	23 (32)
	No preference	34 (47)
Preference for milk or dark chocolate	Milk chocolate	39 (54)
	Dark chocolate	33 (46)
Type of chocolate usually consumed	White chocolate	2 (3)
	Milk chocolate	26 (36)
	Dark chocolate	21 (29)
	Chocolate with fruit, nuts or other flavorings (e.g., almonds, salt, orange)	13 (18)
	Chocolate as part of a mix of multiple ingredients (e.g., O'Henry, Mars, Coffee Crisp, Crispy Crunch)	10 (14)
Consumption frequency for usual type of chocolate	Daily	8 (11)
	3-4 times per week	24 (33)
	Once per week	30 (42)
	Once per month	7 (10)
	A few times per year	3 (4)

Table 3.3 Total % sugar (w/w) and mean sweetness and liking ± standard deviation[1] for the 3D printed chocolates (n=36).

Sample[2]	Total % Sugar	Sweetness[3]	Liking[4]
HHH	51.5	3.3a ± 0.8	6.6 ± 1.5
HLH	41.6	3.2ab ± 0.7	6.9 ± 1.1
HHL	41.6	2.9ab ± 0.9	6.5 ± 1.5
LHL	34.9	2.7bc ± 0.8	6.6 ± 1.4
HLL	34.0	2.4c ± 0.9	6.8 ± 1.4
LLL	26.7	2.3c ± 1.0	6.4 ± 1.6

1 Samples with different lower case superscripted letters within a column are significantly different ($p \leq 0.05$).

2 Upper case letters represent the layering order from bottom to top (H:51.5%, L:26.7% total sugar). Participants were instructed to place the bottom layer on the tongue for evaluations.

3 Samples were evaluated on a 5-pt scale (1=not at all sweet, 5=extremely sweet).

4 Samples were evaluated on a 9-pt scale (1=dislike extremely, 9=like extremely).

3.3.3 TDS curves

TDS curves of the 8 sensory attributes were plotted for each 3D printed chocolate sample **(Figure A1)** to observe the temporal sensory profile of each sample. The chance (0.125) and significance (0.204) levels are indicated as dotted lines on the plots. Attributes were considered to be dominant when the dominance rate exceeded the significance level. The peak dominance rates for all attributes ranged from 0.22-0.47. To observe possible layering effects, the dynamic profile of the chocolates was interpreted by attribute and standardized time quadrants: Q1 (0.00-0.24), Q2 (0.25-0.49), Q3 (0.50-0.74), Q4 (0.75-1.00).

"Milky flavor" was never dominant in any of the samples, whereas **"Hard/Brittle"** was dominant for all samples at the beginning of evaluations (Q1, around 0.00-0.15) with peak dominance rate of 0.36 (HHH), 0.42 (HLH), 0.31 (HHL), 0.44 (LHL), 0.47 (HLL) and 0.44 (LLL).

"Chocolate flavor" was also dominant for all samples with peak dominance rate of 0.33 (HHH), 0.39 (HLH), 0.36 (HHL), 0.39 (LHL), 0.47 (HLL) and 0.36 (LLL), but varied in dominance periods. For HHH, it was dominant in intervals during Q1-Q3 (0.16-0.29, 0.33-0.38, 0.44-0.45, 0.48-0.53, 0.59-0.67). For HLH, it was most dominant in the beginning (Q2, 0.10-0.36) and in the second half (Q3-Q4, 0.58-1.0) of the evaluation. For HHL, it was dominant in intervals from Q2-Q4 (0.26-0.42, 0.44-0.47, 0.55-1.00). For LHL, it was dominant in intervals throughout the evaluation (Q1-Q4, 0.10-0.33, 0.36-0.75, 0.81-0.95). For HLL, it was dominant throughout the evaluation (Q1-Q4, 0.01-0.03, 0.10-0.69, 0.83-1.0) but especially Q3. For LLL, it was dominant in intervals in Q1-Q3 (0.13-0.18, 0.26-0.57), but especially Q2.

"Bitter" was dominant for all samples except HHH with peak dominance rate of 0.25 (HLH), 0.31 (HHL), 0.36 (LHL), 0.33 (HLL) and 0.47 (LLL). For HLH, it was dominant towards the middle of the evaluation (Q2, 0.38-0.43). For HHL, it was dominant in the first half of the evaluation (Q1-Q2, 0.00-0.19 and 0.22-0.43). For LHL, bitter was dominant in intervals from Q2-Q3 (0.22-0.41, 0.57-0.61, 0.72-0.78). For HLL, it was dominant in intervals throughout the evaluation (Q1-Q4, 0.08-0.49, 0.60-0.64, 0.66-0.86 and 0.89-1.00). For LLL, it was dominant throughout the evaluation (Q1-Q4, 0.03-1.00).

"Sweet" was dominant for samples with 43.6% sugar (HLH, HHL) or 51.5% sugar (HHH) at peak dominance rate of 0.31 (HHH) and 0.25 (HLH, HHL). It was dominant in intervals throughout the evaluation (Q1-Q4, 0.09-1.00) for HHH, but especially near the end in Q4 (0.75-1.0). For HLH, it was dominant in Q3 (0.57-0.63 and 0.67-0.70). For HHL, it was dominant at the beginning of evaluations (Q1-Q2, 0.13-0.0.16 and 0.31-0.36).

"Creamy" was dominant for samples with 2 or 3 H layers (HHH, HLH, HHL), or 1 H layer on the bottom (HLL), but only very briefly (0.01-0.04 standardized time intervals) and very

slightly (peak dominance rate of 0.22 for all). Creamy was dominant for HHH towards the end of Q2 (0.32-0.33, 0.46-0.47 and 0.49-0.51), for HLH in the middle of Q2 (0.33-0.34), for HHL in Q3 (0.58-0.62), and for HLL in Q4 (0.83-0.86).

"Melting" was dominant for all samples with peak dominance rate of 0.25 for samples with 2 or more L layers (LHL, HLL, LLL) or 0.28 for samples with 2 or more H layers (HHH, HLH, HHL). For HHH melting was dominant in Q2 (0.31-0.38) and towards the end of Q3 (0.69-0.77). For HLH melting was dominant at the beginning and towards the end of Q3 (0.51-0.58, 0.69-0.78), while for HHL it was dominant at the beginning of Q3 (0.48-0.55) and throughout Q4 (0.68-1.00). LHL was dominantly melting near the end of Q4 (0.79-0.92). Melting was briefly dominant in Q2 (0.36-0.41) for HLL, and Q4 (0.78-0.85) for LLL.

The TDS curves suggested that the sensory profile of the 3D printed chocolates was influenced by the order in which H and L chocolate layers were arranged. Samples with the same amount of total sugar but different layering order (e.g., HLH and HHL or LHL and HLL) had similar dominant attributes but differed in peak dominance rates, and the time periods and duration that the attributes were dominant.

3.3.4 TDS difference curves

TDS difference curves were plotted to highlight differences in dominance rates between samples with similar **(Figure 3.2)** and significantly different **(Figure A2)** mean sweetness intensity.

For almost all of the samples with similar overall sweetness, differences were observed in the dominance rates for sweet, bitter, chocolate flavor, creamy and soft. The exception was between LHL and HLL, where no differences were observed. HLH was more dominant in chocolate flavor in Q3 compared to HHH **(Figure 3.2a)**. HHH was more dominantly creamy in Q2, soft in Q3, and sweet in Q4 compared to HHL, while HHL was more dominantly bitter in Q1-Q2 **(Figure 3.2b)**. HLH was more dominant in chocolate flavor in Q1 and creamy in Q2 compared to HHL, while HHL was more bitter in Q1 **(Figure 3.2c)**. LHL was more dominant in chocolate flavor in Q2 compared to HLH **(Figure 3.2d)**. HHL was sweeter in Q1 compared to LHL, while LHL was more dominant in chocolate flavor in Q1 **(Figure 3.2e)**. LLL was more dominantly bitter in Q3 and Q4 compared to LHL **(Figure 3.2f)**. LLL was more dominantly bitter in Q3, while HLL was more dominant in chocolate flavor in Q2 and Q3 **(Figure 3.2g)**.

As samples perceived to be similar in overall sweetness intensity differed in their TDS profile, the TDS difference curves suggested that other sensory attributes influenced overall sweetness perception. Furthermore, H and L chocolate layering order could have influenced the sensory profile of 3D printed chocolates, which could have affected overall sweetness. The 3D printed chocolate with a H layer in both the top and bottom (HLH) had the most similar temporal sensory profile to the sweetest control sample (HHH) **(Figure 3.2a)**, while the sample with a H layer in the bottom only (HLL) had a profile that was most similar to the chocolate with the least amount of total % sugar (w/w) (LLL) **(Figure 3.2g)**.

Among samples with significantly different sweetness intensity, differences were observed in the dominance rates for sweet, bitter, chocolate flavor and creamy. HHH was more dominantly sweet in Q1-Q2 and Q4 compared to LHL, while LHL was more dominantly bitter in Q2 and Q4 **(Figure A2a)**. HLL was more dominantly bitter in Q1-Q2 and Q4 compared to HHH, while HHH was more dominantly sweet in Q1 and Q3-4 and creamy in Q2 and Q3 **(Figure A2b)**. LLL was more dominantly bitter from Q1-Q4 compared to HHH, while HHH was more dominantly sweet in Q1-Q2 and Q4 **(Figure A2c)**. HLL was more dominantly bitter in Q1 and Q4 and had more dominant chocolate flavor in Q3 compared to HLH, while HLH was more dominantly sweet in Q1 and Q3 and creamy in Q2 **(Figure A2d)**. LLL was more dominantly bitter in Q1 and Q3-4 compared to HLH, while HLH was more dominant in chocolate flavor in Q4 **(Figure A2e)**. HLL was more dominant in chocolate flavor in Q1 and Q3, while HHL was more dominantly sweet in Q1 **(Figure S2f)**. LLL was more dominantly bitter in Q3-Q4 compared to HHL, while HHL was more dominantly sweet in Q2 **(Figure A2g)**.

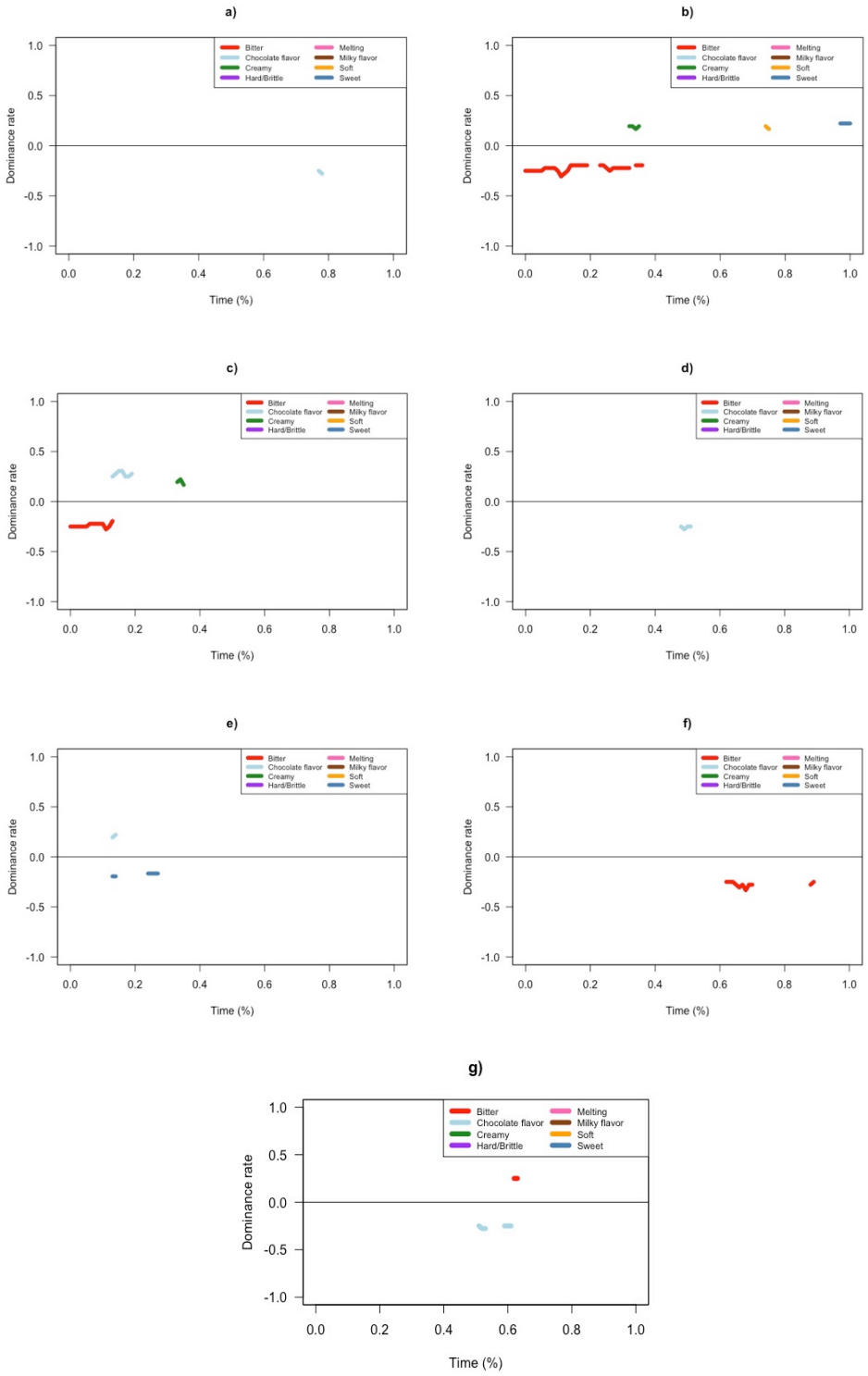

Figure 3.2 TDS difference curves comparing samples with similar overall sweetness: a) HHH-HLH b) HHH-HHL c) HLH-HHL d) HLH-LHL e) LHL-HHL f) LHL-LLL g) LLL-HLL

3.3.5 Principal components analysis (PCA)

The first two dimensions explained 64.88% of the variance observed among the products **(Figure 3.3)**. Dimension 1 was associated with the evaluation time points and the attributes "Hard/Brittle," "Melting" and "Chocolate flavor" while dimension 2 was strongly associated with the opposing taste attributes "Bitter" and "Sweet."

For all six 3D printed chocolates, the first perceived dominant attribute was "Hard/Brittle," and the last perceived dominant attributes were "Chocolate flavor" and "Melting," as evidenced by dimension 1. Three groupings were defined by dimension 2. HHH was its own group and was most associated with sweet. The sweetness dominance of HHL, HLH and LHL were perceived similarly, while the group of HLL and LLL was more associated with bitter compared to the other two groups. Dimension 1 indicated that the similarities in sweetness within the three groups occurred towards the end of the evaluation. For the HLL and LLL group, in the middle of the evaluation, HLL was more dominant in sweet while LLL was more dominant in bitter. For the grouping of HHL, HLH and LHL, in the middle of the evaluation, HHL and LHL had a similar trajectory, but HLH had a trajectory more similar to HHH.

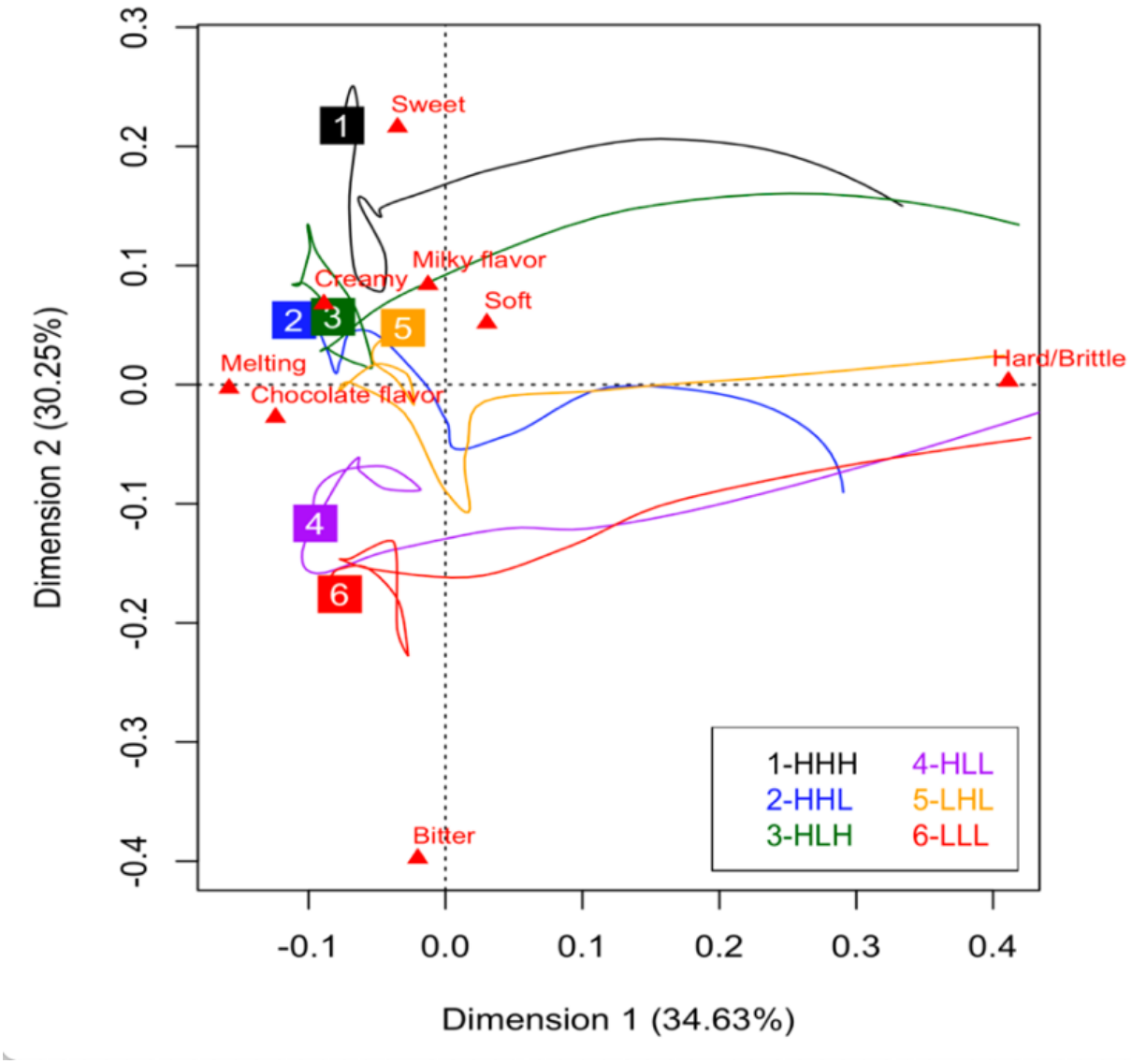

Figure 3.3 PCA biplot representing the product trajectories of the six 3D printed chocolates during the TDS evaluation. Numbered squares represent trajectory end-points for the corresponding sample.

3.4 Discussion

This study explored the effect of layering high and low sugar concentration chocolate on the temporal sensory profile of sugar-reduced and non-sugar-reduced 3D printed chocolates, and the layering influence on sweetness perception and liking. Sugar-reduced 3D printed chocolates were generated with layering arrangements to taste as sweet as samples with 19% greater total sugar content. A sugar concentration gradient between the layers was important for sweetness enhancement. The position of H and L chocolate layers was found to influence the temporal sensory profile and perceived overall sweetness. Overall, the 3D printed chocolates were well liked, and temporal changes did not affect these ratings.

Layering chocolates with different amounts of sugar achieved a 19% reduction in sugar without changes in overall sweetness perception. However, a 32% sugar reduction in sweetness was detected by participants. These results are similar to other studies that arranged tastants in specific layers. In four-layered agar/gelatin gels, an inhomogeneous spatial distribution of sucrose compensated for a 20% overall sucrose reduction when there was a large concentration gradient between the layers (Mosca et al., 2010). This gradient was important because of the contrast effect that was created. By alternating concentrations of sucrose in layers, taste receptors are stimulated in intervals with either low or high sugar concentrations, causing a sweetness enhancement effect. Similar results were observed for liquid solutions, where sweetness was perceived to be more intense by using an alternating presentation of high and low sucrose aqueous solutions in short intervals (Burseg et al., 2010). It was concluded that a conscious perception of the contrast was not required for taste enhancement by this method. The contrast effect may also reduce adaptation, the gradual decrease in taste receptor response with continuous stimulation (Meiselman & Halpern, 1973). In the present research, LHL (34.9%

sugar) was perceived to be similar in sweetness to samples with 41.6% sugar (HHL and HLH), while HLL (34.0% sugar) was not. The mechanism of discontinuous taste receptor stimulation may also be responsible for this. In LHL, the L and H layers are alternating from bottom to top resulting in a large contrast between layers 1 and 2, and layers 2 and 3. In HHL, layers 1 and 2 have the same sugar concentration, and only layers 2 and 3 have a gradient between them.

Layering order of H and L chocolates affected the temporal sensory profile of the 3D printed chocolates. Differences were observed in the peak dominance rates, time periods, and duration of the dominant attributes "Bitter," "Chocolate flavor," and "Creamy" for 3D printed chocolates with the same amount of total sugar but different layering order (HLH and HHL). Furthermore, these changes to the temporal sensory profile appeared to affect perceived sweetness. When the H layer was in the bottom only (HLL), or not present at all (LLL), the temporal sensory profiles were more dominantly "Bitter" compared to HHH, which contributed to a significantly decreased perceived overall sweetness. When H chocolate was in the middle layer only (LHL, 35.3% sugar), the temporal sensory attribute profile was most similar to HLH and HHL, which likely contributed to perceived similar sweetness of LHL (34.9% sugar) with HLH and HHL (41.6% sugar). A temporal sensory profile similar to HHH chocolate with the highest total % sugar (w/w) was created by placing the H chocolate in the top and bottom layers (HLH), and this appeared to enhance sweetness as HLH and HHH were perceived to be similar in sweetness by consumers. As other possible layering combinations (LLH, LHH) were not included in this study, evaluating these additional samples could provide more insight on specific influences of placing a H layer only at the top or at the top and middle of the sample.

The expectation that placing sweeter chocolates at bottom layers would increase sweetness perception was true when comparing between the control sample (HHH) and samples

that had a 19% reduction in sugar compared to the control (HLH and HHL). Samples with 43.56% sugar (HLH, HHL) had high sugar chocolate at the bottom, low sugar chocolate in the middle or top layers, and their sweetness was comparable to a conventional 51.52% sugar chocolate (HHH). Similar to HLH, cream-based snacks with a 35% reduction in salt and salt-associated aroma were found to be saltier compared to the reference snack when the salty aroma layer was at the bottom and the saltier layer was at the top (Emorine et al., 2015). In contrast, sweetness intensity was not different among four four-layered gels with different layering arrangements and an overall 10% (w/w) sugar concentration (Mosca et al., 2010). In the present research, LHL with 35.3% sugar did not have a high sugar layer at the bottom but tasted similar in sweetness to HLH and HHL with 43.56% sugar. This suggested an influence of factors in addition to layering order.

Perceived dominance of certain attributes and timing of the dominance perception during consumption may have affected overall sweetness perception. Significantly higher dominance rates for "creamy" or "sweet" appeared to increase sweetness perception. These attributes are more strongly associated with milk chocolate (Gámbaro & Ellis, 2012), which is generally sweeter than dark chocolate due to lower amounts of cocoa and higher amounts of sugar (Thamke et al., 2009). On the other hand, significantly higher dominance rates of attributes associated with dark chocolates, such as "bitter" or "chocolate flavor" (Thamke et al., 2009) appeared to decrease sweetness perception. Dominance time for "bitter" appeared to influence perceived overall sweetness due to primacy and recency effects (Mosca et al., 2014)

For each 3D printed chocolate, each attribute was dominant at some point during the evaluation except for "Milky flavor." Some associations between H or L layers and dominance of specific attributes were observed. Based on previous TDS studies of milk chocolate or

chocolate with cocoa content similar to the chocolate evaluated in this study (41%, 53% or 55%), H chocolate (47% cocoa) was expected to be dominant in the attributes "Hard," "Brittle," "Sweet," "Melting," "Soft," "Cocoa," "Milk," and "Creaminess" (Ares et al., 2017; Olegario et al., 2020; Rodrigues et al., 2016). L chocolate (72% cocoa) was expected to have similar dominant attributes to dark chocolates with 63% or 70% cocoa, described as dominant in "Crunchy," "Cocoa", "Bitter" and "Melting" (Rodrigues et al., 2016; van Bommel et al., 2019). In the present study, dominance of "Hard/Brittle" was likely related to initial chewing as it was consistently dominant at the beginning of evaluations. The hollow shape and thin walls (4.37mm) of the printed chocolates could have contributed to the perceived hardness/brittleness as well. There was a correlation between L chocolate layers and peak dominance rates and times for "Chocolate flavor." As expected, "Bitter" was dominant for all samples with at least one L layer, while "Sweet" was dominant for samples with two or three H layers and a higher total % sugar (41.6% and 51.5%). "Creamy" was associated with H chocolate, as it was only dominant for samples with two or three H layers. In relation to milk chocolates, "Milky flavor" is closely related to "Creamy," and this similarity may be why those two attributes were never chosen as dominant. It was noted that for HLL, both "Bitter" and "Sweet" were dominant in the first half of the evaluation, but during the dominance periods, the dominance rate for "Sweet" was lower than for "Bitter". This suggested that this sample may have been perceived as "Bittersweet" by the participants. Bittersweet was excluded from the TDS attributes list provided to the participants in this research to avoid confusion when selecting an option as dominant.

The dominance rates, number of dominant attributes selected by participants, and number of responses collected in this research were comparable to previous temporal studies on milk and dark chocolate and chocolate products. In previous studies, dominance rates between 0.2-0.6 for

chocolate attributes were observed, and some presented attributes were not dominant at any point during TDS evaluations (Kiumarsi et al., 2021; Ramón-Canul et al., 2020; Rodrigues et al., 2016; Zhu et al., 2020). Higher dominance rates (>0.8) were recorded when there were only a few attributes to select from (e.g., sweetness, bitterness or astringency) (Oberrauter et al., 2018) or for added attributes, such as "fruity" for orange dark chocolate (van Bommel et al., 2019). Since TDS evaluates dominant attributes over time, sub-threshold perception could result in non-dominant attributes. While a higher agreement among consumers could be achieved by using more panelists or separating taste and texture attribute categories, the findings from this research were robust. Differences in dominance were recognized and dominance rates were above significance levels, which indicated an acceptable panelist agreement. An appropriate TDS training procedure was used as recommended in ISO 13299:2016(E) (International Organization for Standardization, 2016), the presented attributes and their definitions were straightforward and typical of milk and dark chocolates, and the participants were familiarized with the attributes prior to evaluations using a warm-up sample of chocolate.

The 3D printed chocolates were well liked by participants, as regular consumption of both milk and dark chocolate was a participation criterion. The differences observed among the TDS profiles of similarly sweet samples did not affect overall liking of the 3D printed chocolates. While the focus of this study was not identification of temporal sensory attributes as drivers of liking, future studies could use a technique such as a penalty lift analysis to link specific temporal attributes to liking scores among chocolates with more variable sensory and quality attributes (Ares et al., 2017).

Similar studies with a larger number of participants would facilitate further insights into the TDS profile of the evaluated samples. This would allow for stratification based on the type of

chocolate that the panelists liked and frequently consumed. Larger studies including all possible variations of the order of the three layers in the 3D printed chocolates, samples with a greater number of layers or greater concentration gradient between the layers, could more clearly elucidate the effect of layering order. There is motivation for the food industry to continue research on sugar reduction strategies to achieve specific sugar reduction targets (HM Government, 2016; World Cancer Research Fund International, 2015). Furthermore, the increasing popularity of certain diets, such as Ketogenic, Mediterranean and Paleo diets (Modi & Priefer, 2020), have promoted reduced consumption of both carbohydrates and high sugar processed foods.

This study evaluated the temporal dominance of sensations of non-sugar-reduced and sugar-reduced chocolates created by layering of high and low sugar chocolate using a 3D printer. This sugar reduction method influenced temporal sensory attributes, which along with layer positioning and the tastant contrast effect, contributed to enhancing sweetness intensity. The 3D printed chocolates were well liked, and temporal sensory profile changes did not negatively affect overall liking.

3.5 Conclusions

Layering of high and low sugar chocolate by 3D printing achieved up to a 19% sugar reduction without changes in overall sweetness perception and overall liking. A discontinuous stimulation of the taste receptors with a sufficient sugar concentration gradient between the layers contributed to this sweetness enhancement. The layering order from bottom to top of alternating high and low concentration sugar layers changed the temporal sensory attribute profile of 3D printed chocolates, but these changes did not influence overall liking. Future

studies could utilize 3D printing to generate chocolates with varying numbers of layers, different concentration gradients between the layers, and all possible layering orders to more clearly describe the effect of these variables on perceived temporal sensory profile and overall sweetness. 3D food printing technology is progressing rapidly, and further sugar reduction could be achieved with refined research methods.

3.6 References

Ares, G., Alcaire, F., Antúnez, L., Vidal, L., Giménez, A., & Castura, J. C. (2017). Identification of drivers of (dis)liking based on dynamic sensory profiles: Comparison of temporal dominance of sensations and temporal check-all-that-apply. *Food Research International, 92*, 79-87. https://doi.org/10.1016/j.foodres.2016.12.016

Burseg, K. M. M., Brattinga, C., de Kok, Petrus Maria Theresia, & Bult, J. H. F. (2010). Sweet taste enhancement through pulsatile stimulation depends on pulsation period not on conscious pulse perception. *Physiology & Behavior, 100*(4), 327-331. https://doi.org/10.1016/j.physbeh.2010.03.007

Castura, J. (2020). *tempR; temporal sensory data analysis.* http://www.cran.r-project.org/package=tempR/

De Pelsmaeker, S., De Clercq, G., Gellynck, X., & Schouteten, J. (2019). Development of a sensory wheel and lexicon for chocolate. *Food Research International, 116*, 1183-1191. https://doi.org/10.1016/j.foodres.2018.09.063

Emorine, M., Septier, C., Andriot, I., Martin, C., Salles, C., & Thomas-Danguin, T. (2015). Combined heterogeneous distribution of salt and aroma in food enhances salt perception. *Food & Function, 6*(5), 1449-1459. https://doi.org/10.1039/c4fo01067a

Gámbaro, A., & Ellis, A. C. (2012). Exploring consumer perception about the different types of chocolate. *Brazilian Journal of Food Technology, 15*(4), 307-316. https://doi.org/10.1590/S1981-67232012005000021

HM Government. (2016). *Childhood obesity: A plan for action*. Crown.

Holm, K., Wendin, K., & Hermansson, A. (2009). Sweetness and texture perceptions in structured gelatin gels with embedded sugar rich domains. *Food Hydrocolloids, 23*, 2388-2393.

International Organization for Standardization. (2008). *ISO 5492:2008(en) sensory analysis - vocabulary*

International Organization for Standardization. (2016). *Sensory analysis - methodology - general guidance for establishing a sensory profile* (Second ed.)

Kiumarsi, M., Majchrzak, D., Jäger, H., Song, J., Lieleg, O., & Shahbazi, M. (2021). Comparative study of instrumental properties and sensory profiling of low-calorie chocolate containing hydrophobically modified inulin. part II: Proton mobility, topological, tribological and dynamic sensory properties. *Food Hydrocolloids, 110*, 106144. https://doi.org/10.1016/j.foodhyd.2020.106144

Langlois, K., Garriguet, D., Gonzalez, A., Sinclair, S., & Colapinto, C. K. (2019). Change in total sugars consumption among Canadian children and adults. *Health Reports, 30*(1), 10-19. https://www.ncbi.nlm.nih.gov/pubmed/30649778

Lenfant, F., Loret, C., Pineau, N., Hartmann, C., & Martin, N. (2009). Perception of oral food breakdown. the concept of sensory trajectory. *Appetite, 52*(3), 659-667. https://doi.org/10.1016/j.appet.2009.03.003

Lenth, R. V. (2016). *Least-squares means: The R package lsmeans.* doi:10.18637/jss.v069.i01

Liu, S., Munasinghe, L. L., Ohinmaa, A., & Veugelers, P. J. (2020). Added, free and total sugar content and consumption of foods and beverages in canada. *Health Reports, 31*(10), 14-24. https://doi.org/10.25318/82-003-x202001000002-eng

Meiselman, H. L., & Halpern, B. P. (1973). Enhancement of taste intensity through pulsatile stimulation. *Physiology & Behavior, 11*(5), 713-716. https://doi.org/10.1016/0031-9384(73)90257-6

Modi, N., & Priefer, R. (2020). Effectiveness of mainstream diets. *Obesity Medicine, 18*, 100239. https://doi.org/10.1016/j.obmed.2020.100239

Mosca, A. C., Velde, F. v. d., Bult, J. H. F., van Boekel, Martinus A. J. S, & Stieger, M. (2010). Enhancement of sweetness intensity in gels by inhomogeneous distribution of sucrose. *Food Quality and Preference, 21*(7), 837-842. https://doi.org/10.1016/j.foodqual.2010.04.010

Mosca, A. C., Rocha, J. A., Sala, G., van de Velde, F., & Stieger, M. (2012). Inhomogeneous distribution of fat enhances the perception of fat-related sensory attributes in gelled foods. *Food Hydrocolloids, 27*(2), 448-455. https://doi.org/10.1016/j.foodhyd.2011.11.002

Mosca, A. C., van de Velde, F., Bult, J. H. F., van Boekel, Martinus A. J. S, & Stieger, M. (2012). Effect of gel texture and sucrose spatial distribution on sweetness perception. *LWT - Food Science and Technology, 46*, 183-188.

Mosca, A. C., Bult, J. H. F., & Stieger, M. (2013). Effect of spatial distribution of tastants on taste intensity, fluctuation of taste intensity and consumer preference of (semi-)solid food products. *Food Quality and Preference, 28*(1), 182-187. https://doi.org/10.1016/j.foodqual.2012.07.003

Mosca, A. C., Bult, J. H. F., Velde, F. v. d., van Boekel, M. A. J. S., & Stieger, M. (2014). Effect of successive stimuli on sweetness intensity of gels and custards. *Food Quality and Preference, 31*, 10-18. https://doi.org/10.1016/j.foodqual.2013.07.009

Noort, M. W. J., Bult, J. H. F., Stieger, M., & Hamer, R. J. (2010). Saltiness enhancement in bread by inhomogeneous spatial distribution of sodium chloride. *Journal of Cereal Science, 52*(3), 378-386. https://doi.org/10.1016/j.jcs.2010.06.018

Oberrauter, L. M., Januszewska, R., Schlich, P., & Majchrzak, D. (2018). Sensory evaluation of dark origin and non-origin chocolates applying temporal dominance of sensations (TDS). *Food Research International, 111*, 39-49. https://doi.org/10.1016/j.foodres.2018.05.007

Olegario, L. S., González-Mohino, A., Estévez, M., Madruga, M. S., & Ventanas, S. (2020). Impact of 'free-from' and 'healthy choice' labeled versions of chocolate and coffee on temporal profile (multiple-intake TDS) and liking. *Food Research International, 137*, 109342. https://doi.org/10.1016/j.foodres.2020.109342

Pineau, N., Schlich, P., Cordelle, S., Mathonnière, C., Issanchou, S., Imbert, A., Rogeaux, M., Etiévant, P., & Köster, E. (2009). Temporal dominance of sensations: Construction of the TDS curves and comparison with time–intensity. *Food Quality and Preference, 20*(6), 450-455. https://doi.org/10.1016/j.foodqual.2009.04.005

Pineau, N., & Schilch, P. (2015). 13 - temporal dominance of sensations (TDS) as a sensory profiling technique. *Rapid sensory profiling techniques and related methods* (pp. 269-306). Elsevier Ltd. https://doi.org/10.1533/9781782422587.2.269

Pinheiro, J., Bates, D., DebRoy, S. & Sarkar, D. (2020). *Nlme: Linear and nonlinear mixed effects models.* https://CRAN.R-project.org/package=nlme

Ramón-Canul, L. G., Ramón-Canul, F. C., Moo-Huchin, V. M., Herrera-Corredor, J. A., Cabal-Prieto, A., Ramírez-Sucre, M. O., & Ramírez-Rivera, E. J. (2020). Sensory characterisation, dominant attributes in time and consumer preference of industrial and artisanal mexican chocolates. *International Food Research Journal 27, 27*(5), 941-950.

Rodrigues, J. F., Condino, J. P. F., Pinheiro, A. C. M., & Nunes, C. A. (2016). Temporal dominance of sensations of chocolate bars with different cocoa contents: Multivariate approaches to assess TDS profiles. *Food Quality and Preference, 47*, 91-96. https://doi.org/10.1016/j.foodqual.2015.06.020

Rodrigues, J. F., de Souza, V. R., Lima, R. R., Carneiro, João de Deus Souza, Nunes, C. A., & Pinheiro, A. C. M. (2016). Temporal dominance of sensations (TDS) panel behavior: A preliminary study with chocolate. *Food Quality and Preference, 54*, 51-57. https://doi.org/10.1016/j.foodqual.2016.07.002

Sun, J., Peng, Z., Zhou, W., Fuh, J. Y. H., Hong, G. S., & Chiu, A. (2015). A review on 3D printing for customized food fabrication. *Procedia Manufacturing, 1*, 308-319. https://doi.org/10.1016/j.promfg.2015.09.057

Thamke, I., Dürrschmid, K., & Rohm, H. (2009). Sensory description of dark chocolates by consumers. *Food Science & Technology, 42*(2), 534-539. https://doi.org/10.1016/j.lwt.2008.07.006

van Bommel, R., Stieger, M., Schlich, P., & Jager, G. (2019). Dutch consumers do not hesitate: Capturing implicit 'no dominance' durations using hold-down temporal dominance methodologies for sensations (TDS) and emotions (TDE). *Food Quality and Preference, 71*, 332-342. https://doi.org/10.1016/j.foodqual.2018.08.008

World Cancer Research Fund International. (2015). *Curbing global sugar consumption: Effective food policy actions to help promote healthy diets & tackle obesity.*

World Health Organization. (2015). *Guideline: Sugars intake for adults and children*

Chapter 4 - Conclusions and recommendations

4.1 Summary and conclusions

Despite sugar reduction initiatives to reduce sugar in foods, excess sugar consumption remains a global concern. Confectionary items such as chocolate are one of the top contributors to daily total sugar intake. As sugar provides sweetness and texture variety in chocolate, substitution or removal of sucrose can influence these sensory properties. Therefore, new and more efficient strategies to reduce sugar that maintain sweetness and consumer acceptance could be developed for this food category. Spatial distribution is a tastant-reduction technique that has been proven to reduce sugar content in gels, as well as salt and fat in breads and sausages, without negatively affecting sweetness and saltiness. For sugar reduction, this method involves layering of high and low sugar concentrations of a food matrix to maintain an equi-sweet perception. As 3D food printing (3DFP) technology extrudes materials in layers and can create intricate 3D structures, it can be used to achieve spatial distribution. A dual-extruder 3D food printer is more efficient in creating layers of two types of chocolate than conventional chocolate molding and does not require expertise in chocolate making. However, methods to optimize chocolate material formulations and 3D printing parameters must be developed to create high-quality prints.

In chapter 2, 3D food printing was found to be an effective method to create prototype sugar-reduced and non-sugar-reduced 3D printed chocolates with different total % sugar concentrations by the spatial distribution method. A novel, four-step 3D printing parameter optimization procedure was proposed, which included the quantification of 3D printer speeds and extruder flow rates, a qualitative screening assessment to determine optimal printer settings,

validation of printed product accuracy and precision, and confirmation of product quality. This approach determined an optimal print speed setting and flow rate setting combination for a dual-extruder 3D printer with two chocolate types. This optimal print setting combination created 3D printed chocolates with small % error in average measured mass, height, wall thickness, and diameter of the 3D printed chocolates compared to 3D digital designs. Melting properties determined by differential scanning calorimetry revealed that the chocolates were properly tempered prior to 3D printing and remained tempered after 3D printing when the printing temperature was set to 28℃ (for low sugar concentration chocolate) or 32℃ (for high sugar concentration chocolate). The six final designs of manufactured sugar-reduced and non-sugar-reduced 3D printed chocolates were verified to have total % sugar (w/w) concentrations of 51.5%, 41.6%, 41.6%, 34.9%, 34.0%, and 26.7%. As sensory analysis is important for implementation of novel 3D printed foods, a subsequent sensory study using these manufactured designs was conducted (Chapter 3).

In chapter 3, the temporal sensory profile, perceived overall sweetness and overall liking of the sugar-reduced 3D printed chocolates that were manufactured using the spatial distribution method were evaluated. A consumer panel completed a temporal dominance of sensations (TDS) evaluation by selecting from a list of attributes, the one that stood out to them the most during consumption over a period of 120 seconds and rated overall sweetness intensity and liking. TDS curves, TDS difference curves, and principal components analysis (PCA) were computed to determine the differences in temporal sensory attribute profiles among the six 3D printed chocolates. Samples with up to 19% sugar reduction from the high sugar control were perceived to be similarly sweet to the control. This result was attributed to the influence of layering order and a sufficiently large concentration gradient between the layers. Interactions between layering

order, the sensory attribute profile, and overall sweetness perception were elucidated. Layering by 3D printing changed the temporal sensory profiles of the 3D printed chocolates and facilitated sugar reduction without affecting acceptance and sweetness intensity by enhancing desired chocolate taste and texture properties such as “sweet” and “creamy.”

4.2 Significance of this work

This study described a new sugar-reduction method using 3DFP technology, where sugar-reduced 3D printed chocolates were manufactured by alternating layers of high and low sugar concentration dark chocolates. The novel, four-step, semi-quantitative method for optimizing printing parameters that was presented in this research could be adapted and applied to optimize 3D printing of a variety of foods to improve the quality of final prints. Future 3D chocolate printing studies could use the seed-tempering method presented in this research; melting properties indicated that the chocolates were tempered before 3D printing and would remain tempered after 3D printing if printing temperature remained at the working temperature of dark chocolate (28-32℃).

This study also elucidated the temporal sensory perceptions, perceived overall sweetness and liking of the manufactured sugar-reduced and non-sugar-reduced 3D printed chocolates. Layering sugar concentrations within a food structure to modulate the sensory profile has not previously been demonstrated using 3DFP, and not in chocolates. Consumer sensory evaluation verified that sugar reduction could be achieved without affecting sweetness perception and liking of the 3D printed chocolates, which was explained by the alternating stimulation of taste receptors created by layers of chocolate with different sugar concentrations.

The findings from this work suggested that 3DFP using a dual-extruder system could be used as an alternative to conventional molding methods to create layered chocolates with reduced sugar. Furthermore, optimizing printing parameters by the proposed four-step process ensured the creation of high-quality 3D printed chocolates that had dimensions as designed. The sensory results could also encourage food manufacturers to implement 3DFP to provide sugar-reduced products.

4.3 Limitations and future research

It is important to optimize printing parameters to improve the quality of final printed products. As print speed and flow rate are closely related, one often influences the other. In chapter 2, nine combinations using a print speed of 35, 65, or 95 and a flow rate of 70, 100 or 130 (all printing software settings, no units) were investigated to find the most suitable setting for both a high and low sugar concentration chocolate. In future research, other combinations with smaller intervals between settings (less than 30 as was used in the present research) should be considered as other suitable print settings could exist for the chocolates used. Investigation of the effect of 3D printing on chocolate flow properties is needed, as relating the flow properties to other 3D printing parameters could further improve the quality of the 3D chocolate prints.

Chapter 3 provided valuable information for product development of sugar-reduced foods by the spatial distribution method and offered guidance for sugar-reduction using 3D printing. Future studies could explore different layering orders such as concentric designs, or other tastant arrangements such as specific patterns created by placing highly concentrated sugar areas in designated areas of the food. The influence of sugar particle shape, size and type could also be examined. Additionally, samples with a greater number of layers or larger concentration

gradients between the layers could be investigated to ascertain the effects of layering order more precisely. Finally, mixing the high and low sugar concentration chocolate used in this research could create a chocolate with an intermediate sugar concentration that could be used to create different concentration gradients in the chocolate sample.

The temporal sensory perceptions of three-layered, 3D-printed, sugar-reduced chocolates with different sugar concentrations were described in chapter 3. The dominance rates (0.2-0.4), number of dominant attributes selected by participants (six out of eight presented), and number of responses collected in this research (36 for each chocolate sample) were comparable to previous temporal studies on milk and dark chocolate and chocolate products. However, as participants were consumers, this experiment could be strengthened by including more panelists to achieve even higher agreement of dominant attributes (dominance rates closer to 1.0). Chocolates with more variable sensory and quality attributes (e.g., fruits, nuts, and other flavorings) or a greater difference in sugar concentration could also be explored to identify if the spatial distribution method would also enhance sweetness for those chocolates. Finally, since chocolate undergoes a phase change during consumption, it could be helpful to separate taste and texture attribute categories in a subsequent study for more discriminative results. Field notes indicated that a few participants were challenged to select only one attribute as dominant when a taste and texture attribute both stood out at the same time.

Bibliography

Afoakwa, E. O., Paterson, A., Fowler, M., & Vieira, J. (2008). Characterization of melting properties in dark chocolates from varying particle size distribution and composition using differential scanning calorimetry. *Food Research International, 41*(7), 751-757. https://doi.org/10.1016/j.foodres.2008.05.009

Ares, G., Alcaire, F., Antúnez, L., Vidal, L., Giménez, A., & Castura, J. C. (2017). Identification of drivers of (dis)liking based on dynamic sensory profiles: Comparison of temporal dominance of sensations and temporal check-all-that-apply. *Food Research International, 92*, 79-87. https://doi.org/10.1016/j.foodres.2016.12.016

Azam, S. M. R., Zhang, M., Mujumdar, A. S., & Yang, C. (2018, Apr 6,). Study on 3D printing of orange concentrate and material characteristics. *Journal of Food Process Engineering, 0*, e12689. https://doi.org/10.1111/jfpe.12689

Baiano, A. (2020). 3D printed foods: A comprehensive review on technologies, nutritional value, safety, consumer attitude, regulatory framework, and economic and sustainability issues. *Food Reviews International, ahead-of-print*(ahead-of-print), 1-31. https://doi.org/10.1080/87559129.2020.1762091

Beckett, S. T., Fowler, M. S., & Ziegler, G. R. (2017). *Beckett's industrial chocolate manufacture and use* (Fifth ed.). John Wiley & Sons Ltd. https://doi.org/10.1002/9781118923597

Belščak-Cvitanović, A., Komes, D., Dujmović, M., Karlović, S., Biškić, M., Brnčić, M., & Ježek, D. (2015). Physical, bioactive and sensory quality parameters of reduced sugar chocolates formulated with natural sweeteners as sucrose alternatives. *Food Chemistry, 167*, 61-70. https://doi.org/10.1016/j.foodchem.2014.06.064

Burseg, K. M. M., Brattinga, C., de Kok, Petrus Maria Theresia, & Bult, J. H. F. (2010). Sweet taste enhancement through pulsatile stimulation depends on pulsation period not on conscious pulse perception. *Physiology & Behavior, 100*(4), 327-331. https://doi.org/10.1016/j.physbeh.2010.03.007

Canadian Diabetes Association. (2021). *Sugar & diabetes.* https://www.diabetes.ca/advocacy---policies/our-policy-positions/sugar---diabetes#b

Canadian Food Inspection Agency. (2021). *Specific nutrient content claim requirements: Carbohydrate and sugars claims.* https://inspection.canada.ca/food-label-requirements/labelling/industry/nutrient-content/specific-claim-requirements/eng/1389907770176/1389907817577?chap=11

Caporizzi, R., Derossi, A., & Severini, C. (2019). *Cereal-based and insect-enriched printable food*. Elsevier. https://doi.org/10.1016/b978-0-12-814564-7.00004-3

Castura, J. (2020). *tempR; temporal sensory data analysis.* http://www.cran.r-project.org/package=tempR/

Cohen, D., Lipton, J., Cutler, M., Coulter, D., Vesco, A., & Lipson, A. (2009). Hydrocolloid printing: A novel platform for customized food production. Paper presented at the *20th Annual International Solid Freeform Fabrication Symposium, SFF 209,* 807-818. https://search.datacite.org/works/10.1080/10408398.2015.1094732

de melo, Bolini, & Efraim. (2009). Sensory profile, acceptability, and their relationship for diabetic/reduced calorie chocolates. *Food Quality and Preference, 20*(2), 138-143. https://doi.org/10.1016/j.foodqual.2008.09.001

De Pelsmaeker, S., De Clercq, G., Gellynck, X., & Schouteten, J. (2019). Development of a sensory wheel and lexicon for chocolate. *Food Research International, 116*, 1183-1191. https://doi.org/10.1016/j.foodres.2018.09.063

Derossi, A., Caporizzi, R., Azzollini, D., & Severini, C. (2018). Application of 3D printing for customized food. A case on the development of a fruit-based snack for children. *Journal of Food Engineering, 220*, 65-75. https://doi.org/10.1016/j.jfoodeng.2017.05.015

Derossi, A., Caporizzi, R., Ricci, I., & Severini, C. (2019). *Critical variables in 3D food printing*. Elsevier. https://doi.org/10.1016/b978-0-12-814564-7.00003-1

Emorine, M., Septier, C., Andriot, I., Martin, C., Salles, C., & Thomas-Danguin, T. (2015). Combined heterogeneous distribution of salt and aroma in food enhances salt perception. *Food & Function, 6*(5), 1449-1459. https://doi.org/10.1039/c4fo01067a

Fernandes, V. A., Müller, A. J., & Sandoval, A. J. (2013). Thermal, structural and rheological characteristics of dark chocolate with different compositions. *Journal of Food Engineering, 116*(1), 97-108. https://doi.org/10.1016/j.jfoodeng.2012.12.002

Gámbaro, A., & Ellis, A. C. (2012). Exploring consumer perception about the different types of chocolate. *Brazilian Journal of Food Technology, 15*(4), 307-316. https://doi.org/10.1590/S1981-67232012005000021

Glicerina, V., Balestra, F., Dalla Rosa, M., & Romani, S. (2016). Microstructural and rheological characteristics of dark, milk and white chocolate: A comparative study. Journal of Food Engineering, 169, 165-171. https://doi.org/10.1016/j.jfoodeng.2015.08.011

Godoi, F. C., Bhandari, B. R., Prakash, S., & Zhang, M. (2019). *An introduction to the principles of 3D food printing*. Elsevier. https://doi.org/10.1016/b978-0-12-814564-7.00001-8

Godoi, F. C., Prakash, S., & Bhandari, B. R. (2016). 3d printing technologies applied for food design: Status and prospects. *Journal of Food Engineering, 179*, 44-54. https://doi.org/10.1016/j.jfoodeng.2016.01.025

Hamilton, C. A., Alici, G., & in het Panhuis, M. (2018). 3D printing vegemite and marmite: Redefining "breadboards". *Journal of Food Engineering, 220*, 83-88. https://doi.org/10.1016/j.jfoodeng.2017.01.008

Hao, L., Mellor, S., Seaman, O., Henderson, J., Sewell, N., & Sloan, M. (2010). Material characterisation and process development for chocolate additive layer manufacturing. *Virtual and Physical Prototyping, 5*(2), 57-64. https://doi.org/10.1080/17452751003753212

Heart and Stroke Foundation of Canada. (2020). *Reduce sugar.* https://www.heartandstroke.ca/healthy-living/healthy-eating/reduce-sugar

Hertafeld, E., Zhang, C., Jin, Z., Jakub, A., Russell, K., Lakehal, Y., Andreyeva, K., Bangalore, S. N., Mezquita, J., Blutinger, J., & Lipson, H. (2019). Multi-material three-dimensional food printing with simultaneous infrared cooking. *3D Printing and Additive Manufacturing, 6*(1), 13-19. https://doi.org/10.1089/3dp.2018.0042

HM Government. (2016). *Childhood obesity: A plan for action*. Crown.

Hodgson, G., Ranellucci, A. & Moe, J. (2021). *Flow math.* Slic3r Manual. https://manual.slic3r.org/advanced/flow-math

Holm, K., Wendin, K., & Hermansson, A. (2009). Sweetness and texture perceptions in structured gelatin gels with embedded sugar rich domains. *Food Hydrocolloids, 23*, 2388-2393.

International Organization for Standardization. (2008). *ISO 5492:2008(en) sensory analysis - vocabulary*

International Organization for Standardization. (2016). *Sensory analysis - methodology - general guidance for establishing a sensory profile* (Second ed.)

Karavasili, C., Gkaragkounis, A., Moschakis, T., Ritzoulis, C., & Fatouros, D. G. (2020). Pediatric-friendly chocolate-based dosage forms for the oral administration of both hydrophilic and lipophilic drugs fabricated with extrusion-based 3D printing. *European Journal of Pharmaceutical Sciences, 147*, 105291. https://doi.org/10.1016/j.ejps.2020.105291

Karyappa, R., & Hashimoto, M. (2019). *Chocolate-based ink three-dimensional printing (Ci3DP)*. Springer Science and Business Media LLC. https://doi.org/10.1038/s41598-019-50583-5

Keerthana, K., Anukiruthika, T., Moses, J. A., & Anandharamakrishnan, C. (2020). Development of fiber-enriched 3D printed snacks from alternative foods: A study on button mushroom. *Journal of Food Engineering, 287*, 110116. https://doi.org/10.1016/j.jfoodeng.2020.110116

Kern, C., Weiss, J., & Hinrichs, J. (2018). Additive layer manufacturing of semi-hard model cheese: Effect of calcium levels on thermo-rheological properties and shear behavior. *Journal of Food Engineering, 235*, 89-97. https://doi.org/10.1016/j.jfoodeng.2018.04.029

Kiumarsi, M., Majchrzak, D., Jäger, H., Song, J., Lieleg, O., & Shahbazi, M. (2021). Comparative study of instrumental properties and sensory profiling of low-calorie chocolate containing hydrophobically modified inulin. part II: Proton mobility, topological, tribological and dynamic sensory properties. *Food Hydrocolloids, 110*, 106144. https://doi.org/10.1016/j.foodhyd.2020.106144

Lanaro, M., Desselle, M. R., & Woodruff, M. A. (2019). In Godoi F. C., Bhandari B. R., Prakash S. and Zhang M.(Eds.), *3D printing chocolate: Properties of formulations for extrusion, sintering, binding and ink jetting*. Academic Press Ltd-Elsevier Science Ltd. https://doi.org/10.1016/B978-0-12-814564-7.00006-7

Lanaro, M., Forrestal, D. P., Scheurer, S., Slinger, D. J., Liao, S., Powell, S. K., & Woodruff, M. A. (2017). 3D printing complex chocolate objects: Platform design, optimization and evaluation. *Journal of Food Engineering, 215*, 13-22. https://doi.org/10.1016/j.jfoodeng.2017.06.029

Landoni, B. (2014). *3Drag is now printing with chocolate!* Open Electronics. https://www.open-electronics.org/3drag-is-now-printing-with-chocolate/

Langlois, K., Garriguet, D., Gonzalez, A., Sinclair, S., & Colapinto, C. K. (2019). Change in total sugars consumption among canadian children and adults. *Health Reports, 30*(1), 10-19. https://www.ncbi.nlm.nih.gov/pubmed/30649778

Le Tohic, C., O'Sullivan, J. J., Drapala, K. P., Chartrin, V., Chan, T., Morrison, A. P., Kerry, J. P., & Kelly, A. L. (2018). Effect of 3D printing on the structure and textural properties of processed cheese. *Journal of Food Engineering, 220*, 56-64. https://doi.org/10.1016/j.jfoodeng.2017.02.003

Lenfant, F., Loret, C., Pineau, N., Hartmann, C., & Martin, N. (2009). Perception of oral food breakdown. the concept of sensory trajectory. *Appetite, 52*(3), 659-667. https://doi.org/10.1016/j.appet.2009.03.003

Lenth, R. V. (2016). *Least-squares means: The R package lsmeans.* doi:10.18637/jss.v069.i01

Liu, S., Munasinghe, L. L., Ohinmaa, A., & Veugelers, P. J. (2020). Added, free and total sugar content and consumption of foods and beverages in canada. *Health Reports, 31*(10), 14-24. https://doi.org/10.25318/82-003-x202001000002-eng

Liu, Z., Bhandari, B., Prakash, S., & Zhang, M. (2018). Creation of internal structure of mashed potato construct by 3D printing and its textural properties. *Food Research International, 111*, 534-543. https://doi.org/10.1016/j.foodres.2018.05.075

Liu, Z., Zhang, M., Bhandari, B., & Wang, Y. (2017). 3D printing: Printing precision and application in food sector. *Trends in Food Science & Technology, 69*, 83-94. https://doi.org/10.1016/j.tifs.2017.08.018

Liu, Z., Zhang, M., Bhandari, B., & Yang, C. (2018). Impact of rheological properties of mashed potatoes on 3D printing. *Journal of Food Engineering, 220*, 76-82. https://doi.org/10.1016/j.jfoodeng.2017.04.017

Liu, Z., Zhang, M., & Yang, C. (2018). Dual extrusion 3D printing of mashed potatoes/strawberry juice gel. *Food Science & Technology, 96*, 589-596. https://doi.org/10.1016/j.lwt.2018.06.014

Mantell, D. A., Hays, A. W., & Langford, Z. C. (2015). In XEROX CORPORATION, Norwalk, CT (US) (Ed.), *Printing 3D tempered chocolate*

Mantihal, S., Prakash, S., & Bhandari, B. (2019). Textural modification of 3D printed dark chocolate by varying internal infill structure. *Food Research International, 121*, 648-657. https://doi.org/10.1016/j.foodres.2018.12.034

Mantihal, S., Prakash, S., & Bhandari, B. (2019). Texture- modified 3D printed dark chocolate: Sensory evaluation and consumer perception study. *Journal of Texture Studies, 50*(5), 386-399. https://doi.org/10.1111/jtxs.12472

Mantihal, S., Prakash, S., Godoi, F. C., & Bhandari, B. (2017). Optimization of chocolate 3D printing by correlating thermal and flow properties with 3D structure modeling. *Innovative Food Science & Emerging Technologies, 44*, 21-29. https://doi.org/10.1016/j.ifset.2017.09.012

Mantihal, S., Prakash, S., Godoi, F. C., & Bhandari, B. (2019). Effect of additives on thermal, rheological and tribological properties of 3D printed dark chocolate. *Food Research International, 119*, 161-169. https://doi.org/10.1016/j.foodres.2019.01.056

Marangoni, A. G., & McGauley, S. E. (2003). Relationship between crystallization behavior and structure in cocoa butter. *Crystal Growth & Design, 3*(1), 95-108. https://doi.org/10.1021/cg025580l

Meiselman, H. L., & Halpern, B. P. (1973). Enhancement of taste intensity through pulsatile stimulation. *Physiology & Behavior, 11*(5), 713-716. https://doi.org/10.1016/0031-9384(73)90257-6

Modi, N., & Priefer, R. (2020). Effectiveness of mainstream diets. *Obesity Medicine, 18*, 100239. https://doi.org/10.1016/j.obmed.2020.100239

Mosca, A. C., Bult, J. H. F., & Stieger, M. (2013). Effect of spatial distribution of tastants on taste intensity, fluctuation of taste intensity and consumer preference of (semi-)solid food products. *Food Quality and Preference, 28*(1), 182-187. https://doi.org/10.1016/j.foodqual.2012.07.003

Mosca, A. C., Bult, J. H. F., Velde, F. v. d., van Boekel, M. A. J. S., & Stieger, M. (2014). Effect of successive stimuli on sweetness intensity of gels and custards. *Food Quality and Preference, 31*, 10-18. https://doi.org/10.1016/j.foodqual.2013.07.009

Mosca, A. C., Rocha, J. A., Sala, G., van de Velde, F., & Stieger, M. (2012). Inhomogeneous distribution of fat enhances the perception of fat-related sensory attributes in gelled foods. *Food Hydrocolloids, 27*(2), 448-455. https://doi.org/10.1016/j.foodhyd.2011.11.002

Mosca, A. C., van de Velde, F., Bult, J. H. F., van Boekel, Martinus A. J. S, & Stieger, M. (2012). Effect of gel texture and sucrose spatial distribution on sweetness perception. *LWT - Food Science and Technology, 46*, 183-188.

Mosca, A. C., Velde, F. v. d., Bult, J. H. F., van Boekel, Martinus A. J. S, & Stieger, M. (2010). Enhancement of sweetness intensity in gels by inhomogeneous distribution of sucrose. *Food Quality and Preference, 21*(7), 837-842. https://doi.org/10.1016/j.foodqual.2010.04.010

Noorani, R. (2017). *3D printing technology, applications, and selection* (1st ed.). CRC Press.

Noort, M. W. J., Bult, J. H. F., & Stieger, M. (2012). Saltiness enhancement by taste contrast in bread prepared with encapsulated salt. *Journal of Cereal Science, 55*(2), 218-225. https://doi.org/10.1016/j.jcs.2011.11.012

Noort, M. W. J., Bult, J. H. F., Stieger, M., & Hamer, R. J. (2010). Saltiness enhancement in bread by inhomogeneous spatial distribution of sodium chloride. *Journal of Cereal Science, 52*(3), 378-386. https://doi.org/10.1016/j.jcs.2010.06.018

Oberrauter, L. M., Januszewska, R., Schlich, P., & Majchrzak, D. (2018). Sensory evaluation of dark origin and non-origin chocolates applying temporal dominance of sensations (TDS). *Food Research International, 111*, 39-49. https://doi.org/10.1016/j.foodres.2018.05.007

OECD, & FAO. (2020). *OECD-FAO agricultural outlook 2020-2029*. OECD Publishing. https://doi.org/10.1787/1112c23b-en

Olegario, L. S., González-Mohino, A., Estévez, M., Madruga, M. S., & Ventanas, S. (2020). Impact of 'free-from' and 'healthy choice' labeled versions of chocolate and coffee on

temporal profile (multiple-intake TDS) and liking. *Food Research International, 137*, 109342. https://doi.org/10.1016/j.foodres.2020.109342

Ostrowska-Ligęza, E., Marzec, A., Górska, A., Wirkowska-Wojdyła, M., Bryś, J., Rejch, A., & Czarkowska, K. (2019). A comparative study of thermal and textural properties of milk, white and dark chocolates. *Thermochimica Acta, 671*, 60-69. https://doi.org/10.1016/j.tca.2018.11.005

Pineau, N., & Schilch, P. (2015). 13 - temporal dominance of sensations (TDS) as a sensory profiling technique. *Rapid sensory profiling techniques and related methods* (pp. 269-306). Elsevier Ltd. https://doi.org/10.1533/9781782422587.2.269

Pineau, N., Schlich, P., Cordelle, S., Mathonnière, C., Issanchou, S., Imbert, A., Rogeaux, M., Etiévant, P., & Köster, E. (2009). Temporal dominance of sensations: Construction of the TDS curves and comparison with time–intensity. *Food Quality and Preference, 20*(6), 450-455. https://doi.org/10.1016/j.foodqual.2009.04.005

Pinheiro, J., Bates, D., DebRoy, S. & Sarkar, D. (2020). *Nlme: Linear and nonlinear mixed effects models.* https://CRAN.R-project.org/package=nlme

Ramón-Canul, L. G., Ramón-Canul, F. C., Moo-Huchin, V. M., Herrera-Corredor, J. A., Cabal-Prieto, A., Ramírez-Sucre, M. O., & Ramírez-Rivera, E. J. (2020). Sensory characterisation, dominant attributes in time and consumer preference of industrial and artisanal mexican chocolates. *International Food Research Journal 27, 27*(5), 941-950.

Rando, P., & Ramaioli, M. (2021). Food 3D printing: Effect of heat transfer on print stability of chocolate. *Journal of Food Engineering, 294* https://doi.org/10.1016/j.jfoodeng.2020.110415

Rodrigues, J. F., Condino, J. P. F., Pinheiro, A. C. M., & Nunes, C. A. (2016). Temporal dominance of sensations of chocolate bars with different cocoa contents: Multivariate approaches to assess TDS profiles. *Food Quality and Preference, 47*, 91-96. https://doi.org/10.1016/j.foodqual.2015.06.020

Rodrigues, J. F., de Souza, V. R., Lima, R. R., Carneiro, João de Deus Souza, Nunes, C. A., & Pinheiro, A. C. M. (2016). Temporal dominance of sensations (TDS) panel behavior: A preliminary study with chocolate. *Food Quality and Preference, 54*, 51-57. https://doi.org/10.1016/j.foodqual.2016.07.002

RTDS Group. (2020). *PERFORMANCE (development of personalised food using rapid manufacturing for the nutrition of elderly consumers).* https://www.rtds-group.com/services/projects-performance/?portfolioID=100

Severini, C., Azzollini, D., Albenzio, M., & Derossi, A. (2018). On printability, quality and nutritional properties of 3D printed cereal based snacks enriched with edible insects. *Food Research International, 106*, 666-676. https://doi.org/10.1016/j.foodres.2018.01.034

Severini, C., Derossi, A., Ricci, I., Caporizzi, R., & Fiore, A. (2018). Printing a blend of fruit and vegetables. new advances on critical variables and shelf life of 3D edible objects. *Journal of Food Engineering, 220*, 89-100. https://doi.org/10.1016/j.jfoodeng.2017.08.025

Sun, J., Peng, Z., Zhou, W., Fuh, J. Y. H., Hong, G. S., & Chiu, A. (2015). A review on 3D printing for customized food fabrication. *Procedia Manufacturing, 1*, 308-319. https://doi.org/10.1016/j.promfg.2015.09.057

Sun, J., Zhou, W., Yan, L., Huang, D., & Lin, L. (2018). Extrusion-based food printing for digitalized food design and nutrition control. *Journal of Food Engineering, 220*, 1-11. https://doi.org/10.1016/j.jfoodeng.2017.02.028

Svanberg, L., Ahrné, L., Lorén, N., & Windhab, E. (2011). Effect of pre-crystallization process and solid particle addition on microstructure in chocolate model systems. *Food Research International, 44*(5), 1339-1350. https://doi.org/10.1016/j.foodres.2011.01.018

Svanberg, L., Ahrné, L., Lorén, N., & Windhab, E. (2013). Impact of pre-crystallization process on structure and product properties in dark chocolate. *Journal of Food Engineering, 114*(1), 90-98. https://doi.org/10.1016/j.jfoodeng.2012.06.016

Thamke, I., Dürrschmid, K., & Rohm, H. (2009). Sensory description of dark chocolates by consumers. *Food Science & Technology, 42*(2), 534-539. https://doi.org/10.1016/j.lwt.2008.07.006

U.S. Department of Agriculture and U.S. Department of Health and Human Services. (2020). *Dietary guidelines for americans, 2020-2025* (9th ed.)

van Bommel, R., Stieger, M., Schlich, P., & Jager, G. (2019). Dutch consumers do not hesitate: Capturing implicit 'no dominance' durations using hold-down temporal dominance methodologies for sensations (TDS) and emotions (TDE). *Food Quality and Preference, 71*, 332-342. https://doi.org/10.1016/j.foodqual.2018.08.008

van Malssen, K., van Langevelde, A., Peschar, R., & Schenk, H. (1999). Phase behavior and extended phase scheme of static cocoa butter investigated with real-time X-ray powder diffraction. *Journal of the American Oil Chemists' Society, 76*(6), 669-676. https://doi.org/10.1007/s11746-999-0158-4

Voon, S. L., An, J., Wong, G., Zhang, Y., & Chua, C. K. (2019). 3D food printing: A categorised review of inks and their development. *Virtual and Physical Prototyping, 14*(3), 203-218. https://doi.org/10.1080/17452759.2019.1603508

Wang, J., & Shaw, L. L. (2005). Rheological and extrusion behavior of dental porcelain slurries for rapid prototyping applications. *Materials Science & Engineering. A, Structural Materials: Properties, Microstructure and Processing, 397*(1), 314-321. https://doi.org/10.1016/j.msea.2005.02.045

Wang, L., Zhang, M., Bhandari, B., & Yang, C. (2018). Investigation on fish surimi gel as promising food material for 3D printing. *Journal of Food Engineering, 220*, 101-108. https://doi.org/10.1016/j.jfoodeng.2017.02.029

World Cancer Research Fund International. (2015). *Curbing global sugar consumption: Effective food policy actions to help promote healthy diets & tackle obesity.*

World Health Organization. (2015). *Guideline: Sugars intake for adults and children*

Xie, Y., Tan, Y., Ma, G., Zhang, J., & Zhang, F. (2016). *Design and implementation of chocolate 3D printer*. Destech Publications, Inc.

Yang, F., Zhang, M., Bhandari, B., & Liu, Y. (2018). Investigation on lemon juice gel as food material for 3D printing and optimization of printing parameters. *Food Science & Technology, 87*, 67-76. https://doi.org/10.1016/j.lwt.2017.08.054

Zeleny, P., & Ruzicka, V. (2017). The design of the 3d printer for use in gastronomy. *MM Science Journal, 2017*(1), 1744-1747. https://doi.org/10.17973/MMSJ.2017_02_2016187

Zhu, Y., Bhandari, B., & Prakash, S. (2020). Relating the tribo-rheological properties of chocolate flavoured milk to temporal aspects of texture. *International Dairy Journal, 110*, 104794. https://doi.org/10.1016/j.idairyj.2020.104794

Zhuoqun, L., & Jiazhe, Y. (2018). PID control of chocolate 3D printer heating system. Paper presented at the 298-301.

Appendices

Appendix 1. Supplemental tables of Chapter 2

Table A1. Ingredients list and nutrition facts table for high (H, 51.5% total sugar) and low (L, 26.67% total sugar) sugar concentration chocolates.

	H	L
	Ingredients: sugar, chocolate liquor, cocoa butter, soy lecithin, natural flavor.	**Ingredients: chocolate liquor, sugar, cocoa butter, cocoa powder, natural flavor.**
	Quantity (g/100g)	**Quantity (g/100g)**
Energy (Cal)	599.99	633.33
Total Fat	33.33	46.66
Saturated Fat	19.99	26.67
Sodium	0.0033	0.0099
Sugars	51.52	26.67
Protein	6.66	6.66

Table A2. Density of the high (H) and low (L) sugar concentration chocolates.

Chocolate sample	Sample mass (g)	Sample volume (cm^3) ± SD	Sample density (g/cm^3) ± SD
H	2.8164	2.3541 ± 0.0023	1.3244 ± 0.0014
L	2.8928	2.3184 ± 0.0016	1.2478 ± 0.0008

Table A3. Mean ± standard deviation (SD), design value and % error in measured parameters from the design for three-layered high (HHH) and low sugar (LLL) 3D printed chocolates using print setting PS 35, FR 100 or PS 65, FR 70.

Chocolate Sample	Print Setting	Measured Parameter	Mean ± SD	Design Value	% Change from Design Value
HHH	PS 35, FR 100	Mass (g)	3.49 ± 0.12	3.36	3.65
		Height (mm)	9.70 ± 0.10	10.80	-10.22
		Wall thickness (mm)	4.68 ± 0.05	4.37	7.17
		Diameter (mm)	28.36 ± 0.25	28.00	1.30
	PS 65, FR 70	Mass (g)	2.13 ± 0.09	3.36	-36.58
		Height (mm)	6.81 ± 0.18	10.80	-36.98
		Wall thickness (mm)	3.98 ± 0.11	4.37	-9.00
		Diameter (mm)	26.51 ± 0.23	28.00	-5.32
LLL	PS 35, FR 100	Mass (g)	3.30 ± 0.05	3.17	4.23
		Height (mm)	10.01 ± 0.07	10.80	-7.35
		Wall thickness (mm)	5.02 ± 0.14	4.37	14.80
		Diameter (mm)	27.94 ± 0.08	28.00	-0.21
	PS 65, FR 70	Mass (g)	2.25 ± 0.03	3.17	-29.01
		Height (mm)	7.31 ± 0.09	10.80	-32.35
		Wall thickness (mm)	4.42 ± 0.08	4.37	1.22
		Diameter (mm)	25.87 ± 0.10	28.00	-7.61

Table A4. The mean ± standard deviation (SD), design value and % change in measured parameters from the design for individual layers of 3D printed chocolates at print setting PS 35, FR 100 by chocolate type (H, L).

Chocolate Type	Measured Parameter	Mean ± SD	Design Value	% Change from Design Value
H	Mass (g)	1.04 ± 0.13	1.12	-6.91
	Height (mm)	3.02 ± 0.34	3.60	-16.14
	Wall thickness (mm)	4.36 ± 0.20	4.37	-0.23
	Diameter (mm)	28.17 ± 0.26	28.00	0.62
L	Mass (g)	1.13 ± 0.10	1.06	6.70
	Height (mm)	3.20 ± 0.36	3.60	-11.13
	Wall thickness (mm)	4.76 ± 0.30	4.37	8.79
	Diameter (mm)	27.78 ± 0.29	28.00	-0.40

Appendix 2. Supplemental figures of Chapter 3

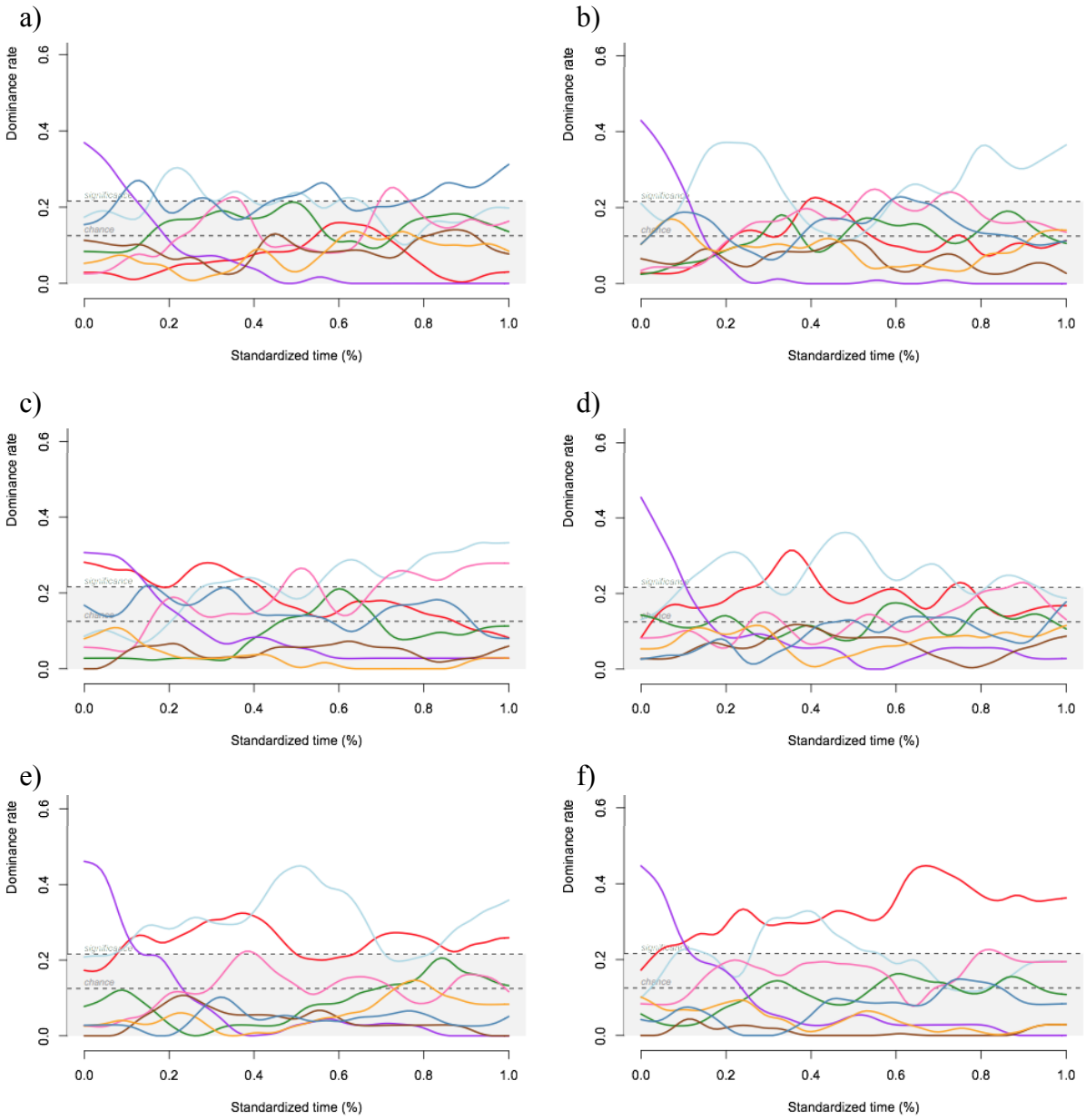

Figure A1. TDS curves for each 3D printed chocolate sample: a) HHH b) HLH c) HHL d) LHL e) HLL f) LLL. Colored lines represent: Bitter, Chocolate flavor, Melting, Milky flavor, Creamy, Soft, Hard/Brittle, Sweet.

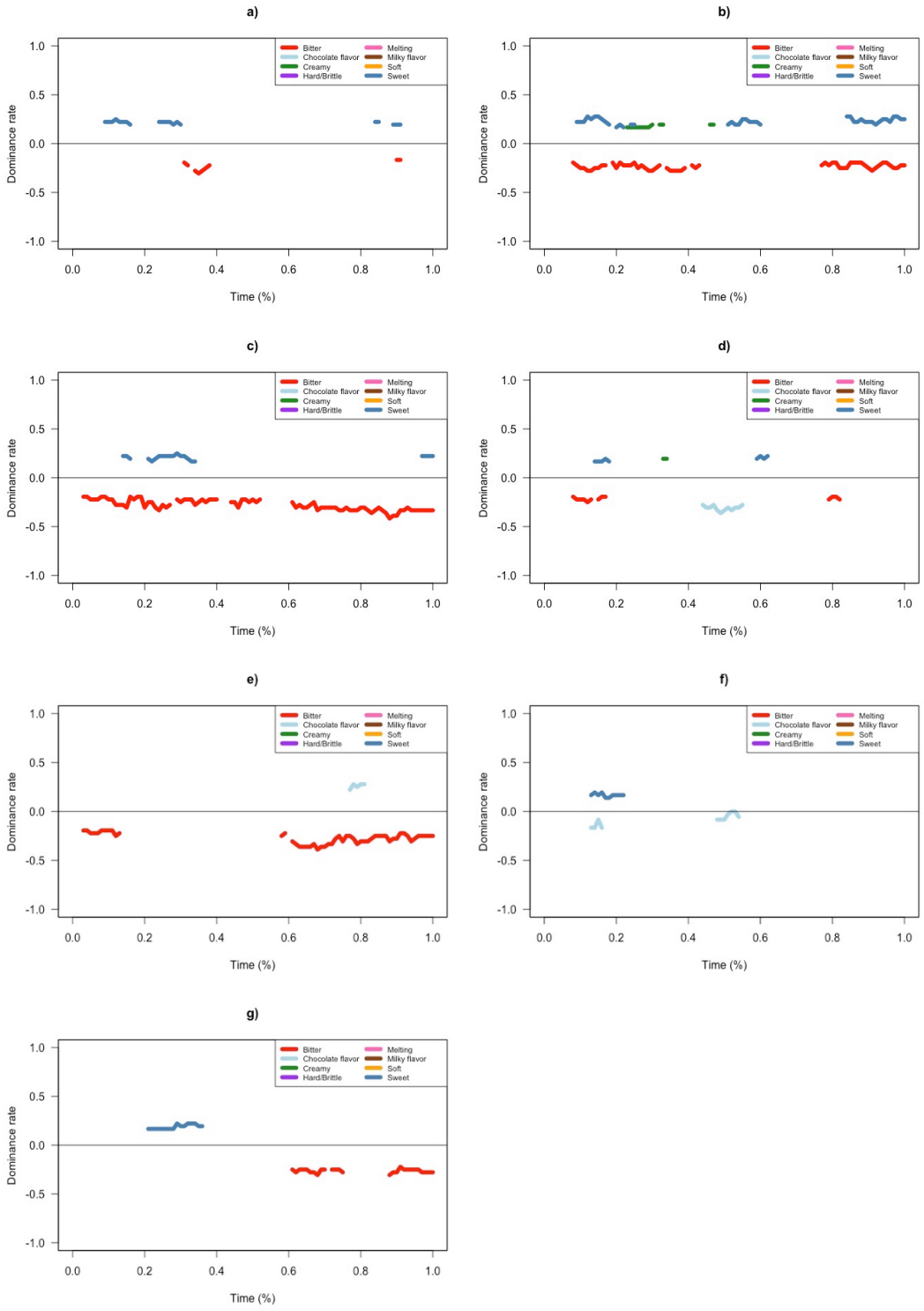

Figure A2. TDS difference curves comparing samples with significantly different sweetness: a) HHH-LHL b) HHH-HLL c) HHH-LLL d) HLH-HLL e) HLH-LLL f) HHL-HLL g) HHL-LLL